Department of Materials Science and Engineering

Water-based boundary lubrication with biomolecule additives on diamond-like carbon and stainless steel surfaces

Timo J. Hakala

Aalto University

DOCTORAL DISSERTATIONS

Aalto University publication series
DOCTORAL DISSERTATIONS 144/2015
VTT SCIENCE 118

Water-based boundary lubrication with biomolecule additives on diamond-like carbon and stainless steel surfaces

Timo J. Hakala

A doctoral dissertation completed for the degree of Doctor of Science (Technology) to be defended, with the permission of the Aalto University School of Chemical Technology, at a public examination held at the lecture hall V1 of the school on 29 January 2016 at 12.

Aalto University
School of Chemical Technology
Department of Materials Science and Engineering

Supervising professor
Prof. Jari Koskinen, Aalto University, Finland

Thesis advisor
Prof. Kenneth Holmberg, VTT Technical Research Centre of Finland Ltd, Finland

Preliminary examiners
Prof. Arto Lehtovaara, Tampere University of Technology, Finland
Dr. Patrick P.L. Wong, City University of Hong Kong, Hong Kong

Opponent
Prof. Ardian Morina, University of Leeds, United Kingdom

Aalto University publication series
DOCTORAL DISSERTATIONS 144/2015

VTT SCIENCE 118

ISBN 978-952-60-6572-4 (printed)
ISBN 978-952-60-6573-1 (pdf)
ISSN-L 1799-4934
ISSN 1799-4934 (printed)
ISSN 1799-4942 (pdf)
http://urn.fi/URN:ISBN:978-952-60-6573-1

ISBN 978-951-38-8375-1 (printed)
ISBN 978-951-38-8374-4 (pdf)
ISSN-L 2242-119X
ISSN 2242-119X (printed)
ISSN 2242-1203 (pdf)
http://urn.fi/URN:ISBN:978-951-38-8374-4

Unigrafia Oy
Helsinki 2015

Finland

441 697
Printed matter

Aalto University

Abstract

Aalto University, P.O. Box 11000, FI-00076 Aalto www.aalto.fi

Author
Timo J. Hakala

Name of the doctoral dissertation
Water-based boundary lubrication with biomolecule additives on diamond-like carbon and stainless steel surfaces

Publisher School of Chemical Technology

Unit Department of Materials Science and Engineering

Series Aalto University publication series DOCTORAL DISSERTATIONS 144/2015

Field of research Tribology

Manuscript submitted 10 September 2015 **Date of the defence** 29 January 2016

Permission to publish granted (date) 18 November 2015 **Language** English

☐ **Monograph** ☒ **Article dissertation (summary + original articles)**

Abstract

Friction and wear incur high economic costs globally. It has been estimated that approximately 30% of energy is used to overcome friction. Developing new solutions, such as coatings, surface texturing and lubricants, to reduce friction in the boundary lubrication regime can have great importance to global energy savings in the future.

In this thesis, water-based lubricants with hydrophobin protein (HFBI, HFBII and FpHYD5) and quince mucilage additives were used to lubricate engineering materials such as diamond-like carbon (DLC) coatings, stainless steels and plastics. It was found that hydrophobins can form monolayers on stainless steel, diamond-like carbon (a-C:H) and PDMS surfaces. On stainless steel surfaces, HFBI and FpHYD5 layers contain 40-64% water. Increasing the water content in hydrophobin film reduced friction in hydrophobin-lubricated stainless steel vs stainless steel contacts. The same effect was seen in quince mucilage-lubricated UHMWPE vs stainless steel contact.

The lowest friction coefficients (COF) were measured in FpHYD5 hydrophobin-lubricated contacts where COF as low as 0.03 was measured. Quince mucilage-lubricated UHMWPE vs stainless steel reduced the friction coefficient to as low as 0.02. Of all the tests, the lowest friction coefficients (close to 0.01) were measured with HFBI and FpHYD5 hydrophobins in PDMS vs PDMS contacts.

Based on the results, it can be suggested that the requirements for water-based lubrication with biomolecule additives in industrial applications are
- A mild temperature range, T= 4 - 95°C
- Low contact pressures, 0.1-5 MPa
- Hydrophobic surfaces, contact angle of water >90°
- Stable conditions (pH, ionic strength)

In the future, water-based lubricants could be used in, among others, the food and beverage industry, the textile industry and biomedical applications.

Keywords Friction, Wear, Hydrophobins, Quince mucilage, Water-based lubrication

ISBN (printed) 978-952-60-6572-4 **ISBN (pdf)** 978-952-60-6573-1

ISSN-L 1799-4934 **ISSN (printed)** 1799-4934 **ISSN (pdf)** 1799-4942

Location of publisher Helsinki **Location of printing** Helsinki **Year** 2015

Pages 166 **urn** http://urn.fi/URN:ISBN:978-952-60-6573-1

Tekijä
Timo J. Hakala

Väitöskirjan nimi
Timantinkaltaisten pinnoitteiden ja ruostumattoman teräksen rajavoitelu vesipohjaisten voiteluaineiden ja biomolekyylien avulla

Julkaisija Kemian tekniikan korkeakoulu

Yksikkö Materiaalitekniikan laitos

Sarja Aalto University publication series DOCTORAL DISSERTATIONS 144/2015

Tutkimusala Tribologia

Käsikirjoituksen pvm 10.09.2015 **Väitöspäivä** 29.01.2016

Julkaisuluvan myöntämispäivä 18.11.2015 **Kieli** Englanti

☐ **Monografia** ☒ **Yhdistelmäväitöskirja (yhteenveto-osa + erillisartikkelit)**

Tiivistelmä

Kitka ja kuluminen aiheuttavat vuosittain merkittäviä taloudellisia menetyksiä. On arvioitu, että noin 30 % maailman energiankulutuksesta kuluu kitkahäviöihin. Uusien teknologisten ratkaisujen, kuten pinnoitteiden, pinnan teksturoinnin sekä voiteluaineiden, avulla voidaan kitkaa alentaa erityisesti rajavoitelualueella.

Tässä väitöskirjassa on tutkittu erilaisten hydrofobiini-proteiinien sekä kvitten hedelmästä liuotetun liman käytettävyyttä lisäaineena terästen, timantinkaltaisten pinnoitteiden (DLC) sekä muovien vesivoitelussa. Tutkimuksessa havaittiin, että hydrofobiinit kykenevät muodostamaan ruostumattoman teräksen, DLC:n sekä PDMS-muovin pinnoille yhden molekyylin paksuisia kerroksia. Teräksen pinnalle muodostuneessa proteiinikalvossa 40-64 % massasta oli vettä. Veden määrällä hydrofobiinien muodostamassa voitelukalvossa oli positiivinen vaikutus kitkan ja kulumisen alenemiseen teräs vs. teräs-kontaktissa. Myös kvitten limalla voidelluissa polyeteeni vs. teräs - kokeissa havaittiin, että molekyyleihin sitoutuneella vedellä on kitkaa alentava vaikutus.

Alhaisimmat kitkakertoimet (0,03) teräs vs. teräs kontaktissa mitattiin FpHYD5-nimisellä hydrofobiinilla. Alhainen kitka johtui teräskuulan pinnalle syntyneestä proteiinikalvosta. Kvitten limalla pystyttiin saavuttamaan alhaisimmillaan 0,02 kitkakerroin polyeteeni vs. teräs kontaktissa. Kaikista alhaisimmat kitkakertoimet saavutettiin PDMS vs. PDMS - kontaktissa, missä HFBI ja FpHYD5 hydrofobiinit alensivat kitkan lähelle 0,01:tä.

Tulosten perusteella voidaan todeta, että vesipohjaisilla voiteluaineilla on potentiaalia rajavoiteluun teollisissa sovelluksissa esimerkiksi elintarvike-, tekstiili- ja terveysteknologia-aloilla, jos lämpötilat, kontaktipaineet, materiaaliominaisuudet sekä olosuhteet ovat sopivat.

Avainsanat Kitka, Kuluminen, Hydrofobiinit, Kvitten lima, Vesipohjainen voitelu

ISBN (painettu) 978-952-60-6572-4 **ISBN (pdf)** 978-952-60-6573-1

ISSN-L 1799-4934 **ISSN (painettu)** 1799-4934 **ISSN (pdf)** 1799-4942

Julkaisupaikka Helsinki **Painopaikka** Helsinki **Vuosi** 2015

Sivumäärä 166 **urn** http://urn.fi/URN:ISBN:978-952-60-6573-1

Preface

The research work for this PhD thesis was performed between 2010 and 2015 at VTT Technical Research Centre of Finland Ltd. Part of the experiments were carried out at Suzhou Institute of Nano-Tech and Nano-Bionics (SINANO), Aalto University, Technical University of Denmark (DTU), Saarbrücken University and University of Turku. I would like to thank all the personnel at these institutes for their help in conducting the experiments. In addition, I would like to thank the Finnish companies Picosun, Picodeon and Bionavis for their participation in the 'Nanolubrication by functional coatings and biomolecules' project. The research work was conducted in four research projects supported financially by VTT, the Academy of Finland and Tekes – the Finnish Funding Agency for Innovation.

First of all, I would like to thank Aino Helle and Erja Turunen who hired me at VTT and have always encouraged my work. At the beginning of my research career, Aino gave me some good advice and made a few comments that have helped me through these five years with the thesis. I would also like to thank my bosses Maria Oksa and Satu Tuurna at VTT who have always supported and encouraged me. When I arrived at VTT in 2010, I did not know anything about biomimetics or biolubrication. In the beginning, Tiina Ahlroos and Päivi Laaksonen were especially helpful, introducing me to the basics of biomimetics and lubrication.

A big part of the work was carried out in a tribology laboratory at VTT where a real tribology expert, Simo Varjus, taught me how to use different devices and perform the tests carefully to guarantee the reliability of the results. I must admit that sometimes assembling the disc with an error of less than 0.002 mm was frustrating, but at least I can now trust my results.

I would like to acknowledge Prof. Jari Koskinen from Aalto University, Prof. Kenneth Holmberg from VTT and Prof. Feng Li from SINANO. They all have different research backgrounds and they shared their different perspectives on the results.

I would also like to thank my co-authors for their support and advice while writing the thesis and conducting the experimental work. In addition, I would like to thank all my colleagues, especially at MK8 and KT3. Jarkko Metsäjoki must be mentioned. He

has a talent for scanning the samples with electron microscopy and is a professional when it comes to beer brewing.

I spent one and a half years in China while writing my thesis. There, I had the opportunity to work together with the student Shi Zhen at SINANO. He was one of the hardest working people I have ever met and I want to thank him and wish him good luck with his PhD at City University of Hong Kong. Living in Suzhou gave me many new ideas and ways to look at the research results from other perspectives. I hope that getting my PhD will allow me to see more new places and find new adventures.

Finally, I want to thank my mum, dad and little brother Juhani.

Kangasala, September 2015
Timo Hakala 洪天

List of publications

This thesis is based on the following original publications, which are referred to in the text as I-VI (Appendix A). The publications are reproduced with kind permission from the publishers.

I Ahlroos T, Hakala TJ, Helle A, Linder MB, Holmberg K, Mahlberg R, Laaksonen P, Varjus S. Biomimetic approach to water lubrication with biomolecular additives. Proceedings of the Institution of Mechanical Engineers, Part J: *Journal of Engineering Tribology*, 2011; published online: 1-10.

II Hakala TJ, Laaksonen P, Saikko V, Ahlroos T, Helle A, Mahlberg R, Hähl H, Jacobs K, Kuosmanen P, Linder MB, Holmberg K. Adhesion and tribological properties of hydrophobin proteins in aqueous lubrication on stainless steel surfaces. RSC Advances, 2012;2:9867-9872.

III Hakala TJ, Saikko V, Arola S, Ahlroos T, Helle A, Kuosmanen P, Holmberg K, Linder MB, Laaksonen P. Structural characterization and tribological evaluation of quince seed mucilage. *Tribology International*, 2014;77:24-31.

IV Hakala TJ, Laaksonen P, Helle A, Linder MB, Holmberg K. Effect of operational conditions and environment on lubricity of hydrophobins in water based lubrication systems. *Tribology,* 2014:8(4):241-247.

V Hakala TJ, Metsäjoki J, Granqvist N, Milani R, Szilvay GR, Elomaa O, Deng M, Zhang J, Li F. Adsorption and lubricating properties of HFBII hydrophobins and diblock copolymer poly(methyl methacrylate-b-sodium acrylate) additives in water-lubricated copper vs. a-C:H contacts. *Tribology International*, 2015;90:60-66.

VI Shi Z, Hakala TJ, Metsäjoki J, Szilvay GR, Li F. Lubrication of aluminium versus diamond-like carbon contacts with hydrophobin proteins. Accepted to be published in Surface Engineering.

Author's contributions to the publications

I Timo J Hakala wrote the introduction, participated in planning the contact angle measurements and analysed the results in the discussion. Tiina Ahlroos was responsible for the tribological experiments and submission. Riitta Mahlberg performed contact angle measurements.

II Timo J Hakala planned the experiments, performed the tribological experiments, analysed the results and was responsible for writing the manuscript. Päivi Laaksonen carried out QCM and ellipsometer experiments. Riitta Mahlberg performed FTIR experiments. Vesa Saikko carried out CTPOD experiments

III Timo J Hakala planned and performed the tribological experiments, which were carried out with a pin-on-disc tribometer, and analysed the results. Päivi Laaksonen was responsible for writing the manuscript. Vesa Saikko carried out CTPOD experiments

IV Timo J Hakala planned and performed the experiments, analysed the results and was responsible for writing the manuscript. Päivi Laaksonen guided in performing the ellipsometer experiments. Suvi Arola helped in mucilage characterization.

V Timo J Hakala planned and performed the experiments, analysed the results and was responsible for writing the manuscript. Niko Granqvist performed the SPR experiments together with Timo J. Hakala. Roberto Milani produced the polymer lubricant for experiments. Geza R. Szilvay instructed about the HFBII proteins. Mengmeng Deng helped to operate ICP-CVD coating deposition device. Simo Varjus performed part of the tribological experiments.

VI Timo J Hakala planned the tribology experiments, analysed the tribology results and wrote the tribology part of the manuscript. Zhen Shi deposited a-C:H coating together with Timo J. Hakala, arranged the coating characterization and was responsible for writing the manuscript. Geza R. Szilvay

instructed about the HFBII proteins. Jarkko Metsäjoki carried out SEM analysis. Simo Varjus performed the tribological experiments.

Aino Helle, Tiina Ahlroos, Markus B. Linder, Kenneth Holmberg, Petri Kuosmanen, Hendrik Hähl, Karin Jacobs, Feng Li, Oskari Elomaa and Jianjun Zhang read the manuscripts and gave comments.

Contents

List of symbols

a-C:H	Hydrogenated amorphous carbon type of DLC coating
AFM	Atomic Force Microscopy
COF	Coefficient of Friction or Friction Coefficient
Da	Dalton, atomic mass unit, which is usually used to describe the size of biomacromolecules
DLC	Diamond-like carbon coating
IEP	Isoelectric point
MDa	Megadalton, 1000000 Da
OWLS	Optical Waveguide Lightmode Spectroscopy
PDMS	Polydimethylsiloxane
QCM	Quartz Crystal Microbalance
RP-HPLC	Reversed Phase High Performance Liquid Chromatography
SEM	Scanning Electron Microscopy
SFB	Surface Force Balance
SPR	Surface Plasmon Resonance
UHMWPE	Ultra-High Molecular Weight Polyethylene

1. Introduction

Environmental issues such as severe pollution (Fig. 1) and global warming are the result of increased use of fossil fuels and energy consumption. There are two ways to reduce pollution: 1) to find alternative, cleaner methods to produce energy and 2) to reduce the amount of energy needed. It has been suggested that about 15-35% of the world's energy is used to overcome friction (Holmberg, 2012, 2013, 2014). Thus, new ways to reduce friction and wear play an important role in decreasing the overall energy consumption. Friction and wear can be reduced by new low-friction, low-wear coatings, surface treatments and new lubrication solutions (Cai et al., 2013). One new possible lubrication solution includes a biomimetic approach to lubrication (Holmberg et al., 2012), which means learning from low-friction lubrication systems in nature and transferring these mechanisms to engineering lubrication systems.

Figure 1. Pollution is a severe problem, especially in China. Picture taken in Suzhou Industrial Park in 2014.

Lubrication can be improved by developing new solutions, such as coatings, surface texturing and lubricants (Fig. 2) that can reduce friction, especially in the boundary lubrication regime. Traditionally, oil has been the most used lubricant, but the fact that the world is running out of natural resources, such as oil, is a motivator to find alternative lubricants. In addition, there are several application areas in which oil cannot be used as a lubricant due to its harmful additives and the remnants it leaves on the final products. The use of oil also brings with it other problems such as waste treatment and harmful leakages.

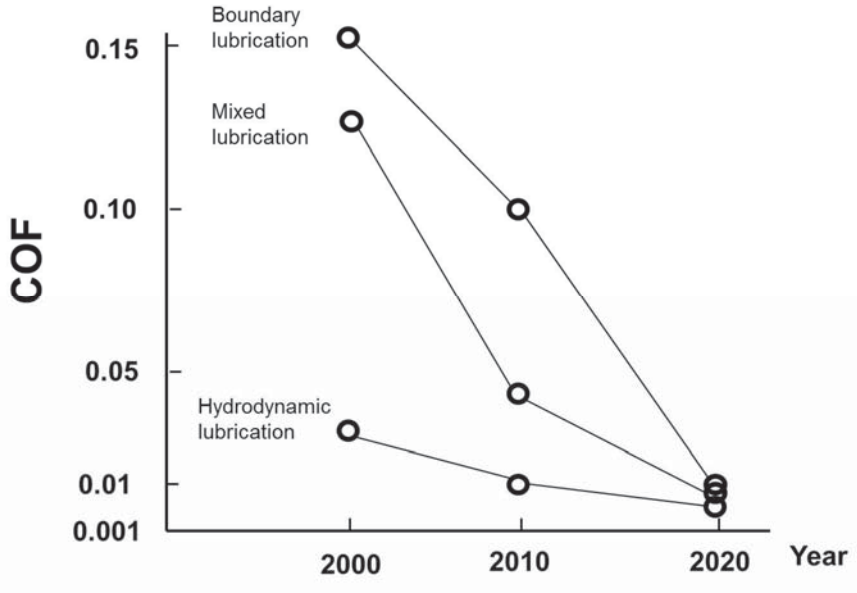

Figure 2. The development of lubricants has reduced friction in different lubrication regimes, and this trend will continue in the near future (modified from Holmberg, 2012).

Water is a fascinating option for a lubricant due to its low viscosity, good thermal conductivity and environmental friendliness. However, water is corrosive for common engineering materials, e.g. steel, and it has poor boundary lubrication properties. The temperature range for water lubrication is also limited compared with the use of oil because of evaporation. Nowadays, water-based lubricants are mainly used in low temperature applications that operate in a hydrodynamic lubrication regime, such as water-lubricated bearings.

Additives can be used to improve wetting, extreme pressure, and the corrosion and lubricating properties of water (Mortier et al., 1997). Improvements in boundary lubrication have attracted great interest from scientist in the past few years. Different additives, such as graphite (Chen et al., 2011), nanodiamonds (Elomaa et al., 2103; Kato et al., 2009), copper-containing nanoparticles (Zhang et al., 2012), ionic liquids (Phillips et al., 2004; Omotowa et al., 2004), amines, glycols (Tomala et al., 2010), polymers (Chawla et al., 2009), surfactants (Briscoe et al., 2006) and biomolecules (Coles et al., 2010; Lee et al., 2005), have been studied. According to patents, new water-based lubricants are proposed for use to lubricate different applications, such as railway switches, conveyors in the beverage industry, textile-processing machines and machining optical glass (N.A., 1980, Ruhr et al., 2004).

1.1 Lubrication regimes

Lubrication can be divided into three regimes: 1) boundary lubrication, 2) mixed lubrication and 3) hydrodynamic lubrication. In the boundary lubrication regime, contacting surface asperities carry the load and only lubricating layers with a thickness of some nanometres can reduce wear and friction. The boundary lubrication (Fig. 3) regime is achieved when the sliding velocity and lubricant viscosity are low or the surface roughness and normal force are high. Water has poor boundary and mixed lubrication properties, but due to its low viscosity it is a fairly good lubricant in the hydrodynamic lubrication regime. Unlike oils, water does not form solid-like layers under high contact pressures and thus it does not help prevent impact wear.

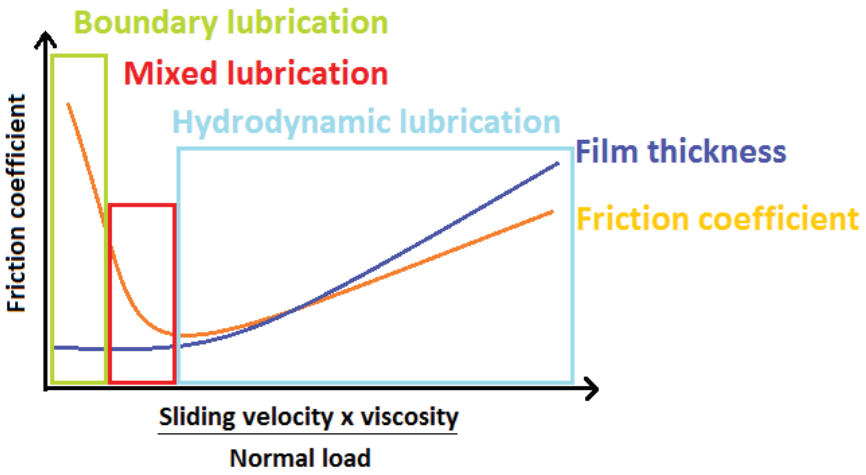

Figure 3. Stribeck's curve and thickness of lubricating film vs lubrication regimes in traditional oil lubrication

Boundary lubrication can be divided further into four regimes (Stachowiak and Batchelor, 2005):

1. Low temperature and low load
2. Low temperature and high load
3. High temperature and medium load
4. High temperature and high load

In the first two boundary lubrication regimes, the lubricating films are formed by surface-adsorbed molecules, called the adsorption lubrication regime (Stachowiak and Batchelor, 2005). These molecules adhere to the surfaces via physical or chemical bonds. The molecules that adhere via physical bonds are usually more easily removed from the surface due to shear and increased temperature. Thus, lubrication with these kinds of additives is limited to low contact pressures and has not gained much interest from scientist before (Fig. 4). In the third and fourth regimes, the lubricity is provided by lubricant additives that can react with the surface. These additives often contain sulphur, chlorine or phosphorus.

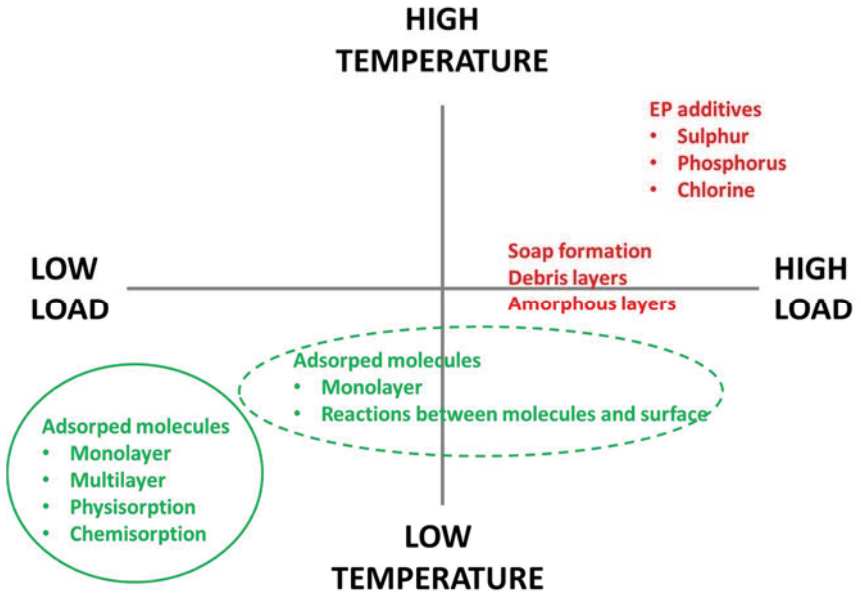

Figure 4. Lubrication mechanisms at different temperatures and under different normal loads (based on information from Stachowiak and Batchelor)

1.2 Boundary lubrication in nature

The interest in biomimetic lubrications comes from nature, where several examples of self-healing, low-friction lubrication systems can be found, such as mammal joints, lungs and eyes for instance (Neville et al., 2007; Dedinaite, 2012). The lubrication systems are complex including multilayer structures and fluid where lubrication is a result of several different molecules, including charged macromolecules and phospholipids. These highly stabilized lubrication systems with superlow friction coefficients below 0.01 can be measured in the boundary lubrication regime (Klein, 2012; IMechE; Dedinaite, 2012). Compared with oil-lubricated contacts, the friction coefficients are approximately 0.1 in the boundary lubrication regime.

The differences compared with man-made lubrication systems are that the lubricated materials are softer than industrially used materials, e.g. steel, the contact pressures and sliding speeds are relatively low, and the lubrication is water based.

1.3 Lubricating biomolecules

In nature, water-based lubrication systems include biomolecules, such as proteins, carbohydrates and phospholipids, and can remain low friction and low wear for close to 100 years, as seen in, e.g., mammal joints (Dedinaite, 2012). The adhesion forces of biomolecules to solid surfaces are high compared with traditional surfactant molecules, which can widen the adsorption lubrication regime to higher contact pressures. In addition, the biomolecules can have superior low friction properties compared with traditional surfactant molecules (Klein, 2012). At high temperatures, biomolecules can denature, which limits their use to low temperatures.

1.3.1 Proteins

Proteins are biopolymers consisting of amino acid units bonded by amide or peptide bonds. The properties of the molecule depend on the existing amino acids as well as primary, secondary, tertiary and quaternary protein structures (Hart et al., 2003; Nelson et al., 2008).
Lubricating glycoproteins in nature, such as mucin, aggrecan and lubricin, are relatively big: their size is usually a few MDas. The layers they form on solid surfaces can be sterically and electrically repulsive. Due to the big hydrophilic brush-like structures, they are able to bind large amounts of water (Lee et al., 2015; Zappone et al., 2007; Yakubov et al., 2009). While the hydrophilic part of the molecules binds water, the hydrophobic part can provide good adhesion to solid surfaces. Strong adhesion to surfaces prevents the molecules from shearing away easily from a surface under mechanical contact. Strong adhesion also helps molecules to be re-adsorbed onto the surface after being sheared away (Coles et al., 2010).

The structures of glycoproteins have inspired scientists to develop a similar type of polymer molecules. Unlike glycoproteins, the polymer molecules can be attached to the substrate via covalent bonding, which improves their load-carrying properties. With chemically attached polyzwitterionic brushes, friction coefficients as low as 0.0004 at contact pressure 7.5 MPa have been achieved (Chen et al., 2011).

1.3.1.1 Hydrophobins

Hydrophobins are small amphiphilic proteins produced by filamentous fungi that consist of about 100 amino acids. Hydrophobins are the most surface-active proteins known so far. Fungi use hydrophobins to modify their surface properties and control the interactions with their environment. For example, hydrophobins reduce the surface tension at the air-water interface to make it easier to breach the water-

air interface during their growth. On other hand, the hydrophobins can also make the surface of fungus more hydrophobic in an air atmosphere (Wösten et al., 1999; Sunde et al., 2008). Hydrophobins are divided into Classes I and II (Linder, 2004). Class II hydrophobins are suitable for lubricant additives in aqueous lubrication because they are water soluble. Class II has only been found in Ascomycetes, while Class I hydrophobins have also been found in Basidiomycetes (Linder et al., 2005).

The structure of Class II hydrophobins, such as HFBI and HFBII, consists of an aliphatic hydrophobic part and a hydrophilic part (Fig. 5). Inside the protein, there are four disulphide bridges that make the protein structure very stable against environmental changes. To act as a lubricant, additives in industrial applications, hydrophobins, have three important properties: 1) self-assembly and strong adhesion to solid surfaces, 2) high water binding ability and 3) stable structure that can withstand high temperatures (up to 90°C) without breaking (Askolin et al., 2006; Hakanpää et al., 2004).

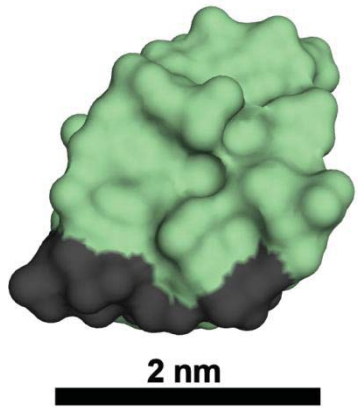

Figure 5. Structure of an HFBII hydrophobin protein. The green colour indicates the hydrophilic-exposed surface and the dark grey colour at the bottom indicates the hydrophobic patch. The diameter of the hydrophobic patch is approximately 2.2 nm. (Structure from Protein Data Bank entry 1R2M; Hakanpää et al., 2004)

The film-forming properties of hydrophobins are well known. They can form monolayer films on both air-water and water-solid interfaces without changes in their structures (Linder et al., 2005). Due to their amphiphilic structure, they can make hydrophobic surfaces more hydrophilic and hydrophilic surfaces more hydrophobic. The cationic and anionic properties also affect the adsorption and alignment of the hydrophobins on solid-water interfaces (Grunér et al., 2012). In solutions,

Class II hydrophobins form dimers and at high concentrations (10 mg/ml) they can form tetramers (Linder et al., 2005).

Earlier studies have shown that Sc3 hydrophobins are able to reduce the contact angle of water and friction in dry conditions measured on polymer surfaces in nanoscale by AFM (Misra et al., 2006). More recent studies have shown that HFBI and FpHYD5 hydrophobins are able to reduce friction significantly in water-based lubricated PMDS/PMDS contact (Lee et al., 2015). In both systems, the friction coefficients dropped to 0.01-0.02. Higher friction coefficients (0.11-1.9) were measured between two HFBI layers by surface force balance (SFB). The friction was dependent on the environment and substrate hydrophobicity, which affects the alignment of the molecules (Goldian et al., 2013).

More than 70 different hydrophobins are found in nature (Linder et al., 2005). In this study, three of these have been studied, namely HFBI, HFBII and FpHYD5. HFBI and HFBII are Class II hydrophobins, which have different amino acid sequences, and their role in the biological function is different in nature, e.g. HFBII is found in spores while HFBI is found in the mycelium of vegetative cultures (Linder et al., 2005). FpHYD5 is a hydrophobin that has a similar structure to HFBI and HFBII except that it has a glycan group (mass 1695 Da) attached to its hydrophilic side (Sarlin et al., 2012).

The isoelectric points of hydrophobins are important because the environment affects the electric charges of the proteins, and the interaction between the proteins and the surface. Thus, the pH can affect the hydrophobin adsorption and film structure on solid surfaces.

1.3.2 Carbohydrates

Carbohydrates are molecules with combined hydroxyl groups and carbonyl groups. Carbohydrates can be divided into monosaccharides, oligosaccharides and polysaccharides depending on their structure. Monosaccharides are the smallest carbohydrate compounds, which means that they cannot be hydrolysed into smaller units. Oligosaccharides consist of at least two monosaccharides, and polysaccharides can contain thousands of monosaccharide units. Cellulose is one example of a polysaccharide (Hart et al., 2003; Nelson et al., 2008).

The high OH-group content of carbohydrate molecules makes them water soluble and highly hydrated (Stokes, et al., 2011). Their lubrication properties are dependent on the shape of the molecule, which affects lubricant rheology, the ability to entrain the contact zone and the adsorption properties (Garrec and Norton, 2012b). Surface hydrophilicity has been observed to improve spreadability of some carbohydrates on surfaces, though sometimes their adsorption is expected to occur via hydrophobic interactions (Zinoviadou et al., 2008; Stokes et al., 2011).

Some carbohydrates can retain their structure and properties in a wide range of environmental condition such as a temperature range of 25-70˚C and pH values of 2-9, but bacterial growth is a problem and thus industrial use in lubrication will be limited.

1.3.2.1 Quince mucilage

Quince mucilage is extracted from the seeds of the quince fruit. When dry seeds are immersed in water, the mucilage is self-formed at room temperature. The quince mucilage contains water-soluble cellulose and other carbohydrates (Vignon and Gey). The cellulose consists of cellulose nanofibrils and hemicelluloses such as glucoronoxylans. The mucilage has several beneficial properties such as a large amount of swelling and a slippery appearance, probably due to the hydration of the carbohydrate structures, which has been observed to enhance lubrication in water-based systems and lower friction to a level of 0.005 measured between the mucilage surface and glass (Li J. et al. 2012). As the bacteria use carbohydrates as a nutrient, the problem with the quince mucilage is the bacterial growth, which contaminates the lubricant relatively quickly if the bacterial growth is not restricted by chemicals.

1.3.3 Phospholipids

Phospholipids are similar to fats and oils with regard to their molecular structure. The phospholipid molecules consist of a non-polar tail and polar headgroup. Phospholipids prefer to arrange membrane structures, which have an important role in, for example, biological systems.
The amphiphilic molecular structure of phospholipids makes them able to adsorb on different surfaces and form multilayer structures (Hills, 2012; Trunfio-Sfarghiu et al., 2008; Goldberg et al., 2011). Although phospholipids are not easily water soluble, they have been used in water-based lubrication systems as a lubricant additive. Their solubility in water requires higher temperatures (~ over 40 ˚C) or carrier molecules, such as lubricin, which improve their solubility in water (Hills, 2002). The lubrication properties of phospholipids are highly dependent on pH and ionic strength (Dekkiche et. al., 2010). Phospholipids are one of the few biomolecules that have been tested to lubricate engineering materials and still been observed to provide low friction under high contact pressures (Goldberg et al. 2011; Hills, 1995).

1.3.4 Buffer solutions

As biomolecules are sensitive to changes in the environment and their properties depend highly on pH and ionic strength, buffer solutions are used. Buffer solutions

are used to stabilize the pH and ionic strength to a chosen level. pH affects the electric charges in molecules, and ionic strength can affect the interaction between molecules as well as the water-binding ability and structure of the lubricating layer (Lee et al., 2005). Buffer solutions consist of small molecules and ions and can have a certain ability to lubricate in themselves. For example, anions can form hydrated structures and increase the local viscosity between sliding surfaces and thus lubricate the contact more effectively than water (Garrec and Norton, 2012a).

1.4 Boundary lubrication mechanisms

Biomolecules can form different kinds of structures on solid surfaces and lubricate the contacts via different mechanisms in the boundary lubrication regime.

1.4.1 Hydration lubrication

Most of the glycoproteins and polymers that form monolayers on surfaces are expected to lubricate solid surfaces via hydration lubrication. In hydration lubrication, the sliding occurs between the hydrophilic parts of the two molecule layers that are adhered to both sliding surfaces (Fig. 6), and low friction is related to the bound water and its fluidity (Klein, 2004).

Lubricating molecules prevent the water from escaping from the contact zone. Under high-contact pressures, the water molecules move between the liquid and the surface-attached molecules. This phenomenon provides low friction in lubrication under higher contact pressures. Due to the nature of water, i.e. that the viscosity is not pressure dependent, its lubrication properties differ significantly from those of oil. The lubricating macromolecules usually contain large carbohydrate structures and thus they have the ability to bind high amounts of water (Roba et al., 2009; Yang et al., 2006; Stokes et al., 2011; Li J. et al.; 2012).

Other important properties of lubricating macromolecules are their strong adhesion to surfaces, repulsion between molecule layers, and lateral forces in the layer and surface. All these properties affect the stability and structure of the lubricating film (Stachowiak and Batchelor, 2005; Klein, 2006). The hydration lubrication mechanism can be disturbed by the bridging of molecule layers adsorbed on both sliding surfaces. The bridging occurs most easily with neutral molecules. The charged molecules have stronger repulsion to each other, which prevents the bridging effectively (Klein, 2003).

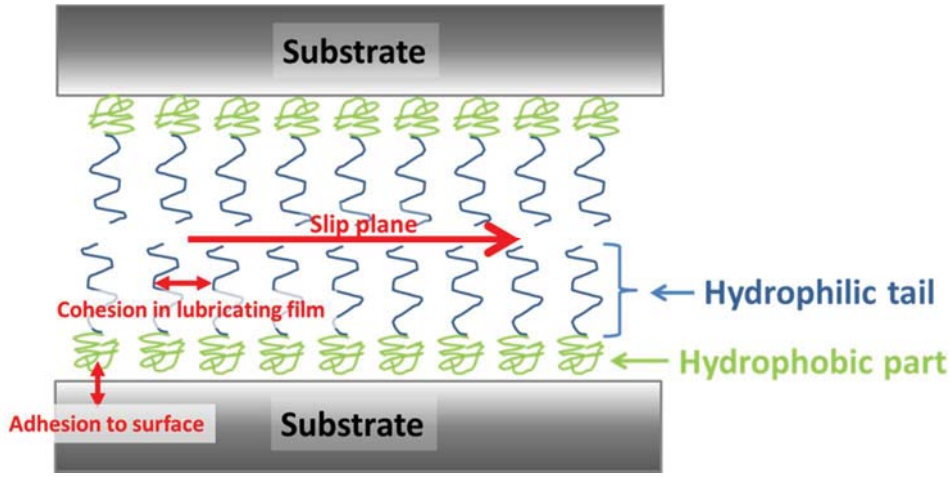

Figure 6. Schematic picture of hydration lubrication where the slip plane is located between adsorbed layers. Strong adhesion to the surface and cohesion inside the lubricating film increase the load-carrying properties of the lubricant film.

In some cases, the hydration lubrication can occur between the lubricating molecules and the substrate. This has been shown with polar surfactants where the sliding occurred between the polar headgroups and substrate via hydration lubrication (Briscoe et al., 2006).

1.4.2 Other boundary lubrication mechanisms

In addition to hydration lubrication, there are different mechanisms to explain low friction achieved by biomolecule additives in the boundary lubrication regime. These mechanisms are viscous boundary lubrication, slip plane between adsorbed layers, slip effect on the surface and graphitization.

In viscous boundary lubrication, friction is dependent on the molecule concentration in the lubricant. In this mechanism, biomolecules form multilayer films between the sliding surfaces, and increasing the concentration increases the film thickness (Fig. 7). An increase in film thickness reduces the local shear rate and shear stress and thus reduces friction in the sliding contact (Yakubov et al., 2009). An increase in local viscosity may also have hydrodynamic effects between two sliding surfaces.

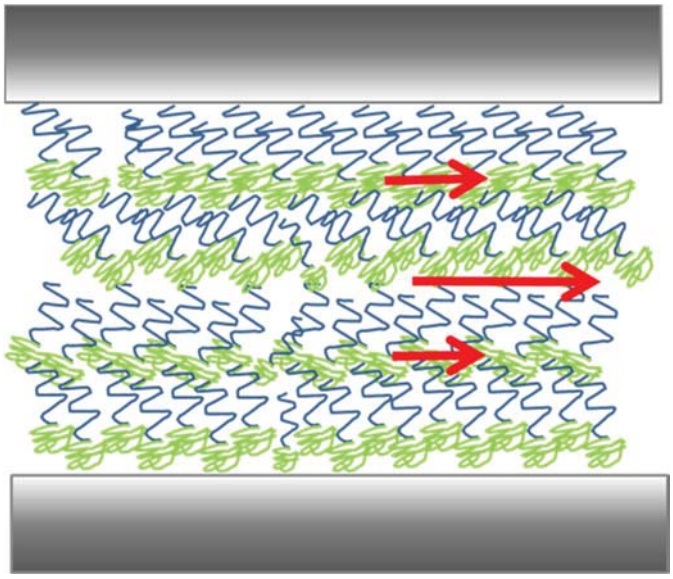

Figure 7. Water-based lubrication improved with biomolecule additives. Biomolecules are attached to the surfaces and bind water between two sliding surfaces.

Biomolecules mainly consist of carbon, nitrogen, oxygen and hydrogen. At high temperatures and pressures, biomolecules can degrade and form graphite on the sliding surfaces (Liao et al., 2011). This phenomenon depends on the surface materials, because the reaction to form graphite requires a catalytic material, e.g. a transition metal such as cobalt. In tribological contact, fresh surfaces are formed that can act as a catalyst for reactions. Graphite is a solid lubricant and known to lubricate well in humid conditions.

1.5 The effect of the environment

Environmental factors, such as ionic strength, pH and temperature, can affect the adsorption and film structure of lubricating films formed of biomolecules on solid surfaces (Lee et al., 2005; Madsen et al., 2014). The film structure affects, for example, the repulsion forces between opposing molecule layers, the cohesive forces in lubricating film, the adhesion forces and the amount of hydration.
It has been found that low friction with brush-like molecules is achieved when hydrophilic brushes protrude away from the solid surface, which happens, e.g., in water (Pettersson et al., 2008). The film may compress due to changes in pH and ionic strength, which can increase friction. There are also examples where the ionic strength affects the film structure but does not affect the lubricating ability of the biomolecule layer, i.e. the friction coefficient, but the wear of the layer at higher normal loads (Macakova, 2011). The wear may be increased due to reduced co-

hesive forces in the film, changes in adhesion forces or an increased number of entanglements in the contact.
It has been found that the larger the area of one molecule on a solid surface, the lower the internal cohesion inside the lubricating film. This has an effect on the adhesion forces between the film and the substrate (Heuberger, et al., 2005; Lee et al. 2015). Stronger adhesion between the molecule and solid surface increases the load-carrying capacity by preventing the shearing away of lubricating film.

High temperatures or shear forces can cause denaturation of the biomolecules. This affects their lubricity because of the formation of compact and well-adhered protein layers onto the sliding surfaces, which have a lower level of hydration (Heuberger et al., 2005; Fang et al., 2007). Unfolded molecules can have a lower water-binding ability than molecules in a natural state.

1.6 Water-based lubricant vs oil

Oil is still the most used lubricant in many applications. It has relatively good boundary lubrication properties and several other benefits compared with water-based lubricants. Oil is not as sensitive to aging and temperatures as water-based lubricants. However, the friction coefficients in the boundary lubrication regime can be magnitudes lower in water- and biomolecule-lubricated contacts than in oil-lubricated contacts (Stachowiak and Batchelor, 2005; Lee et al., 2005; Harvey et al., 2011).

A general comparison between oil and water-based lubricants in the boundary lubrication regime is difficult to make because the lubrication performance is highly dependent on the lubricated materials. For example, oil lubricates hydrophilic vs hydrophilic contacts well but water lubricates hydrophilic vs hydrophobic contact better (Borruto et al., 1998). Water with lubricant additives is found to lubricate hydrophilic-hydrophobic contacts most effectively (Pawlak et al., 2011). Thus, surface wettability has a strong effect on lubrication by water-based lubricants. When lubricating metallic materials under high contact pressures, the oil additives containing reactive groups of sulphur, phosphorus and chlorine can react chemically with the surface and form very thin easily shearing layers that prevent excess wear (Stachowiak and Batchelor, 2005). Most biomolecules are physically adsorbed and cannot form this type of chemically reacted layers. Thus, their ability to lubricate is limited to low-contact pressures.

1.7 Aim of the work

The aim of this thesis is to study the potential of biomolecules for use as lubricant additives in water-based lubrication for materials used in engineering applications in the future (Fig. 8). It requires understanding of the connection between film formation and lubrication performance as well as determining the conditions where low friction and wear can be obtained. The performance of biomolecules in lubrication has been studied with artificial materials before but not with engineering materials such as stainless steel and diamond-like carbon coatings.

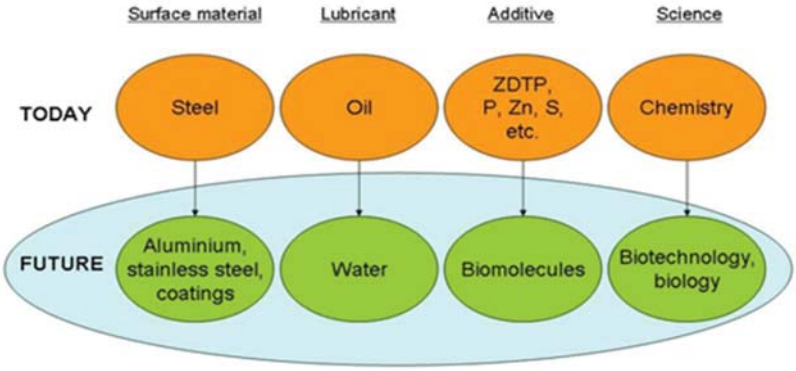

Figure 8. Possible changes in lubrication systems toward environmentally friendly lubrication in the future may include utilizing biotechnology and water (Publication I).

The scientific hypothesis is that biomolecule additives can form lubricating layers on engineering materials and reduce friction in the boundary lubrication regime compared to traditional lubricants such as mineral oil with extreme pressure (EP) additives.

By understanding the molecule structure and properties and their relation to lubrication performance, new lubricant additives with tailored properties can be developed in the future. In addition, new lubrication systems could be designed by taking account of the requirements for operational conditions, environment and lubricated materials.

2. Experimental

2.1 Materials

2.1.1 Lubricants

The hydrophobins (HFBI, HFBII and FpHYD5) and quince mucilage lubricants were all produced at VTT Technical Research Centre of Finland. The lubricants and their most important properties are listed in Table 1.

Table 1. Lubricants and their main properties related to lubrication performance

Lubricant	**Molecule mass (g/mol)**	**Isoelectric point**	**Properties**
HFBI	7540	5.7*	Strong adhesion to solid surfaces
HFBII	7200***	6.7**	Strong adhesion to solid surfaces, lower cost to produce than HFBI
FpHYD5	9210	4-5	Higher water-binding ability compared with HFBI
Quince mucilage	-	-	High water-binding ability

***Wang et al. 2010, **Kisko et al., 2008, ***Staminirova et al., 2013

Hydrophobins were produced using recombinant strains of Trichoderma reesei and purified by two-phase extraction and reversed phase high-performance liquid chromatography (RP-HPLC) as described previously (Linder et al., 2004; Sarlin et al., 2012). The proteins were dissolved in different buffer solutions and water for the experiments.

Quince seeds (Cydoniaoblonga) were separated from fresh fruit, dried in an ambient temperature and stored in dry conditions before use. Mucilage was extracted from the quince seeds by immersing the seeds in fresh water. The seeds were weighed and kept in a 40 mg/ml concentration in deionized water overnight. The solution was decanted and the extraction repeated once more. The extract contained some solid impurities originating from the seeds, which were removed by gentle centrifugation and filtration through three layers of cotton gauze. The mucilage was stored at 4°C. The dry mass of the mucilage, 0.55 m%, was determined by lyophilization. The mucilage could also be lyophilized and re-dispersed in deionized water to gain a higher concentration. The mucilage was washed with ethanol as described earlier (Vignon and Gey, 1998). Concentrated mucilage was dispersed in three parts ethanol and centrifuged. The excess ethanol was removed and the mucilage dialyzed and freeze-dried. Part of the mucilage was freeze-dried without dialysis and used in the lubrication studies (Publication III).

The buffer solutions used in the experiments are listed in Table 2 (Publication IV).

Table 2. Buffer solutions used in the adsorption and tribology experiments

pH	**Ionic Strength**	**Buffer solution**
pH 3	50 mM	50 mM citric acid – sodium citrate
pH 5	50 mM	50 mM sodium acetate
pH 7	50 mM	50 mM tris(hydroxymethyl)aminomethane – HCl
pH 9	50 mM	50 mM glycine-sodium hydroxide
pH 5	500 mM	500 mM sodium acetate

2.1.2 Materials for tribological experiments

Tribological experiments were carried out with pins and discs manufactured from different materials (Fig. 9). The materials and their properties are listed in Table 3.

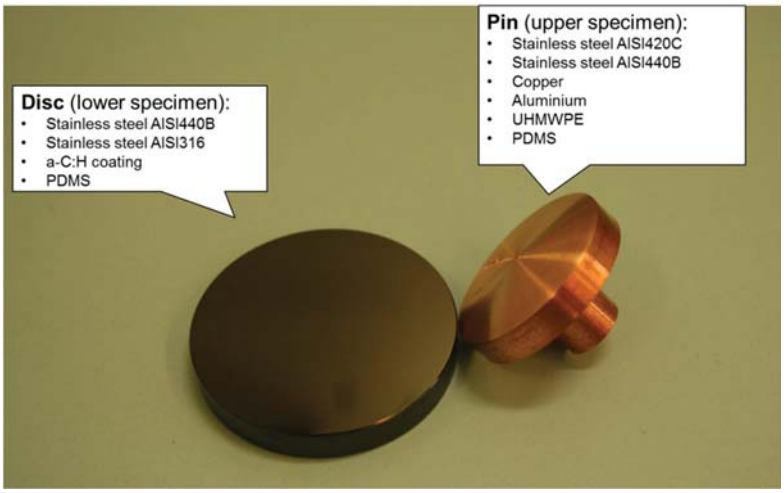

Figure 9. Discs and pins for tribotests

Table 3. Material properties of pins and discs

Pin/disc material	Surface roughness (R_a)	Hardness
AISI440B	0.05 µm or lower	567 HV1
AISI420C		927 ± 22 HV1
a-C:H	below 0.05 µm	20.3 GPa (nanohardness)
AISI316	0.01 µm	200 HV1
Aluminium	0.05 µm or lower	82.1 HV1
Copper	0.44 ± 0.03 µm	96.0 ± 1.1 HV1,
UHMWPE	Not measured	Not measured
PDMS	Not measured	Not measured

Stainless steel spheres (AISI420C) with a diameter of 10 mm were purchased from a commercial source. The spherical-shaped pins with a radius of 50 mm were made of AISI440B, copper and aluminium. PDMS pins were spherical shaped. The ultra-high molecule-weight polyethylene pins (UHMWPE) were used in the POD and CTPOD experiments. The UHMWPE pins had flat contact surface areas of 12.6 mm^2 (POD) and 63.6 mm^2 (CTPOD). An unused surface of the pin was used in each experiment.

Stainless steel (AISI440B) discs were purchased from a commercial source and then polished in-house at VTT. The diameter of the discs was 40 mm and the surface roughness R_a value was 0.05 µm or better. The same disc was used in

several tests and before each tests it was cleaned by ultrasonic washing in petroleum ether and in ethanol, for 5 minutes each.

The a-C:H coatings were deposited on stainless steel discs by ICP-CVD. The coatings had a total thickness of approximately 1 µm. The coating thickness included a SiN_x adhesion layer with a thickness of 300 nm.

2.2 Adsorption measurements

To study the adsorption and film-forming ability of hydrophobin on stainless steel and other surfaces, the experiments were carried out using the following methods: a quartz crystal microbalance with dissipation monitoring (QCM-D; Publication II), an ellipsometer (Publications II and IV), surface plasmon resonance (SPR; Publication V) and optical waveguide lightmode spectroscopy (OWLS; Hakala and Lee, 2011). The ellipsometer, SPR and OWLS measure the dry mass of adsorbed molecules on solid surfaces while QCM-D also takes account of the mass of bound water

Adsorption measurements by QCM-D (Publication II)
A quartz crystal microbalance with dissipation monitoring (QCM-D) was used for simultaneous measurement of frequency and dissipation to follow the binding of proteins to stainless steel sensors (SS2343; Biolin Scientific Sweden). First, the sensor chips were cleaned in a standard UV/ozone chamber for 10 min and then exposed to a hot $H_2O/NH_3/H_2O_2$ mixture (1 : 1 : 5) for 10 min, followed by rinsing with Milli-Q water. The protein adsorption measurements were carried out by injecting 1 ml of protein solutions into either Milli-Q water (Millipore, US) or 50 mM sodium acetate (Sigma-Aldrich, US) using a flow of ~ 0.1 ml/min to the chamber and following the frequency and dissipation responses.

Adsorption measurements in liquid by ellipsometry (Publication II)
Ellipsometric measurements were carried out using a multiwavelength ellipsometer operated at a single wavelength of 532 nm. The device was set up in a PCSA (polarizer-compensator-sample-analyser) configuration with an angle of incidence of 65° to the surface normal. A stainless steel QCM-D sensor was placed in a home-made liquid cell that was filled with the corresponding liquid. After equilibration of the surface, the protein solution was injected into the cell by hand with a syringe. Before performing the experiments, the sensor was cleaned in a similar manner to the QCM-D experiments. The ellipsometric angles D and Y were recorded continuously over time via the nulling ellipsometry principle in two zones (Tompkins and Irene, 2005).

Adsorption measurements of dry films by ellipsometry (Publication IV)
The adsorbed amount of protein was estimated by measuring the effective film thickness using a multiwavelength ellipsometer operated at a single wavelength of 532 nm. A polarizer-compensator-sample-analyser configuration was employed. Data were collected between the angle of incidence from 45 to 83° reflected from a polished stainless steel surface that had been immersed in the liquid of interest for 60 min, rinsed and dried. The experiments were carried out at 40-45% relative humidity and a temperature of 20.4°C. The film thickness results were obtained by fitting the measured data to an optical box model consisting of stainless steel and the protein film. The complex refractive index for the stainless steel was measured from a clean surface, and a constant refractive index of 1.460 was assumed for the protein film (Arwin, 1998). The absolute amount of adsorbed protein for which the effective thickness was calculated was determined with de Feijter's formula (de Feijter et al., 1978).

Surface Plasmon Resonance (SPR; Publication V) is a surface-bound optical phenomenon that can be used to study interactions and optical layer properties, such as the refractive index (RI) and thickness (d) of materials. While commonly applied in biomolecular screening (Rich and Myszka, 2010), new methods such as the now utilized Multi-Parametric surface plasmon resonance (MP-SPR) allow us to characterize interactions between biomolecules and surfactants with different coatings (Granqvist et al., 2013; Orelma et al., 2011).
The MP-SPR instrument together with gold and copper-coated sensors was used in the measurements. The a-C:H coating was deposited on the gold sensor as described in Section 2.1. The measurements were performed at 20°C using a flow rate of 30 µL/min. The HFBII interaction between a-C:H and Cu surfaces was studied in pure water (Milli-Q) and in an acetate buffer (50 mM sodium acetate, pH 5.0). Each interaction experiment consisted of a series of HFBII or polymer injections with concentrations of 3.9, 15.6 and 62.5 µg/mL respectively. An exception to this was a polymer interaction with a Cu surface, which was performed with a single injection of 250 µg/mL. The amount of HFBII was calculated from the SPR signal level after all the injections, and the initial slope of the first HFBII sample injection was used to calculate the relative interaction rate. The a-C:H coating thickness was determined using SPR Navi LayerSolver v.1.0.2.2.4.

Adsorption experiments by Optical waveguide lightmode spectroscopy (OWLS)
OWLS was used to study the adsorption of the proteins on polydimethylsiloxane (PDMS) surfaces. At the inlet of OWLS, hydrophobin sample solution was injected into the device and allowed to mix with the flow of buffer solution (50 mM sodium acetate buffer, pH 5), finally reaching the target surfaces. Adsorption of the proteins was determined as the change in refraction index in the vicinity of the surfaces (Hakala and Lee, 2011).

2.3 Tribological experiments

Tribological experiments were carried out with a pin-on-disc (POD) tribometer designed and manufactured at VTT Technical Research Centre of Finland (Fig. 10; Publications I-V). Ultra-high molecular weight polyethylene (UHMWPE) vs stainless steel experiments were carried out by POD (Publication III) and Circular translation pin-on-disc (CTPOD; Publications II-III; Saikko, 2006). In these experiments, a flat-on-flat type of contact was applied. Polydimethylsiloxane (PDMS) vs PDMS reference tests were carried out with a pin-on-disk tribometer (CSM Instruments, software version 4.4 M, Switzerland). In these tests, 5 N normal load and sliding velocity 50 mm/s were applied (Hakala and Lee, 2011).

In POD tests, different test parameters (normal load, sliding speed, sliding distance) were applied (Fig. 11). Most of the experiments were carried out with 0.05 m/s sliding speed and normal load of 2 N or 10 N. The volume of the lubricants used was 0.6 ml in each experiment. Although here, bath lubrication was not used and the lubricant covered the entire wear track during the experiment (Fig. 12). All the tests were carried out at room temperature (22 ± 1°C) and evaporation was neglected in the tests. The duration was 40 minutes, unless stated otherwise.

The friction force was measured constantly during the tests. After the tests, the wear volume of the ball or pin was measured from the dimensions of the wear track and both sliding surfaces (ball and disc) were examined by optical microscopy. In interesting cases, the wear tracks were studied by scanning electron microscopy (SEM) and a 2D profilometer. It was not possible to determine the wear volume from the disc due to the duration of the experiments (usually 40 minutes), which did not cause a deep wear track on the disc even if lubricated with a relatively poor lubricant such as 50 mM sodium acetate (Fig. 13). Thus, the wear volume of the lubricated contacts was calculated by measuring the dimensions of the wear tracks of the pins that were sliding against the discs. The wear track dimensions have been used to calculate the apparent contact pressures.

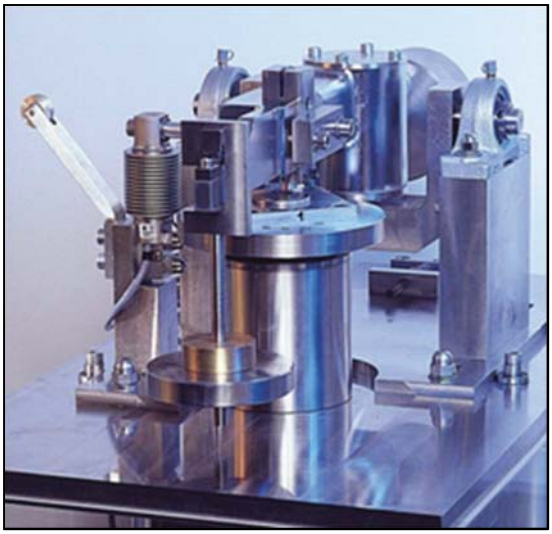

Figure 10. Pin-on-disc designed and manufactured at VTT

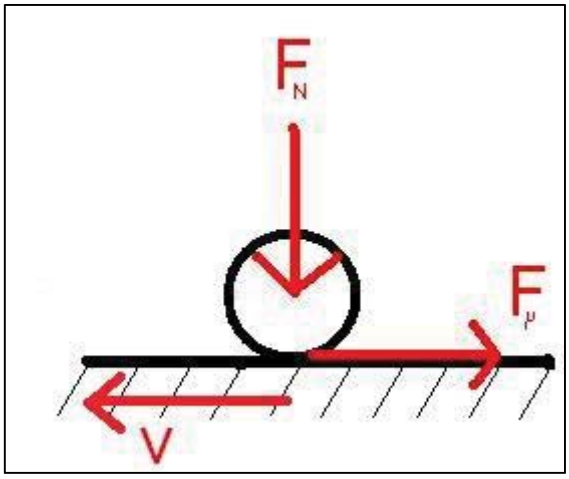

Figure 11. Ball on a flat-type contact. After initial contact of the surfaces, the contact type changes to flat on flat and the contact pressure decreases as a function of wear

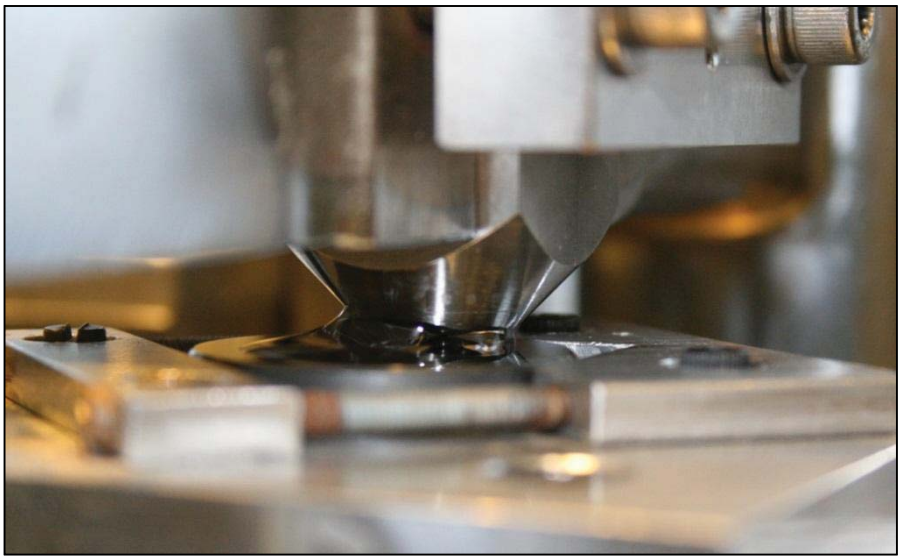

3

Figure 12. Contact of stainless steel ball and stainless steel disc lubricated with 50 mM sodium acetate buffer, pH 5

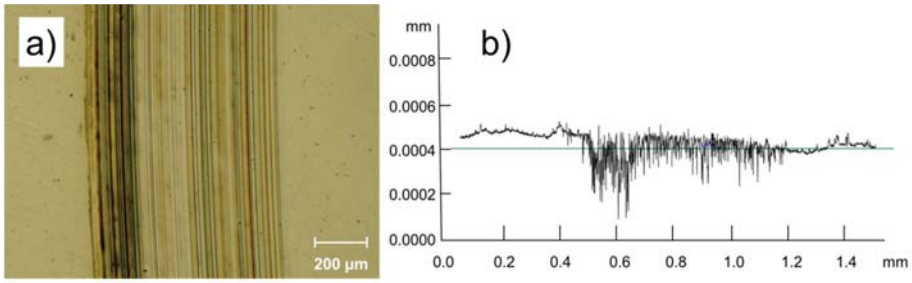

Figure 13. a) Optical microscopy image and b) 2D profile of wear track on stainless steel disc after pin-on-disc experiment lubricated with 50 mM sodium acetate buffer (pH 5). The test parameters were normal load 10 N, sliding velocity 0.1 m/s and duration 40 min. The amount of wear was hard to determine quantitatively.

2.4 Characterization

For the contact angle measurements an Attension Theta optical tensiometer (from Biolin Scientific) was used at 22.5°C and 50% relative humidity (RH). The sessile drop method was used to measure the contact angles of water on surfaces. The Young-Laplace equation was used for fitting the drop profiles. The size of

the water droplet was 5 µl and the contact angle of the water was determined as an average from 5 parallel experiments. For the contact angle, the measurements concentration of HFBII solutions was 0.1 mg/ml. The HFBII layer was formed by an addition of a 0.5 ml solution on the a-C:H surface, and after 30 minutes of adsorption, the excess solution was washed away with 1.0 ml of Milli-Q water. After washing, the a-C:H surface was dried with air (Publication V).

Scanning electron microscopy (SEM) + energy dispersive spectroscopy (EDS) (Zeiss Ultraplus + Thermo Fisher Scientific Ultradry EDS detector) was used to characterize wear tracks on copper and aluminium pins as well as a-C:H coating (Publication V).

Raman spectroscopy (Horiba Jobin-Yvon Labram HR Raman, 488 nm) was used to characterize oxide films on a copper pin (Publication V). The Raman spectrum of tribofilm on a stainless steel surface was obtained with a spectrometer equipped with a microscope with 615 and 640 objectives. The laser was an Innova 300C FreDTM frequency doubled Ar^+ ion laser, which was operated at a 244 nm wavelength. A charge-coupled device camera was used for detecting the scattered light. The system was controlled and the data were processed with Grams32 software.

3. Results and discussion

3.1 Adsorption and film forming

In measurements carried out with a Quartz Crystal Microbalance (QCM) and ellipsometer it was found that both HFBI and FpHYD5 hydrophobins can form monolayers on stainless steel surfaces. On stainless steel surfaces, the maximum adsorbed mass was achieved with a 0.05 mg/ml concentration. The higher concentrations do not increase the amount of adsorbed molecules on the surface, which can be explained by the monolayer formation (Publication II). Similar results were observed in the experiments carried out on a-C:H and PDMS surfaces measured by SPR and OWLS, respectively (Publication V; Hakala and Lee, 2011). The adsorbed masses shown in Fig. 15 represent the maximum amounts of adsorbed molecules after additional injections did not increase the amount of adsorbed mass. Thus the error rates are small.

By comparing the dry masses of adsorbed molecules (Fig. 15) it can be seen that there is no great difference between the adsorbed amounts of hydrophobins on different surfaces. It is interesting that higher amounts of hydrophobins are adsorbed on the surfaces in water than in buffer solution. Water has a higher pH than acetate buffer (pH 5), which affects the surface charges of the hydrophobin proteins. Changes in surface charges may affect lateral interactions between hydrophobins and their interactions with the surface. In water, the net electric charges of hydrophobins are closer to 0 or negative because of the isoelectric points of hydrophobins, which are between 4 and 6.7 (Kisko, 2008; Table 1).

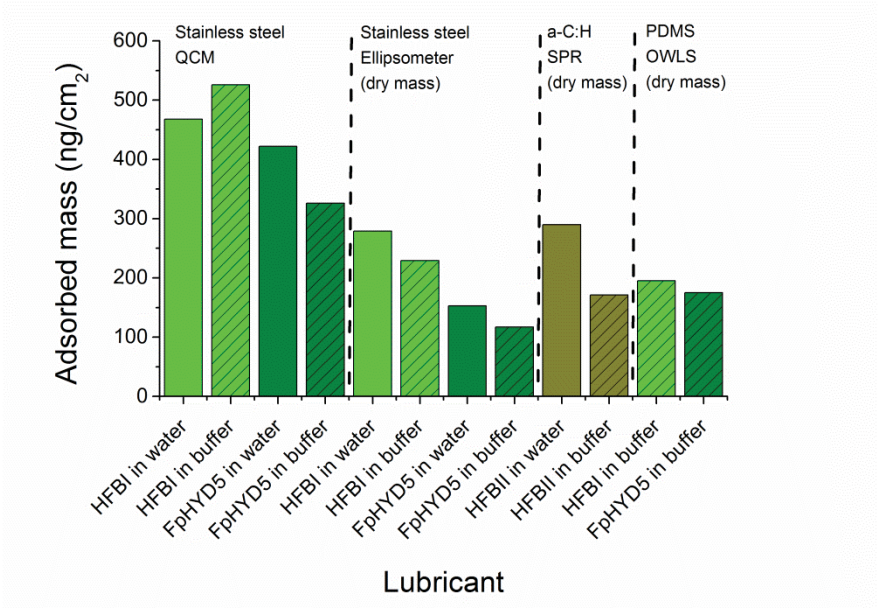

Figure 15. Adsorbed mass of hydrophobins on different surfaces. Ellipsometer, SPR and OWLS measure the dry mass of hydrophobins adsorbed on the surface while QCM takes bound water into account (Publications II and V; Hakala and Lee, 2011).

The effect of pH and ionic strength on the adsorption of FpHYD5 hydrophobins on stainless steel surfaces was studied with an ellipsometer (Publication IV). Increasing the ionic strength clearly decreased the amount of bound protein, whereas an increase in pH from 5 to 9 more than doubled the thickness of the bound protein layer (Fig. 16). The pH affects the net electric charge of the molecule and solid surface. Stainless steel surfaces consist mainly of iron oxides and chromium oxides. The isoelectric points (IEP) for these oxides are 5.2-8.6 and 7.0, respectively (Parks, 1965). For FpHYD5, the isoelectric point is about 4-5. The structure of the glycan group of FpHYD5 molecules is not known exactly and, thus, the exact IEP cannot be calculated. According to the adsorption results, it can be seen that the adhesion is increased significantly when the electric charges are both negative. At pH 5, the adsorbed mass of FpHYD5 on the stainless steel surface was significantly lower.

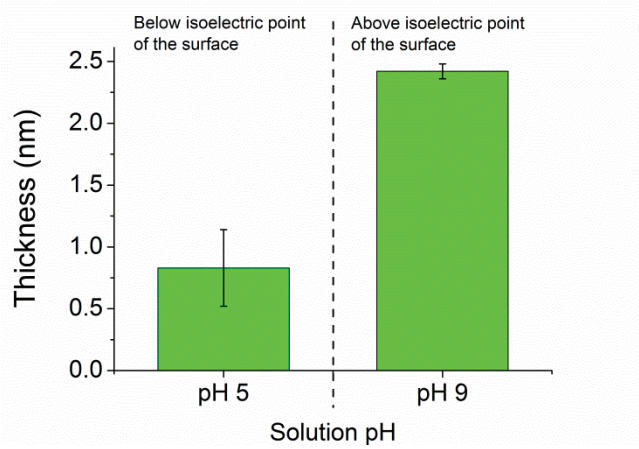

Figure 16. The thickness of FpHYD5 adsorbed on a stainless steel surface at pH 5 and pH 9 (Publication IV).

On the a-C:H surface, the HFBII hydrophobins reduced the contact angle from 75° to 60° (Publication V). On the stainless steel surface, HFBI hydrophobins did not affect the contact angle significantly, which was ~60° for a clean surface except with the highest concentration of 5 mg/ml (Publication I). The water contact angles on FpHYD5 layers formed on stainless steel surfaces at pH 5 and pH 9 were 59 and 40, respectively. It must be taken into account that the contact angles were measured on dried hydrophobin layers that may have had a different structure to the monolayer formed on a solution/solid interface. The results may also have been affected by the surface roughness.

The diameters of HFBI and HFBII hydrophobins are about 2-3 nm. The FpHYD5 molecule has a similar size except that it has a glycan group attached to its hydrophilic part. The size of the hydrophobic patch of hydrophobin proteins is about 4 nm^2. The molecular masses of hydrophobins are HFBII 7200 g/mol, HFBI 7540 g/mol and FpHYD5 9210 g/mol. The average area that the molecules occupy on different surfaces can be calculated from the adsorbed masses with the knowledge that hydrophobins form monolayer structures both on stainless steel and a-C:H surfaces. The average values for area per molecule on different surfaces are presented in Table 4.

Table 4. Area per molecule measured on different surfaces

Molecule	Surface	Area per molecule (nm^2)
HFBI[Publication II]	Stainless steel	4.6
FpHYD5[Publication II]	Stainless steel	14.7
HFBII[Publication V]	a-C:H	4.1
HFBI[Hakala and Lee, 2011]	PDMS	6.4
FpHYD5[Hakala and Lee, 2011]	PDMS	8.7

When comparing the area per molecule on stainless steel and a-C:H surfaces with the area on PDMS surfaces, the density of hydrophobins is higher on stainless steel and a-C:H surfaces. The only exception is the FpHYD5 molecule, which has a higher density on a PDMS surface, which is supported by the results published by Lee et al, 2015. This may originate from different alignments of the molecules on stainless steel surfaces compared with PDMS surfaces where hydrophobins are expected to adhere with their hydrophobic patch.

3.2 Tribology

3.2.1 Friction and wear

The hydrophobins reduced the friction in stainless steel vs stainless steel compared with water in the experiments performed with 2 N normal load and a sliding velocity of 0.05 m/s. In some experiments, the friction decreased to below the level of oil-lubricated contacts, though the wear volume was higher in the hydrophobin-lubricated contacts (Fig. 17). The lowest friction coefficient was 0.09, achieved with FpHYD5 hydrophobins in 50 mM sodium acetate buffer at pH 5. This friction coefficient was 24% lower than for the pure mineral oil-lubricated contact. Addition of 2% EP additives (yellow points in Fig. 17) reduced friction by 0.01 in mineral oil lubricated contacts compared to pure mineral oil. The lowest wear volume for a stainless steel ball was also measured in an FpHYD5-lubricated contact.

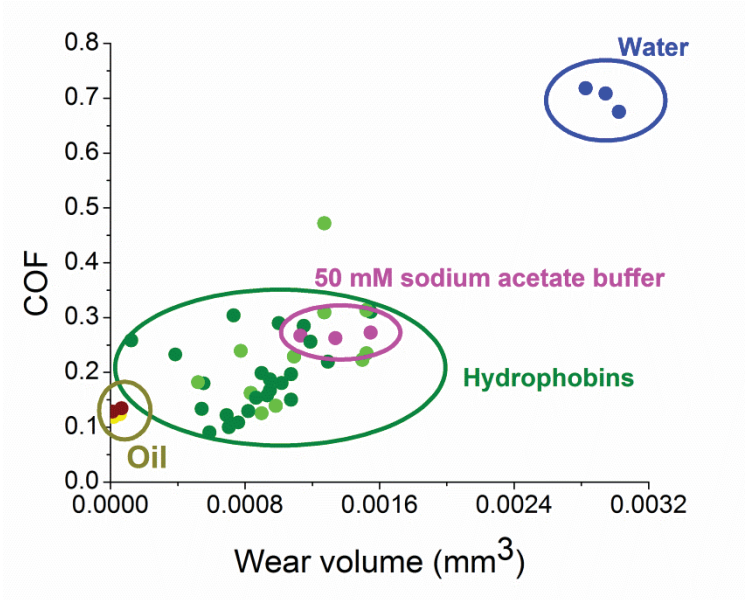

Figure 17. Friction coefficients (COF) vs wear volumes in stainless steel vs stainless steel experiments lubricated with oil, hydrophobins, buffer and water

Hydrophobins were also able to lubricate copper vs a-C:H and PDMS vs PDMS contacts better than water or acetate buffer. Quince mucilage was not an effective lubricant in stainless steel vs stainless steel contact but reduced friction significantly in UHMWPE vs stainless steel contact where hydrophobins had no significant effect on friction (Fig. 18).

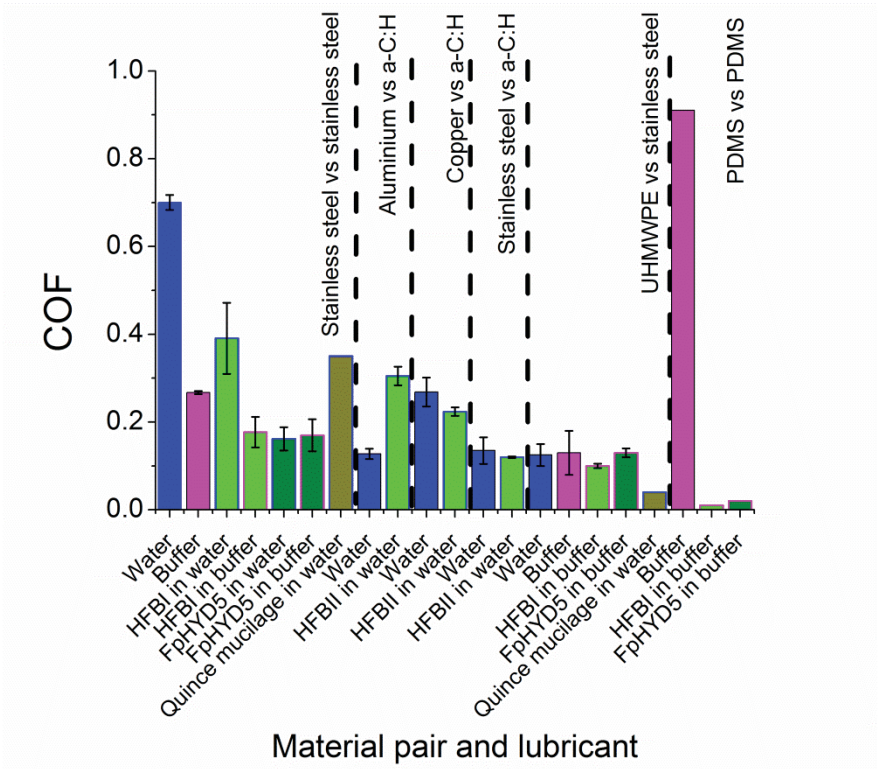

Figure 18. Lubrication of different material pairs with water, 50 mM sodium acetate buffer, hydrophobin proteins and quince mucilage (Publications I-VI; Hakala and Lee, 2011)

Water-lubricated stainless steel vs stainless steel contacts had friction coefficients of approximately 0.6-0.7. In hydrophobin-lubricated contacts, the friction coefficient decreased to a level of 0.1-0.2. Sodium acetate buffer (50 mM) solution was able to reduce the friction coefficient to 0.25-0.35. In hydrophobin-lubricated experiments, the friction coefficient was not dependent on normal load (2-100 N), but an increase in sliding velocity to 0.10 m/s caused an occasional decrease in friction coefficient in FpHYD5-lubricated experiments (Publications II and IV).

Quince mucilage was not able to lubricate stainless steel vs stainless steel contact. The reason for the poor lubricating ability of quince mucilage may be related to the repulsion between the negatively charged quince mucilage and stainless steel surfaces, which led to the removal of the lubricant from the contact zone (Publication III). However, while hydrophobins were not able to reduce the friction in UHMWPE vs stainless steel contact compared with water or sodium acetate buffer solution, the quince mucilage performed as an excellent lubricant reducing the friction down to 0.02-0.07 (Publication III). This shows that the material pair as

well as contact geometry can have a significant effect on lubrication performance with biomolecules.

The hydrophobin concentration did not have a big effect on lubrication after exceeding a concentration of 1.0 mg/ml. In smaller concentrations, there was a slight increase in friction and wear, which may be explained by breakage or partial removal of the lubricating film during the POD experiment (Publication II). The adsorption speed of hydrophobins on a stainless steel surface depends on the concentration. At low concentrations, the sheared molecules are not replaced by new ones as rapidly. The increase in quince mucilage concentration, however, reduced the friction in UHMWPE vs stainless steel contact. This indicated that while hydrophobins do lubricate by a monolayer, the quince mucilage lubricates better when it forms thicker multilayer structures between sliding surfaces (Publications II and III).

The lubrication of contacts with a-C:H-coated surfaces with hydrophobins was challenging. When the HFBII hydrophobins were added to water, the friction coefficient and wear increased in aluminium vs a-C:H contacts compared with water-lubricated experiments (Publication VI). In copper vs a-C:H contacts, the hydrophobins reduced friction by 13-30% compared with water but increased wear (Publication V). In stainless steel vs a-C:H contacts, hydrophobins did not have a significant effect on friction and wear.

The PDMS vs PDMS contact was the only one for which the hydrophobins were able to reduce friction to a level of 0.01-0.02. This contact has significantly lower contact pressures (0.36 MPa) and both surfaces are hydrophobic. In addition, in this contact, no significant wear of the surfaces occur. Lee et al., 2015, have published results on the performance of HFBI and FpHYD molecules in PDMS vs PDMS contact showing that friction was significantly lower compared with pure buffer solution in the boundary lubrication regime.

Determining the effect of hydrophobins and quince mucilage on wear in different contacts was challenging. In many contacts, the wear was below the determination limit, which depends on the profilometer. The effect on wear is presented in Table 5. In stainless steel vs stainless steel contacts, hydrophobins and quince mucilage reduced the wear compared with water. In experiments in which a-C:H coating was used, the wear of the counter materials (aluminium and copper) was increased when hydrophobins were added to the water.

Table 5. The effect of lubricants on wear compared with water or buffer solution in different contacts. (- = no experiments carried out)

Lubricant	Hydrophobins	Quince mucilage
Contact		
Stainless steel vs stainless steel	Reduced	Reduced
UHMWPE vs stainless steel	Not detected	Not detected
Aluminium vs a-C:H	Increased	-
Copper vs a-C:H	Increased	-
Stainless steel vs a-C:H	Not detected	-
PDMS vs PDMS	Not detected	-

3.2.2 The effect of adhered molecules on friction and wear

As seen in Section 3.1, although the hydrophobins form monolayers on different solid surfaces, the amount of adhered hydrophobin can affect the friction and wear. Based on the tribological experiments with stainless steel counter bodies (Publications I, II, IV), the increased dry mass of hydrophobins actually increases the friction and wear (Fig. 19). This indicates that the hydrophobin proteins are not lubricating in themselves. As Heuberger et al. and Lee et al. (2005) have shown, the increased number of adsorbed molecules increases cohesion between lubricant molecules and decreases the adhesion force between molecules and substrate and thus cause increased friction. This can explain the increased friction and wear in hydrophobin-lubricated contacts. However, a certain number of molecules are needed to adhere to surfaces because in pure water and buffer solution, lubricated contacts had higher wear compared with contacts lubricated with hydrophobin proteins.

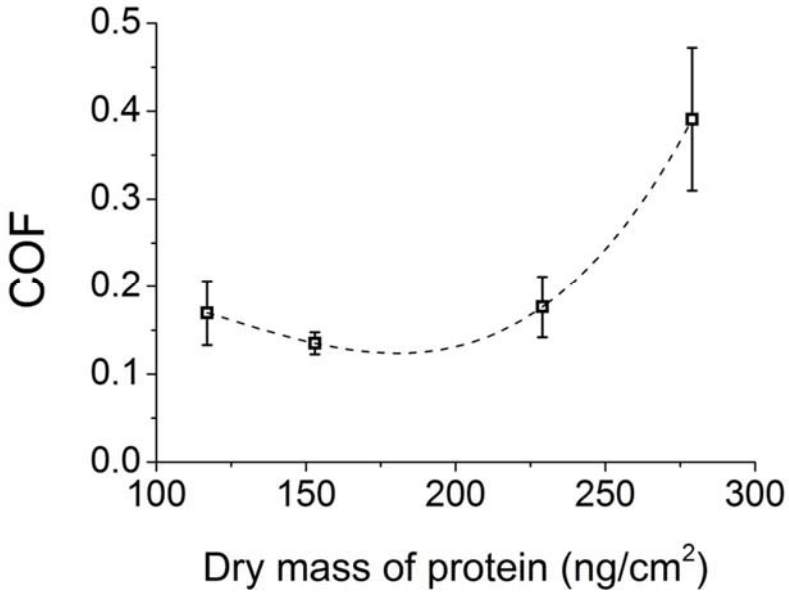

Figure 19. Friction coefficient of the dry mass of hydrophobin proteins adhered to a stainless steel surface (Publication II)

As seen before, the dry mass of FpHYD5 hydrophobins on stainless steel surfaces increased with increasing pH. The friction and wear of FpHYD5-lubricated contacts were measured at different pH levels from pH 3 to pH 9 using a constant load of 10 N and constant sliding velocity of 0.05 m/s (Fig. 20). The buffer solutions were studied as a reference system. At lower pH values, the friction and wear of the stainless steel vs stainless steel contact remained constant, but increasing the pH to 7 caused a small increase in both friction and wear. When the pH was increased to 9, the friction coefficient and wear of the buffer solution-lubricated contacts decreased slightly, whereas the FpHYD5 hydrophobins caused an increase in both friction and wear (Publication IV). The isoelectric point of FpHYD5 proteins is between 4 and 5 and chromium oxide has an isoelectric point at 7 (Parks, 1965). The increase in friction in FpHYD5-lubricated contacts occurs when both surface and molecule are negatively charged and the adsorbed mass of hydrophobins is also high (pH 9). It may be that at pH 9, hydrophobins form a very dense molecule layer on stainless steel surfaces, thus limiting the amount of water bound to the layer. This could explain the higher friction measured at pH 9.

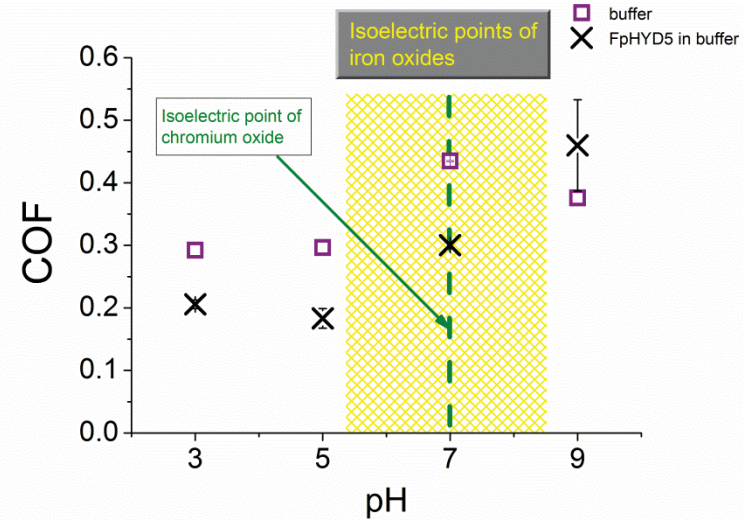

Figure 20. Friction coefficient vs solution pH in FpHYD5-lubricated stainless steel vs stainless steel contacts. The friction below the isoelectric points of chromium oxide and iron oxides is lower than the friction-measured pH above the isoelectric points.

3.2.3 The effect of water content on lubricating film

In nature, the lubricating molecules often contain carbohydrate structures that increase water-binding ability. When comparing the friction and wear results of HFBI and FpHYD5 molecules in stainless steel vs stainless steel contacts, it was observed that the increased water content in the hydrophobin film led to decreased friction and wear (Fig. 21; Publication II). Similar results were achieved with non-treated quince mucilage in UHMWPE vs stainless steel contact when the friction decreased with increased water-binding ability of quince mucilage. Although the lubricated materials are hard and the lubricating film is not stable, the importance of water in the sliding contact to reduce friction and wear seems to be significant.

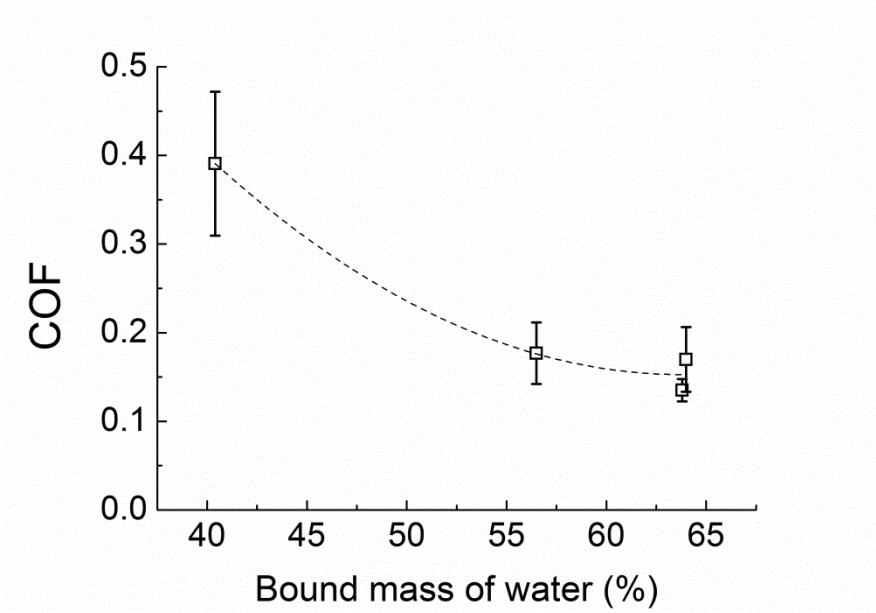

Figure 21. Friction coefficient vs water content in hydrophobin film formed on a stainless steel surface (Publication II)

3.2.4 The effect on tribofilm formation

In the contact with a-C:H-coated surfaces, the hydrophobins disturbed the lubrication by increasing wear. In water-lubricated contacts an oxide-containing tribofilm formed on aluminium and copper surfaces. The hydrophobin prevented the oxide film formation and it also affected friction and wear in the sliding contacts with a-C:H coatings. The wear of copper and aluminium increased because no oxide film was formed. In aluminium vs a-C:H, contact, friction also increased compared with the water-lubricated contacts.

In the water-lubricated contacts, Cu_2O film formed on the copper surface. In the SPR experiments, it was observed that hydrophobins were able to react with a copper surface and remove the oxide layer (Publication V).

3.2.5 Low friction with hydrophobins

Occasionally in the tribotests with FpHYD5 hydrophobins in stainless steel vs stainless steel contacts, friction started to decrease to a level below 0.05 (Fig. 22)

although the conditions were kept identical (Publication IV). Low friction in FpHYD5-lubricated contacts was always related to tribofilm formation on the worn surface on the stainless steel sphere observed by optical microscopy (Fig. 23). The tribofilm appeared as scale-like patterns formed on the sliding surface (Fig. 23 a). The film was studied by Raman spectrometry (Ref. Publication IV), which showed the presence of protein. The spectrum was deconvoluted into separate bands that were identified as amide II and III bands and a c_{α}-H amide bending vibration band and were comparable with those reported in the literature for proteins having b-sheet and random coil secondary structures. (Chi et al., 1998)

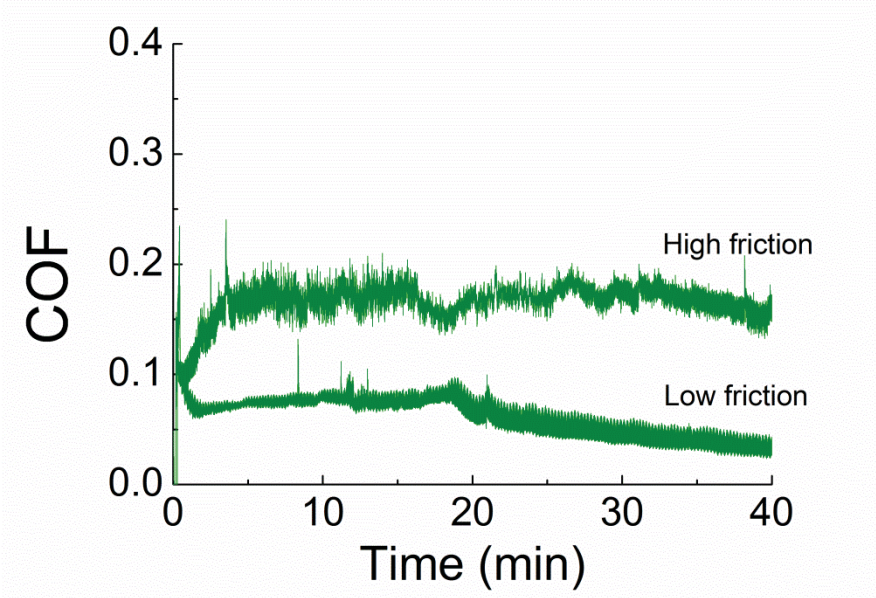

Figure 22. Two friction curves measured in a stainless steel vs stainless steel POD experiment. Although the conditions were identical, the friction was significantly lower in the second experiment. The contacts were lubricated with FpHYD5 in 50 mM acetate buffer. The test parameters were normal load 10 N, sliding velocity 0.1 m/s and duration 40 min.

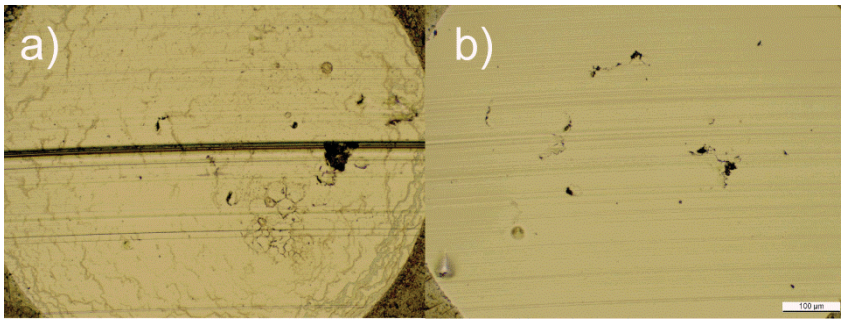

Figure 23. a) Tribofilm formed on the stainless steel surface, b) no tribofilm formed

The Formation of tribofilm, which consists of proteins, on the wear track of the pin allows a situation in which there is a protein layer on both the disc and pin surfaces. This indicates that low friction is achieved when there is a protein layer on both sliding surfaces. However, the layer on the ball/pin surface is not a monolayer of hydrophobins because a monolayer (thickness ~2-3 nanometres) cannot be detected by optical microscopy.

.

4. Discussion on lubrication performance

4.1 Film formation, friction and wear performance

To provide effective boundary lubrication, the biomolecule additives need to adhere to sliding surfaces and prevent the contact between surface asperities. In biomolecule-lubricated contacts, low friction coefficients are usually achieved via hydration lubrication. Hydration lubrication requires:

1. Hydrated molecules on both sliding surfaces
2. Perfect alignment of the molecules, which allows the sliding to occur between the hydrated moieties
3. Low contact pressures

Hydrophobins are well known for their adsorption properties. The adsorption experiments showed that hydrophobins adhered well to stainless steel, a-C:H and PDMS surfaces. There is no significant difference in the amounts of hydrophobins that adhered to different surfaces. Although the surface properties did not affect the amount of adsorbed molecules, the environment in which adsorption occurs had an effect on adsorption. It was observed that the amount of adsorbed molecules was higher from water than 50 mM sodium acetate buffer solution. It may be that the ions in buffer solutions and pH affect the interactions between hydrophobins on solid surfaces. In water, hydrophobins are able to form a more closely packed monolayer compared with a buffer solution at pH 5. Strong lateral interactions are typical for hydrophobin films and have been observed earlier in an air/water interface (Szilvay et al., 2007). The adsorbed amount of FpHYD5 molecules on the stainless steel surface was lower than the amount of HFBI molecules. A probable reason for this is the rather large carbohydrate structure (1.7 kDa) in the FpHYD5 molecule, which may cause electrostatic repulsion and steric hindrance between the molecules, thus weakening the lateral interaction in the protein layer. This can also explain why the FpHYD5-lubricated contacts showed more wear than the HFBI-lubricated contacts.

Hydrophobins have relatively large hydrophilic parts for their size, which makes them able to bind high amounts of water. The water-binding ability of the lubricating hydrophobin films was dependent on both the environment and the molecule

structure. The glycosylated FpHYD5 formed layers on stainless steel with over 60% of the mass being water. An increased water-binding ability compared with the HFBI molecule is assumed to be due to the carbohydrate structures attached to the FpHYD5 molecule. Thus, a combination of an anchoring group (hydrophobin) and a water-absorbing group (carbohydrate) enabled the formation of a reasonably thick layer of water on the surface. In stainless steel vs stainless steel contacts, the FpHYD5 molecule generally lubricated more effectively than HFBI. These results indicate that the hydrophobin proteins do not lubricate in themselves very effectively but, at the same time, the bound water plays an important role in lubrication. The experiments with quince mucilage in UHMWPE vs stainless steel contact also showed the importance of water in lubrication. The addition of 1M NaCl increased friction by 36% in quince mucilage-lubricated contact, most probably due to the reduced level of hydration of the mucilage.

The alignment of hydrated molecules is an important property in hydration lubrication because low friction is achieved when the sliding occurs between the hydrated moieties. Although adsorption experiments showed that hydrophobins are able to form monolayers on different surfaces, we do not know how they are aligned. The adsorption of hydrophobins is affected by both hydrophobic interactions and electric charges. The alignment on different surfaces may be different although the amounts of adsorbed molecules would be similar. The HFBI, HFBII and FpHYD5 molecules have hydrophobic patches that are similar in size (4 nm^2) in all of the molecules. If we assume that on hydrophobic PDMS surfaces, which have contact angles of water over 90°, the FpHYD5 and HFBI hydrophobins are adhered with their hydrophobic patch. In addition, in PDMS vs PDMS contacts, both hydrophobins were able to reduce the friction coefficients close to 0.01, which is at similar level to friction coefficients in effective hydration lubrication. We do not know the alignment of the molecules on stainless steel and a-C:H surfaces, which have lower hydrophobicity compared with PDMS surfaces. It is interesting that the area per FpHYD5 molecule on a stainless steel surface was 14.7 nm^2 but on a PDMS surface, the area for the same molecule was only 8.7 nm^2. As the environment (pH, ionic strength) was the same in both cases, there should be no difference in the interaction between molecules. Thus, the results indicate that there are differences in the molecule alignment. The possible alignments on stainless steel and PDMS surfaces are schematically illustrated in Fig. 24. For a smaller HFBI molecule, there was no such difference in the amount of adsorbed molecules on stainless steel and PDMS surfaces, which can be explained by the globular shape of the molecule.

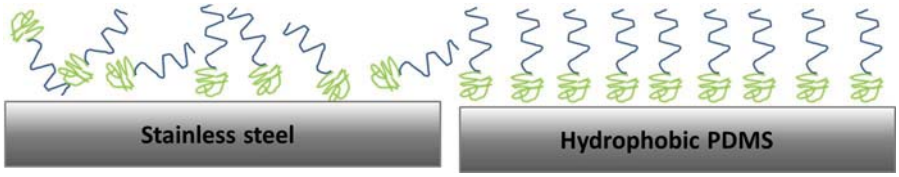

Figure 24. Adsorption and possible alignment of FpHYD5 molecules on stainless steel and hydrophobic PDMS surfaces

The lowest friction coefficients for all the experiments were measured in PDMS vs PDMS contacts lubricated with HFBI and FpHYD5 hydrophobins. The friction coefficients decreased from ~0.9 to close to 0.01 when hydrophobins were added to the buffer solution. Low friction compared with other lubrication systems may be explained by three main differences. The first factor is the hydrophobicity of PDMS surfaces. In PDMS vs PDMS contacts, the hydrophobins are probably adhered on both surfaces with their hydrophobic patches. This leads to a situation in which sliding can occur between the hydrated moieties as illustrated in Fig. 6. Secondly, in PDMS vs PDMS contacts, there are low contact pressures. While in other lubricated contacts, the contact pressures decreased down to a few MPas due to wear. Those are significantly higher than for the PDMS vs PDMS contacts for which the contact pressure is approximately 0.36 MPa. However, when the contact pressure exceeded a few MPas it had no effect on lubrication with hydrophobin molecules (Fig. 25). At higher contact pressures, the material pair has more effect on lubrication performance than contact pressure itself. Thirdly, PDMS surfaces do not wear significantly. In the contacts with the harder materials, the upper specimen in particular has wear because it is constantly in sliding contact.

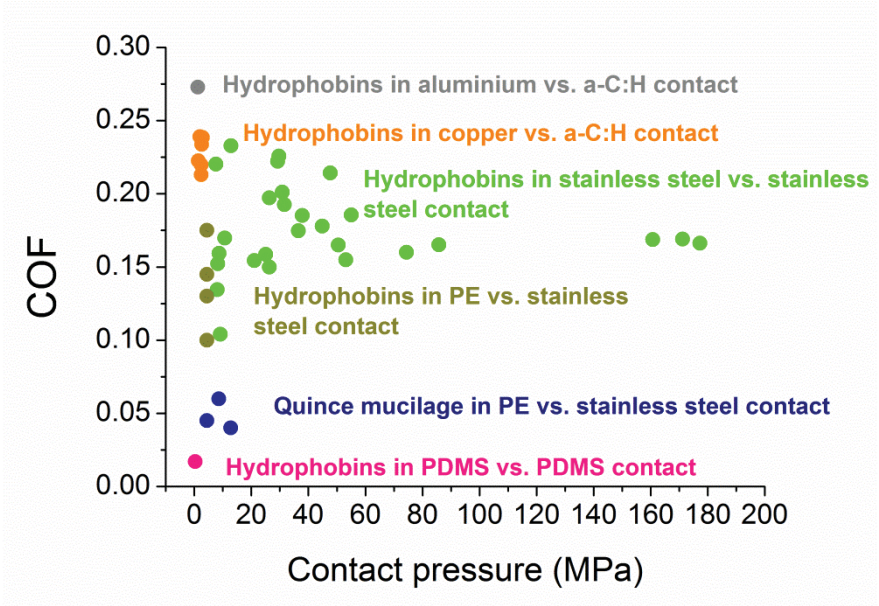

Figure 25. COF vs contact pressure in different lubricated contacts.

As seen in Fig. 25, the friction coefficients in hydrophobin-lubricated contacts are usually between 0.1 and 0.3. Relatively high friction coefficients could be explained by higher contact pressures that may disturb low friction mechanisms by causing the entanglement of molecule layers adsorbed on both sliding surfaces (Klein, 2012; Harvey et al., 2011), removal of surface- adhered molecules (Raviv et al., 2008) and bridging where molecules are adhered on both sliding surfaces (Harvey et al. 2011; Carapeto et al., 2010). The importance of the correct alignment of molecules on surfaces in hydration lubrication was discussed earlier. In the contacts in which stainless steel, aluminium, copper and a-C:H were used, there was also wear of the materials. Due to the wear, stable lubricating films cannot be formed by adhered hydrophobins on both sliding surfaces, which prevents the existence of a hydration lubrication situation (Fig. 26 a). When surfaces are worn, the molecules are also sheared away from the contact (Fig. 26 b). The wear rates and contact pressures decrease during the experiment, and at some points there may be a situation in which the molecules are adhered on both surfaces, as seen in tribological experiments with FpHYD5. It was observed that FpHYD5 was able to form a protein layer occasionally on the worn surface of the stainless steel ball, and that led to low-friction coefficients below 0.05 in stainless steel vs stainless steel contacts. This is not the case with all materials. It is not likely that hydrophobins could form stable lubricating film on a constantly sliding pin/ball surface because the adsorption of hydrophobins on stainless steel and a-C:H surfaces takes a few minutes and hence so does the formation of a full mono-

layer. Thus, the formation of a monolayer in a kinetic situation, such as tribocontact, may be impossible. In addition, the adsorption rates of the hydrophobins depends on their concentration, which means that the recovery of the hydrophobin layer on the disc surface was faster at higher protein concentrations. This could explain why the friction remained low with higher protein concentrations while at a concentration of 0.1, friction and wear increased compared with the buffer solution. The higher protein concentration in the lubricant may also affect the amount of molecules between the sliding surfaces and the local viscosity. An increase in local viscosity can improve the lubrication by causing a hydrodynamic effect between the sliding surfaces.

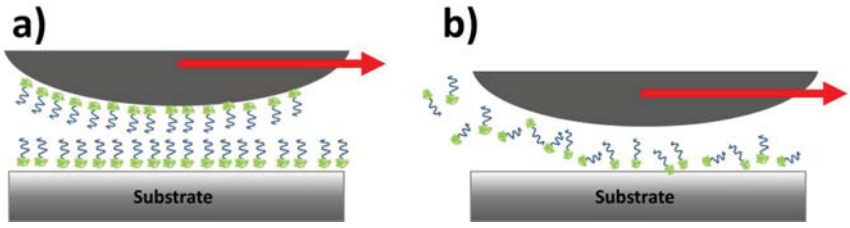

Figure 26. a) A situation in which hydration lubrication is possible in a POD experiment, b) a situation with hard materials in which wear and shear force have removed molecules from the upper surface, which is constantly in contact

In the contacts where the upper specimen was made of copper or aluminium there was also significant wear of the upper sliding surface. It was also observed that hydrophobins prevented the formation of oxides on the sliding surfaces. In SPR experiments, it was seen that HFBII hydrophobins actually removed the oxide film from the copper surface in a static situation without any mechanical contact. Thus, in these cases, the hydrophobins were not able to form lubricating layers on the upper surface, which can explain the relatively high friction coefficients of 0.2-0.3. When no oxide film was formed on the pin surface, the wear on the pin increased.

A summary of the results is presented in Table 6. It can be seen that the best results were achieved by FpHYD5 in stainless steel vs stainless steel contact, HFBI and FpHYD5 in PDMS vs PDMS contacts and quince mucilage in UHMWPE vs stainless steel contact.

Table 6. Summary of the friction and wear results for different lubricated contacts

Lubricant / Materials		Water	Buffer	Oil	HFBI	HFBII	FpHYD5	Quince mucilage
Stainless steel vs stainless steel	COF	0.6-0.8	0.25-0.35	0.1-0.15	0.15-0.25		**0.1-0.25**	0.3-0.4
	Wear	High	Aver-age	Low	Average		Average	High
UHMWPE vs stain-less steel	COF	0.1-0.15	0.08-0.18		0.1-0.18		0.1-0.18	**0.02-0.09**
Stainless steel vs a-C:H	COF	0.13-0.14				0.12		
	Wear	Low				Average		
Alumini-um vs a-C:H	COF	0.12-0.14				0.28-0.32		
	Wear	Aver-age				High		
Copper vs a-C:H	COF	0.24-0.30				0.21-0.24		
	Wear	Aver-age				High		
PDMS vs PDMS	COF		0.8-0.9		**0.01-0.05**		**0.01-0.02**	

4.2 Potential application areas for biomolecular lubrication in the future

Based on the tribotests and literature, it can be suggested that the requirements for water-based lubrication with biomolecule additives in industrial applications are

- a mild temperature range that is suitable for water lubrication and bio-molecules, T= 4-95°C
- low contact pressures, 0.1- 5 MPa
- hydrophobic surfaces, contact angle of water >90°
- a stable environment (pH, ionic strength)

Compared with oil lubrication, water-based lubrication with biomolecules is sensitive to changes in the environment, such as temperature, pH and ionic strength. In short-term lubrication processes, such as metal working, there may be fewer limitations regarding contact pressures and temperatures, because no long stability of the molecules is needed. In these kinds of processes, for example the graphitiza-

tion mechanism, in which molecules are broken down and form graphite on sliding surfaces, can provide effective lubrication.

Possible applications for water-based lubrication improved with biomolecule additives could be existing applications in which water is already used and there is a need for lubricants that are not harmful to the environmental or humans and do not leave harmful remnants on the products. With biomolecule lubricants, friction can also be reduced compared with water-lubricated contacts as seen in the tribological experiments with quince mucilage. Aging and bacterial growth can of course cause problems in biomolecule-lubricated contacts, as carbohydrates are especially sensitive to bacterial growth. Hydrophobin proteins can survive longer without any clear worsening of performance. However, the aging of hydrophobin solutions has not yet been studied properly.

The benefit of using biomolecule-containing lubricants is their low friction in the boundary lubrication regime. This could lead to energy savings in various bearings and motors for instance. In addition, waste treatment of lubricants is much easier compared with oil lubricants because biomolecules are environmentally friendly.

Examples of some of the lubrication systems and applications with most potential in which biomolecules could be used in the future are described below.

The food and beverage industry

In certain applications in the food industry, lubrication must be arranged so that the lubricant cannot contaminate the food or beverage. There are several applications in which there is a high risk of leakage. Thus, lubricants suitable for the food and beverage industry are National Sanitary Foundation (NSF) H1 grade lubricants. The NSF H1 grade is given to lubricants that do not contaminate the food in case of contact between the food or beverage and the lubricant. The certificate also takes into account hygiene during processing and storage of the lubricant. It is important for food grade biolubricants to prevent the growth of bacteria without poisonous additives. For carbohydrate-containing lubricants, this can cause limitations on their usage. Hydrophobins can survive for a relatively long time if stored properly. The hydrophobin lubricants did not have any visual changes even after 1-2 years when stored in a refrigerator. In addition, hydrophobins can be ingested by human without health risks.

Traditional oil lubricants and their additives cannot meet the requirements for the NSF H1 grade, and synthetic lubricants have been developed for the food and beverage industry. Non-harmful bio-based lubricants could be one alternative for the food and beverage industry if they satisfy the health requirements for food grade lubricants. Many biomolecules are extracted from plants, such as the quince fruit, and are not harmful to humans (Florea and Luca, 2008).

Nowadays, food grade grease is commonly used in many applications because the risks of leakage are small compared with low viscosity oils. However, replacing grease with low viscosity lubricants would have a great effect on energy savings. Examples of applications in which bio-based lubricants could be used in the food industry are shafts and bearings, depending on the materials and conditions.

The textile industry

In the textile industry, lubricants are used in, for example, fibre processing. Lubricants need to prevent abrasive wear of the fibres. Water-based lubricants can easily be removed from the final products by washing, unlike oil-based lubricants (Li, Y et al., 2012). Textile materials, such as polyethylene and polypropylene, are hydrophobic and can be lubricated well by water-based lubricants and additives that are adsorbed to surfaces by hydrophobic forces (Song et al., 2014). The problem of hydrophobins and some other biomolecule additives in the textile industry could be high velocities of lubricated systems. Hydrophobins easily form foam, which should be avoided.

Biomedical and pharmaceutical applications

Biomolecules can be used as surgical or medical lubricants to make operations more comfortable. In some applications, the surfaces can be tailored by biomolecule additives to reduce friction and, especially, wear of the biomaterials, e.g. catheters (Zhang et al, 2013). The biomolecule layer on the surface could be used as an alternative to synthetic polymers with enhanced lubricating ability and environmental friendliness. The manufacturing of biomedical devices may need lubricants that are easily removed from the final products. Biomolecules could act as anti-stick coatings in certain production steps, e.g. printing or pressing in tablet processing and other pharmaceutical processes. For example, hydrophobins can easily be washed away with ethanol.

Conclusions

In this thesis, water-based lubricants with hydrophobin proteins (HFBI, HFBII and FpHYD5) and quince mucilage additives were used to lubricate engineering materials such as diamond-like carbon (DLC) coatings, stainless steels and plastics.

Generally, the lowest friction coefficients were measured in contacts where at least one of the surfaces was a polymeric material. In hard vs hard-type contacts, low friction coefficients and wear rates were occasionally achieved.

The main results of this thesis are as follows:

- Hydrophobins can form monolayers on stainless steel, diamond-like carbon (a-C:H) and PDMS surfaces. On stainless steel surfaces, HFBI and FpHYD5 layers contain 40-64% water (Publication II).
- An increase in water content in lubricating film reduced friction in hydrophobin-lubricated stainless steel vs stainless steel contacts (Publication II). The same effect was seen in quince mucilage-lubricated UHMWPE vs stainless steel contact (Publication III).
- FpHYD5 hydrophobins reduced the friction coefficient in stainless steel vs stainless steel contacts from about 0.7 to as low as 0.03. Low friction was related to protein film formation on the wear track of the stainless steel ball (Publication IV).
- Quince mucilage-lubricated UHMWPE vs stainless steel reduced the friction coefficient from about 0.12 to as low as 0.02 (Publication III).
- HFBI and FpHYD5 hydrophobins decreased the friction coefficient from 0.9 to close to 0.01 in PDMS vs PDMS contacts (Hakala and Lee, 2011).

Based on these results from adsorption and tribological experiments, biomolecules can form lubricating layers on engineering materials and lubricate with friction coefficients well below the friction coefficients measured with mineral oil and EP additives. This is in accordance with the scientific hypothesis of this thesis.

It can be suggested that the requirements for water-based lubrication with biomolecule additives in industrial applications are

- a mild temperature range that is suitable for water lubrication and bio-molecules, T= 4-95°C
- low contact pressures, 0.1- 5 MPa
- hydrophobic surfaces, contact angle of water >90°
- Stable conditions (pH, ionic strength)

From the work, it can be concluded that biomolecules have the potential to act as effective lubricants in the boundary lubrication regime when the conditions are mild and the environment stable.

References

Arwin, H. 1998. 'Spectroscopic ellipsometry and biology: Recent developments and challenges'. *Thin Solid Films*, 313-314, pp. 764-774.

Askolin, S, Linder, M, Scholtmeijer, K, Tenkanen, M, Penttila, M, de Vocht, ML and Wösten, HAB. 2006. Interaction and Comparison of a Class I Hydrophobin from Schizophyllum commune and Class II Hydrophobins from Trichoderma reesei, *Biomacromolecules*, 7, pp. 1295-1301.

Borruto, A, Crivellone, G, Marani, F. 1998. Influence of surface wettability on friction and wear tests, *Wear*, 222 (1), pp. 57-65.

Briscoe, WH, Titmuss, S, Tiberg, F, Thomas, RK, McGillivray, DJ and Klein, J. 2006. Boundary lubrication under water, Nature Letters, 444, pp. 191-194.

Cai, M, Guo, R, Zhou, F and Liu, W. 2013. Lubricating a bright future: Lubrication contribution to energy saving and low carbon emission. Science China Technological Sciences, 56 (12), pp. 2888-2913.

Carapeto, AP, Serro, AP, Nunes, BMF, Martins, MCL, Todorovic, S, Duarte, MT and André, V. 2010. Characterization of two DLC coatings for joint prosthesis: The role of albumin on the tribological behavior, *Surface & Coatings Technology*, 204, pp. 3451-3458.

Chawla, K, Lee, S, Lee, BP, Dalsin, JL, Messersmith, PB and Spencer, ND. 2009. A novel low-friction surface for biomedical applications: Modification of poly(dimethylsiloxane) (PDMS) with polyethylene glycol(PEG)-DOPA-lysine, *Journal of Biomedical Materials Research* Part A, 90, 3, pp. 743-749.

Chen, M, Briscoe, WH, Armes, SP, Cohen and H, Klein, J. 2011. Polyzwitterionic brushes: Extreme lubrication by design. *European Polymer Journal*, 47 (4), pp. 511-523.

Chen, Q, Wang, X., Wang, Z, Liu, Y and You, T. 2013. Preparation of water-soluble nanographite and its application in water-based cutting fluid, Nanoscale Research Letters, 8, 1, pp. 1-8.

Chi, Z, Chen, XG, Holtz, JSW and Asher, SA. 1998. UV resonance raman-selective amide vibrational enhancement: quantitative methodology for determining protein secondary structure, *Biochemistry*, 37, pp. 2854-2864.

Coles, JM, Chang, DP and Zauscher, S. 2010. Molecular mechanisms of aqueous boundary lubrication by mucinous glycoproteins, *Current Opinion in Colloid & Interface Science*, 12, 15, pp. 406-416.

Dedinaite, A. 2012. Biomimetic lubrication. *Soft Matter*, 8, pp. 273-284.

de Feijter, JA, Benjamins, J and Veer, FA. 1978. Ellipsometry as a tool to study the adsorption behavior of synthetic and biopolymers at the air-water interface, *Biopolymers*, 17, 1759-1772.

Dekkiche, F, Cornecic, MC, Trunfio-Sfarghiuc, AM, Munteanu, B, Berthier, Y, Kaabar, W and Rieu, JP. 2010. Stability and tribological performances of fluid phospholipid bilayers: Effect of buffer and ions, *Colloids and Surfaces B: Biointerfaces*, 80, pp. 232-239.

Elomaa, O, Hakala, TJ, Myllymäki, V, Oksanen, J, Ronkainen, H, Singh, VK and Koskinen, J. 2013. Diamond nanoparticles in ethylene glycol lubrication on steel-steel high load contact. *Diamond and Related Materials*, 34, pp. 89-94.

Fang, H-W, Shih, M-L, Zhao, J-H, Huang, H-T, Lin, H-Y, Liu, H-L, Chang, C-H, Yang, C-B and Liu, H-C. 2007. Association of polyethylene friction and thermal unfolding of interfacial albumin molecules, *Applied Surface Science*, 253, 16, pp. 6896-6904.

Florea, O and Luca, M. 2008. Multipurpose lubricating greases for food-grade applications, Proceedings of the 3rd International Conference on Manufacturing Engineering (ICMEN), October 1-3, pp. 673-680.

Garrec, DA and Norton, IT. 2012a. Boundary lubrication by sodium salts: A Hofmeister series effect, J. *Colloid Interface Sci.*, 379, pp. 33-40.

Garrec, DA and Norton, IT. 2012b. The influence of hydrocolloid hydrodynamics on lubrication, *Food Hydrocolloids*, 26, pp. 389-397.

Goldberg, R, Schroeder, A, Silbert, G, Turjeman, K, Barenholz, Y and Klein, J. 2011. Boundary Lubricants with Exceptionally Low Friction Coefficients Based on 2D Close-Packed Phosphatidylcholine Liposomes, *Adv. Mater*, 23, 3517-3521.

Goldian, I, Jahn, S, Laaksonen, P, Linder, M, Kampf, N and Klein, J. 2013. Modification of interfacial forces by hydrophobin HFBI. *Soft Matter*, 9 (44), pp. 10627-10639.

Granqvist, N, Liang, H, Laurila, T, Sadowski, J, Yliperttula, M and Viitala, T. 2013. Characterizing ultrathin and thick organic layers by surface plasmon res-

onance three-wavelength and waveguide mode analysis, *Langmuir*, 29 (27), pp. 8561-8571.

Grunér, MS, Szilvay, GR, Berglin, M, Lienemann, M, Laaksonen, P and Linder, MB. 2012. Self-assembly of class II hydrophobins on polar surfaces. *Langmuir*, 28 (9), pp. 4293-4300.

Hakala, TJ, Laaksonen, P, Helle, A, Linder, MB and Holmberg, K. 2014. Effect of operational conditions and environment on lubricity of hydrophobins in water based lubrication systems, *Tribology - Materials, Surfaces and Interfaces,* 8 (4), pp. 241-247

Hakala, TJ and Lee, S. 2011.Scientific report – Short term scientific mission, COST Action TD1003, A collaborative research on bio-inspired approaches to lubricate engineering materials on nanometer scale, 1-7, available online at http://www.bioinspirednano.eu/docs/files/Timo%20Hakala.pdf (16.7.2015)

Hakala, TJ, Saikko, V, Arola, S, Ahlroos, T, Helle, A, Kuosmanen, P, Holmberg, K. Linder, MB and Laaksonen, P. 2014. Structural characterization and tribological evaluation of quince seed mucilage, *Tribology International*, 77, pp. 24-31.

Hakanpää, J, Paananen, A, Askolin, S, Nakari-Setälä, T, Parkkinen, T, Penttilä, M, Linder, MB and Rouvinen, J. 2004. Atomic Resolution Structure of the HFBII Hydrophobin, a Self-assembling Amphiphile. *Journal of Biological Chemistry*, 279 (1), pp. 534-539.

Hart, H, Craine, LE and Hart, DJ. 2003. Organic Chemistry – a short course, 11th edition, Houghton Mifflin, USA, ISBN:0-618-215360.

Harvey, NM, Yakubov, GE, Stokes, JR and Klein, J. 2011. Normal and Shear Forces between Surfaces Bearing Porcine Gastric Mucin, a High-Molecular-Weight Glycoprotein, *Biomacromolecules*, 12, pp. 1041-1050.

Heeb, R, Lee, S, Venkataraman, NV and Spencer, ND. 2009. Influence of salt on the aqueous lubrication properties of end-grafted, ethylene glycol-based self-assembled monolayers, *ACS Applied Materials and Interfaces*, 1, 5, pp. 1105-1112.

Heuberger, MP, Widmer, MR, Zobeley, E, Glockshuber, R and Spencer, ND. 2005. Protein-mediated boundary lubrication in arthroplasty, *Biomaterials*, 26 (10), pp. 1165-1173.

Hills, BA. 1995. Remarkable Anti-Wear Properties of Joint Surfactant, *Annals of Biomedical Engineering*, 23, pp. 112-115.

Hills, BA. 2002. Review – Surface-active phospholipid: A Pandora's box of clinical applications'. Part II. Barrier and lubricating properties, *Internal Medicine Journal*, 32, pp. 242-251.

Holmberg, K, Andersson, P and Erdemir, A. 2012. Global energy consumption due to friction in passenger cars. *Tribology International*, 47, pp. 221-234.

Holmberg, K, Andersson, P, Nylund, N-O, Mäkelä, K and Erdemir, A. 2014. Global energy consumption due to friction in trucks and buses. *Tribology International*, 78, pp. 94-114.

Holmberg, K, Siilasto, R, Laitinen, T, Andersson, P and Jäsberg. A. 2013. Global energy consumption due to friction in paper machines. *Tribology International*, 62, pp. 58-77.

Kato, T, Ohmori, H, Lin, W and Osawa, E. 2009. Lubrication property of single-digit-nanodiamond in an aqueous colloid, *Journal of Japanese Society of Tribologists*, 54, 2, pp. 122-129.

Kisko, K, Szilvay, GR, Vainio, U, Linder, MB and Serimaa, R. 2008. Interactions of hydrophobin proteins in solution studied by small-angle X-ray scattering, *Biophysical Journal*, 94 (1), pp. 198-206.

Klein, J., Raviv, U., Perkin, S., Kampf, N., Chai, L., Giasson, S. 2004. Fluidity of water and of hydrated ions confined between solid surfaces to molecularly thin films, *Journal of Physics Condensed Matter*, 16 (45), pp. S5437-S5448.

Klein, J. 2006. Molecular mechanisms of synovial joint lubrication. Proceedings of the Institution of Mechanical Engineers, Part J: *Journal of Engineering Tribology*, 220 (8), pp. 691-710.

Klein, J. 2012. Polymers in living systems: from biological lubrication to tissue engineering and biomedical devices, *Polymers for Advanced Technologies*, 23, 4, pp. 729-735.

Lee, S, Müller, M, Rezwan, K and Spencer, ND. 2005. Porcine Gastric Mucin (PGM) at the Water/Poly(Dimethylsiloxane) (PDMS) Interface: Influence of pH and Ionic Strength on Its Conformation, Adsorption, and Aqueous Lubrication Properties, *Langmuir*, 21,18, pp. 8344-8353.

Lee, S, Røn, T, Pakkanen, KI and Linder, M. 2015. Hydrophobins as aqueous lubricant additive for a soft sliding contact. *Colloids and Surfaces B: Biointerfaces*, 125, pp. 264-269.

Li, J, Liu, Y, Luo, J, Liu, P and Zhang, C. 2012. Excellent Lubricating Behavior of Brasenia schreberi Mucilage, *Langmuir*, 28, 20, pp. 7797-7802

Li, Y, Rojas, OJ and Hinestroza, JP. 2012. Boundary Lubrication of PEO-PPO-PEO Triblock Copolymer Physisorbed on Polypropylene, Polyethylene, and Cellulose Surfaces, *Ind. Eng. Chem. Res*., 51, pp. 2931-2940.

Liao, Y, Pourzal, R, Wimmer, MA, Jacobs, JJ, Fischer, A and Marks, LD. 2011. Graphitic tribological layers in metal-on-metal hip replacements, *Science* 334, 6063, pp. 1687-1690.

Linder, MB. 2009. Hydrophobins: Proteins that self assemble at interfaces. Curr. Opin. *Colloid Interface Sci*., 14, pp. 356-363.

Linder, MB, Qiao, M, Laumen, F, Selber, K, Hyytiä, T, Nakari-Setälä, T and Penttilä, ME. 2004. Efficient purification of recombinant proteins using hydrophobins as tags in surfactant-based two-phase systems, *Biochemistry*, 43 (37), pp. 11873-11882.

Linder, MB, Szilvay, GR, Nakari-Setälä, T and Penttilä, ME. 2005. Hydrophobins: The protein-amphiphiles of filamentous fungi. FEMS Microbiology Reviews, 29 (5), pp. 877-896.

Macakova, L, Yakubov, GE, Plunkett, MA and Stokes, JR. 2011. Influence of ionic strength on the tribological properties of pre-adsorbed salivary films, *Tribology International*, 44, 9, pp. 956-962.

Madsen, JB, Pakkanen, KI and Lee, S. 2014. Thermostability of bovine submaxillary mucin (BSM) in bulk solution and at a sliding interface, *Journal of Colloid and Interface Science*, 424, pp. 113-119.

Misra, R, Li, J, Cannon, GC and Morgan, SE. 2006. Nanoscale reduction in surface friction of polymer surfaces modified with Sc3 hydrophobin from Schizophyllum commune, *Biomacromolecules*, 7, 5, pp. 1463-1470.

Mortier, RM and Orszulik, ST. 1997. Chemistry and Technology of Lubricants, 2nd edition, Chapman & Hall, Great Britain, ISBN: 0-7514-0246-X.

NA, 1980. Lubricants for railway switches, JP55027599, July 22.

Nelson, DL, Lehninger, AL and Cox, MM. 2008. Lehninger principles of biochemistry, 5th edition, New York, W.H. Freeman, USA, ISBN:978-0716771081.

Neville, A, Morina, A, Liskiewicz, T and Yan, Y. 2007. Synovial joint lubrication – Does nature teach more effective engineering lubrication strategies? Proceedings of the Institution of Mechanical Engineers, Part C: *Journal of Mechanical Engineering Science*, 221 (10), pp. 1223-1230.

Omotowa, BA, Phillips, BS, Zabinski, JS and Shreeve, JM. 2004. Phosphazene-based ionic liquids: Synthesis, temperature-dependent viscosity, and effects as additives in water lubrication of silicon nitride ceramics, *Inorg. Chem*., 43, pp. 5466-5471.

Orelma, H, Filpponen, I, Johansson, L-S, Laine, J and Rojas, OJ. 2011. Modification of cellulose films by adsorption of cmc and chitosan for controlled attachment of biomolecules, *Biomacromolecules*, 12 (12), pp. 4311-4318.

Parks, GA. The isoelectric points of solid oxides, solid hydroxides, and aqueous hydroxo complex systems, *Chemical Reviews*, 1965, 65 (2), pp. 177-198.

Park, M-S, Chung, J-W, Kim, Y-K, Chung, S-C and Kho, H-S. 2007. Viscosity and wettability of animal mucin solutions and human saliva, *Oral Diseases*, 13, pp. 181-186.

Pawlak, Z, Urbaniak, W and Oloyede, A. 2011. The relationship between friction and wettability in aqueous environment, *Wear*, 271 (9-10), pp. 1745-1749.

Pettersson, T and Dedinaite, A. 2008. Normal and friction forces between mucin and mucin–chitosan layers in absence and presence of SDS, *Journal of Colloid and Interface Science*, 324, 246-256.

Phillips BS and Zabinski JS. 2004. Ionic lubrication effects on ceramics in a water environment, Tribology Letters, 17, pp. 533-541.

Raviv, U, Giasson, S, Kampf, N, Gohy, J-F, Jerome, R and Klein, J. 2008. Normal and Frictional Forces between Surfaces Bearing Polyelectrolyte Brushes, *Langmuir*, 24, pp. 8678-8687.

Rich, RL and Myszka, DG. 2010. Grading the commercial optical biosensor literature – Class of 2008: 'The Mighty Binders', *Journal of Molecular Recognition*, 23 (1), pp. 1-64.

Roba, M, Naka, M, Gautier, E, Spencer, ND and Crockett, R. 2009. The adsorption and lubrication behavior of synovial fluid proteins and glycoproteins on the bearing-surface materials of hip replacements, *Biomaterials*, 30, pp. 2072-2078.

Ruhr, RO, Wichman, G, Paquette, C and Gutzman, T. 2004. Conveyor lubricants for use in the food and beverage industries, US6696394, Abbrev. February 2.

Saikko, V. 2006. Effect of contact pressure on wear and friction of ultra-high molecular weight polyethylene in multidirectional sliding, Proceedings of the Institution of Mechanical Engineers, Part H: *Journal of Engineering in Medicine*, 220 (7), pp. 723-731.

Sarlin, T, Kivioja, T, Kalkkinen, N, Linder, MB and Nakari-Setälä, T. 2012. Identification and characterization of gushing-active hydrophobins from Fusarium graminearum and related species. *Journal of Basic Microbiology*, 52 (2), pp. 184-194.

Schweigkofler, M and Kilthau, T. 2011. Water-based lubricating oils containing water-soluble polymers for textile-processing machines, WO2011131331, October 27.

Seror, J, Merkher, Y, Kampf, N, Collinson, L, Day, AJ, Maroudas, A and Klein, J. 2011. Articular Cartilage Proteoglycans as Boundary Lubricants: Structure and Frictional Interaction of Surface-Attached Hyaluronan and Hyaluronan Aggrecan Complexes, *Biomacromolecules*, 12, pp. 3432-3443.

Song, J, Li, Y and Cheng, Q. 2014. Adsorption of a Silicone-Based Surfactant on Polyethylene and Polypropylene Surfaces and Its Tribologic Performance, *Journal of Applied Polymer Science*, 131, p. 19.

Sotres, J, Madsen, JB, Arnebrant, T and Lee, S. 2014. Adsorption and nanowear properties of bovine submaxillary mucin films on solid surfaces: Influence of solution pH and substrate hydrophobicity, *Journal of Colloid and Interface Science*, 428, pp. 242-250.

Stachowiak, GW and Batchelor, AW. 2005. Engineering tribology, 3rd edition, Elsevier, Amsterdam, The Netherlands, ISBN: 978-0-7506-7836-0.

Stanimirova, RD, Gurkov, TD, Kralchevsky, PA, Balashev, KT, Stoyanov, SD and Pelan, EG. 2013. Surface pressure and elasticity of hydrophobin HFBII layers on the air-water interface: Rheology versus structure detected by AFM imaging, *Langmuir*, 29 (20), pp. 6053-6067.

Stokes, JR, Macakova, L, Chojnicka-Paszun, A, de Kruif, CG and de Jongh, HHJ. 2011. Lubrication, Adsorption, and Rheology of Aqueous Polysaccharide Solutions, *Langmuir*, 27, pp. 3474-3484.

Sunde, M, Kwan, AHY, Templeton, MD, Beever, RE and Mackay, JP. 2008. Structural analysis of hydrophobins. *Micron*, 39 (7), pp. 773-784.

Szilvay, GR, Paananen, A, Laurikainen, K, Vuorimaa, E, Lemmetyinen, H, Peltonen, J and Linder, MB. 2007. Self-assembled hydrophobin protein films at the air-water interface: Structural analysis and molecular engineering. *Biochemistry*, 46, pp. 2345-2354.

Tomala, A, Karpinska, A, Wernera, WSM, Olver, A and Störi, H. 2010. Tribological properties of additives for water-based lubricants, *Wear*, 269, 11-12, pp. 804-810.

Tompkins, HG and Irene, EA. ed. 2005. Handbook of Ellipsometry, Heidelberg, Springer.

Trunfio-Sfarghiu, A-M, Berthier, Y, Meurisse, MH and Rieu, JP. 2008. Role of Nanomechanical Properties in the Tribological Performance of Phospholipid Biomimetic Surfaces, *Langmuir* 24, pp. 8765-8771.

Veerman, ECI, Valentijn-Benz, M and Nieuw, AV, Amerongen. 1989. Viscosity of human salivary mucins, J. *Biol. Buccale*, 17, pp. 297-306.

Vignon, MR and Gey, C. 1998. Isolation, 1H and 13C NMR studies of (4-O-methyl-D-glucurono)-D- xylans from luffa fruit fibres, jute bast fibres and mucilage of quince tree seeds, *Carbohydrate Research*, 307 (1-2), pp. 107-111.

Wang, Z, Lienemann, M, Qiau, M and Linder, MB. 2010. Mechanisms of protein adhesion on surface films of hydrophobin, *Langmuir*, 26 (11), pp. 8491-8496.

Wösten, HAB, Van Wetter, M-A, Lugones, LG, Van der Mei, HC, Busscher, HJ and Wessels, JGH. 1999. How a fungus escapes the water to grow into the air. *Current Biology*, 9 (2), pp. 85-88.

Yakubov, GE, McColl, J, Bongaerts, JHH and Ramsden, JJ. 2009. 'Viscous Boundary Lubrication of Hydrophobic Surfaces by Mucin', *Langmuir*, 25, pp. 2313-2321.

Yang, CB, Fang, H-W, Liu, H-L, Chang, C-H, Hsieh, M-C, Lee, W-M and Huang, HT. 2006. Frictional characteristics of the tribological unfolding albumin for polyethylene and cartilage, Chemical Physics Letters, 431, pp. 380-384.

Zagidullin, RN, Abdrashitov, YM, Abdrafikova, LS, Rasulev, ZG and Gil'mutdinova, ES. 1991. Lubricating-cooling fluid for machining of optical glass, SU1694633, Abbrev. November 30.

Zappone, M, Ruths, GW, Greene, GD, Jay and Israelachvili, JN. 2007. Adsorption, Lubrication, and Wear of Lubricin on Model Surfaces: Polymer Brush-Like Behavior of a Glycoprotein, *Biophysical Journal*, 92, pp. 1693-1708.

Zhang, C, Zhang, S, Yu, L, Zhang, Z, Wu, Z and Zhang, P. 2012. Preparation and tribological properties of water-soluble copper/silica nanocomposite as a water-based lubricant additive, *Applied Surface Science*, 259, pp. 824-830.

Zhang, W, Yang, FK, Han, Y, Gaikwad, R, Leonenko, Z and Zhao, B. 2013. Surface and Tribological Behaviors of the Bioinspired Polydopamine Thin Films under Dry and Wet Conditions, *Biomacromolecules*, 14, pp. 394-405.

Zinoviadou, KG, Janssen, AM and de Jongh, HHJ. 2008. Tribological Properties of Neutral Polysaccharide Solutions under Simulated Oral Conditions, *Journal of Food Science*, 73, 2, pp. 88-94.

I

Ahlroos, T., Hakala, T.J., Helle, A., Linder, M.B., Holmberg, K., Mahlberg, R., Laaksonen, P., Varjus, S. (2011) Biomimetic approach to water lubrication with biomolecular additives. *Proceedings of the Institution of Mechanical Engineers, Part J: Journal of Engineering Tribology*, 225 (10), 1013-1022.
DOI:10.1177/1350650111406635

Biomimetic approach to water lubrication with biomolecular additives

T Ahlroos, T J Hakala, A Helle, M B Linder, K Holmberg*, **R Mahlberg, P Laaksonen,** and **S Varjus**
VTT Technical Research Centre of Finland, VTT, Finland

The manuscript was received on 30 November 2010 and was accepted after revision for publication on 21 March 2011.

DOI: 10.1177/1350650111406635

Abstract: The aim of this study is to find a connection between mechanical engineering and biotechnology by utilizing biomimetics in lubrication. The objective is to improve boundary lubrication by biomolecules in water-based systems. Proteins were used because they can form films and multilayers on the surfaces and thus prevent direct contact between them. In this study, hydrophobin and albumin proteins are studied as additives to enable water lubrication.

Keywords: biomimetics, boundary lubrication, biomolecules, hydrophobins

1 INTRODUCTION

In the future, one major trend is to move away from oil-based systems to renewable bio-based processes. Oil has been readily available, and oil-based products have been useful in lubrication. However, a major disadvantage of oil-based lubrication is the dependence on additives that are harmful to the environment [**1**]. On the other hand, there are many applications in which the use of water would be desirable. Potential applications for water-based lubricants include paper machinery, process equipments in food industry, mining industry, fire-resistant hydraulic fluids, and cold forming. The presence of lubricating oil in these industries causes a continual risk of contamination.

1.1 Biomimetics

Learning from natural systems and applying this knowledge to engineering is called biomimetics [**2**, **3**]. The basic idea of this study is to use a biomimetic approach to solve the problems of water lubrication in boundary lubrication regime. Boundary lubrication usually occurs under high-load and low-speed conditions in bearings and gears, e.g. when the motion starts and stops. Boundary lubrication is the last protection for the surface before wear failure, but it requires a good adhesion of the lubricant to the surfaces [**4**].

In this study, boundary lubrication is chosen to be the target to be improved by biomimetics, because it is a major challenge in machine design and this area offers many interesting possibilities for bio-based systems. There are several examples of excellent boundary lubrication systems in nature, such as mammalian joints.

Hills and Schwarz [**5**, **6**] have studied surface-active phospholipids of mammalian joints and reported that they act as back-up boundary lubricants if there is no fluid film available, e.g. after standing still for a long time. Healthy joints can still operate after long standing, although the fluid has been squeezed out from between the contacting surfaces. This indicates that boundary lubrication occurs also in mammalian joints [**5**–**7**].

Affinity to surfaces and attainment of hierarchical structures are the benefits of biomimetic approach, by which a low-friction nanostructure to the surface is achieved. This nanostructure may also be self-healing. Problems related to the use of biolubricants (whether bio-based oils or water) need to be solved,

**Corresponding author: VTT Technical Research Centre of Finland, P.O. Box 1000, FI-02044 VTT, Finland.*
email: Kenneth.Holmberg@vtt.fi

and new self-healing, low-friction, low-wear solutions need to be designed. Biomolecules can form films consisting of one or several layers. The film-forming ability is based on surface adhesion that can be customized [**8**]. Thus, natural-derived bionanocomposites can be used to solve lubrication problems. They are environmentally friendly, which is of major importance in tomorrow's lubricants [**5**]. The possibilities in the biomimetic approach to lubrication are in the utilization of existing biomolecules or in designing and synthesizing totally new ones. One possibility for tailoring molecules is to use directed evolution of peptides. Biomimetics can teach how water-based lubricants work. In this study, smart compounds are added to water to make water lubrication possible. The advantage in the use of biomolecules for this is that they function naturally in water.

1.2 Water lubrication

There are examples in nature where non-oil water-based systems have excellent performance [**3**], and in principle, there are no reasons why lubricating systems would have to be oil-based, and why for example, bio-based systems could not be practical. It is clear that a switch from oil-based systems would need a complete rethinking and redesign of practical details. In fact, there are even today several applications where non-oil-based solutions are being sought.

Water has been used as a lubricant in hydraulic systems in nuclear engineering, coal mines, steel foundries, desalination plants, fire-fighting, food/beverage production, and plastics moulding. Due to its low viscosity, water is used only for hydrodynamic lubrication where its low viscosity and high thermal conductivity are advantages [**9**]. Water is not environmentally harmful so it reduces the hydraulic oil waste, but it requires corrosion-resistant materials, better surfaces, closer tolerances for the materials, limited operating temperature area, and water quality control. The corrosion resistance of steel surfaces in hydrodynamic lubrication can be improved by corrosion-resistant coatings, such as diamond-like carbon or multifunctional, tailored sol–gel coatings. Alternatively, corrosion-resistant alloys and engineering ceramics can be considered [**9**, **10**].

Water-based boundary lubrication requires changes in the design of the tribological machine components and materials used in them. Challenge is the low viscosity of water, which has an important effect on the lubricating properties and sets high demands for the boundary lubrication additives, i.e. for the biomolecules to be developed.

1.3 Water lubrication with biomolecules as additives

In the nature, water usually has different kinds of natural additives, such as proteins, carbohydrates, and lipids, that can improve the boundary lubrication properties of water. It is shown that corrosion can also be avoided by using additives in water that adsorb on the surface [**11**]. Traditional mineral oils usually consist of phosphorus-, sulphur-, and zinc-containing additives that can form tribolayer on the top of the surface by chemical reactions. It causes low shear layer that reduces friction between two moving surfaces. Adhesive biomolecules can also form tribolayers by adsorbing on surfaces and preventing the contact between them. To find good biolubricants is challenging, because the requirements for the stability of the molecules are usually higher in engineering applications than in the biological systems. The molecules should be able to function under high pressures, temperatures, and shear rates [**4**].

The important properties of the bio-based boundary lubrication layer are as follows [**2**].

1. It spontaneously forms through intimate contact/interaction between the surface and the lubricant additives.
2. It has a layered structure on a nanometric scale comprising a base glassy structure and an upper organic-rich layer.
3. It is self-healing.
4. It is smart – it reacts to changes in load, temperature, pressure, and sliding speed.

1.4 Biomolecules in engineering

Proteins were chosen to be the starting point, and selected proteins have been evaluated with respect to their boundary lubrication ability. The adsorption of certain proteins on steel surface has been also studied before [**12**]. It has been noticed that the protein adsorption depends on the chemical properties of proteins, solutions, and surfaces.

In solutions, pH, ionic strength, and temperature can affect the adsorption properties of protein molecules. Also, macromolecular crowding affects the properties of protein. Shear stress due to flow can remove the protein molecules from the surface. It has also been found that the longer the proteins are allowed to adsorb at surface, the stronger their adhesion will be [**12**].

Surface hydrophobicity and ionic interactions between surface and molecule can have a great influence on the adsorption and conformation of the protein molecules; hence, on a hydrophilic surface, the

conformational changes can be more pronounced. The behaviour at the interfaces of different proteins cannot be generalized due to the great differences in protein molecules [**12**–**15**].

It is shown before that the concentration of the additives has crucial role in friction and wear reduction [**11**]. By tribological means, it is important to know that the properties of proteins may vary with temperature and pressure, because these properties have effect on lubrication performance [**16**, **17**].

In this study, the proteins were hydrophobins (HFBIs) and bovine serum albumin (BSA). HFBIs were chosen for the first preliminary tests because they can form monolayer and multilayer films on the interfaces [**18**–**20**]. HFBI molecules consist of hydrophobic and hydrophilic parts and that gives unique properties for the molecules. The film-forming ability is based on the improvement of surface adhesion where the hydrophobic part of the HFBIs adheres to the hydrophobic surface. The adsorption and film structure properties can vary among different HFBIs [**18**–**21**]. The HFBIs used are small proteins produced by filamentous fungi and used in nature for adhesion and coatings [**20**]. The fluids of natural joints also contain proteins. The aim is to develop effective lubrication conditions for industrial machines and equipments that fulfil future environmental requirements by biomolecularly enhanced water lubrication. This would be a breakthrough in future industrial lubrication in a situation when the use of oil is restricted due to environmental reasons or non-availability (Fig. 1). The biomimetic approach is based on the hierarchic structures of nature and self-assembly of molecules. By these means, one can achieve crucial self-healing, load-carrying capacity, and smart characteristics.

1.5 Friction and wear with water-based protein lubrication

The effectiveness of proteins to reduce friction and wear depends on the ability of the protein to adhere tightly to the surface and their ability to replace immediately those proteins that are removed from the surface by shear. It also requires low surface energy of the protein molecule [**22**]. Lubrication properties of different proteins such as albumin and mucin have been studied by research groups around the world, but there are only a few published test results with HFBI proteins as lubricant additives [**23**].

Common for these studies is that they have been usually carried out with other surface materials than steel against steel, which is the most common material pair in machine design. Many of the studies are related to orthopaedic implants and their polymeric materials [**24**, **25**].

Researchers have so far been more interested in adsorption properties, molecular structure, and steric repulsions of protein molecules than their effect on friction and wear. If the friction properties of the protein layers have been tested, they have usually been carried out in nanoscale by atomic force microscopy or in microscale by mini traction machine [**22**, **24**, **26**].

Lee *et al.* have studied with pin-on-disc (POD) tribometer how pH and ionic strength affect lubricating properties of mucin upon the self-mated sliding contact of poly(dimethylsiloxane). They have noticed that the adsorbed amount of mucin and lubricating properties are not always in straight correlation. Large amount of adsorbed molecules did not always guarantee good lubricating properties [**27**].

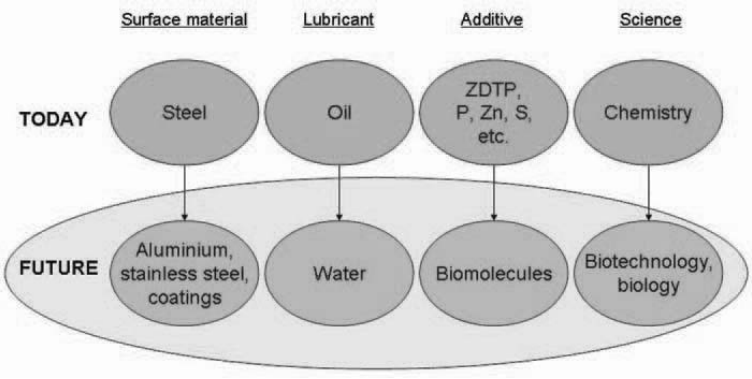

Fig. 1 Potential forthcoming change in industrial lubrication with driving forces arising from environmental requirements and diminishing oil resources

The aim of this study is to study how boundary lubrication properties of water can be improved in steel-on-steel contact with protein molecules and how HFBI molecules adsorb to the steel surface.

2 EXPERIMENTAL

2.1 POD tribometer tests

Friction and wear testing were carried out using POD tribometer to study the boundary lubrication ability of the selected biomolecules at different concentrations. The concentrations used were 0.1, 1, and 5 mg/mL for both the HFBIs and the BSA. The HFBI molecules were studied in 50 mM sodium acetate buffer pH 5 solution (HFBI), and the albumin molecules were studied in both 50 mM sodium acetate buffer pH 5 (BSAB) and in double deionized water (BSADDIW). Acetate buffer and a rather neutral pH were chosen to maintain the pH of the lubricant constant throughout the experiment. Reference tests were carried out with ion-exchanged water and mineral oil. In the first tests, the amount of lubricant used was 1 mL but since part of the lubricant spread over the edge of the disc during the test, the volume of the lubricants used was reduced to 0.6 mL. The lubricant was added onto the disc by a syringe. Figure 2 shows the disc with HFBI on the disc before and after a test.

The test specimens were stainless steel discs (AISI 440B) with a diameter of 40 mm (R_a value 0.01 μm or better) and stainless steel balls (AISI 420) with a diameter of 10 mm. The same disc was used in several tests, and before each tests, it was cleaned by ultrasonic washing in petroleum ether and in ethanol, 5 min each. A new ball was used in every test.

The test parameters were selected to give boundary lubrication conditions: normal force 2 N, sliding velocity 0.1 m/s (sliding diameter varied within 24–30 mm), sliding distance 200 m, and test duration 33 min [**28**]. The tests were carried out at room temperature ($22 \pm 1^{\circ}$C).

The friction force was measured during the tests. After the tests, the wear of the balls was measured, and all the sliding surfaces were examined by optical microscopy. The wear measurement was made by measuring the diameters of the wear scars of the balls by optical microscopy and then the wear volume was calculated from the wear scar and the ball diameter.

2.2 Adsorption tests by contact angle measurements

The adsorption of HFBI molecules to stainless steel discs was tested by measuring the contact angles of water from discs similar to the ones used in the tribological experiments. Before the measurements, the discs were cleaned in ultrasonic bath with three different solvents each for 5 min. The solvents used were petroleum ether, ethanol, and acetone, respectively. The solvents did not affect significantly the surface chemistry of the discs. After cleaning, the discs were dried with air flow. Cleaning of the discs with solvents does not change the topography of the discs, and the contact angles between washed and unwashed discs are in same order of magnitude (results not shown here).

After cleaning, the contact angles for bare discs were measured. Bare disc means the disc after cleaning and before the HFBI solution was added. Then, 0.5 mL of HFBI solution was added on the disc for 2 h. Concentrations of HFBI solutions were 0.1, 1.0, and 5.0 mg/mL. All the lubricants were in 50 mM sodium acetate buffer solution, but concentration 1.0 mg/mL existed also in water solution without buffer. Area on the disc for the HFBI solution was restricted with rubber O-ring (Fig. 3). HFBI solutions were rinsed carefully away after 2 h with 5 or 20 mL ion-exchanged water and dried overnight. Sample of 0 mL indicates that the solution was not rinsed away with water, but only the excess solution was poured out after 2 h and then dried like the other discs.

Residues of the different lubricating solutions of HFBI on the stainless steel surfaces were evaluated by

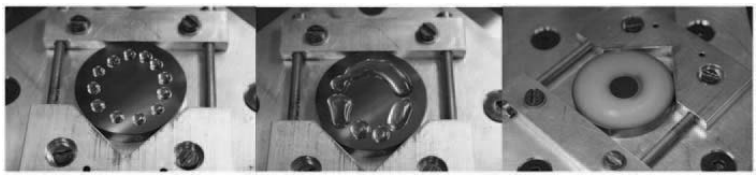

Fig. 2 HFBI of concentration 0.1 mg/mL on the disc before and after the test
Note: The lubricant was added onto the disc by a syringe drop by drop and it did not spread to the whole disc surface. During the test, the lubricant changed its colour to white because of the protein agglomerates, as shown in the picture on right. The diameter of the discs is 40 mm

measuring the contact angles of ion-exchanged water on the substrates rinsed as described above. The instrument used for the contact angle measurements was CAM200 (KSV Instruments Limited, Finland). Ion-exchanged water droplets with the volume of 6–7 μL were placed on the substrates, and the static contact angles were recorded as a function of time (up to 300 s). Prior to the contact angle measurements, the rinsed specimens were conditioned at 20°C and 50 per cent relative humidity for 16 h. Three measurements (droplets) for each sample surface were carried out.

3 RESULTS

3.1 Pin-on-disc

Visual examination during the tests showed that the smallest concentration of HFBIs stayed clear longer than the higher concentrations which changed the colour to white soon after the test started. BSA did not change its colour but stayed clear. Changes taking place in the HFBIs during the tests may be one possible reason for the variation in their wear results. On the discs of the water tests, there was clearly rust present. Optical microscopy was carried out after the tests, and it revealed that all the test specimens were worn in a similar way, and no significant tribolayer was observed. Figure 4 shows examples of the wear scars on the balls and discs. It was observed that when the HFBI concentration increased, the wear decreased. The results of the average friction coefficient values and wear of the balls are shown in Figs 5 and 6. In Fig. 5, the average friction coefficient and wear values are presented as the mean values of all the tests carried out with each concentration of the molecules being tested. Figure 6 shows the values of individual tests. All the values of HFBIs and BSA obtained in the tests were between those of mineral oil and water.

Fig. 3 Different concentrations of HFBI molecules in 50 mM sodium acetate buffer (pH 5) were added on stainless steel discs before contact angle measurements. Discs were exposed for HFBI solution for 2 hours and then rinsed away with ion exchanged water and dried. Contact angles of water were measured on dried discs

3.2 Contact angle measurements

There was great influence of the concentration of HFBI solutions to the hydrophilicity of the surfaces. All the HFBI solutions reduced the contact angle before rinsing. The concentrations of HFBI (in sodium acetate buffer) lowered the contact angle of water on steel surface from 60° to 10° (Figs 7 to 9). Rinsing of the protein films increased the contact angles of all the samples indicating that some of the protein could be removed by rinsing. The highest HFBI concentration was the only one where the final contact angle after rinsing with 20 mL of water was still significantly lower than the contact angle of the bare discs.

Contact angles with concentration of 1.0 mg/mL of HFBI in water (Fig. 10) and in buffer did not differ significantly from each other after rinsing, but

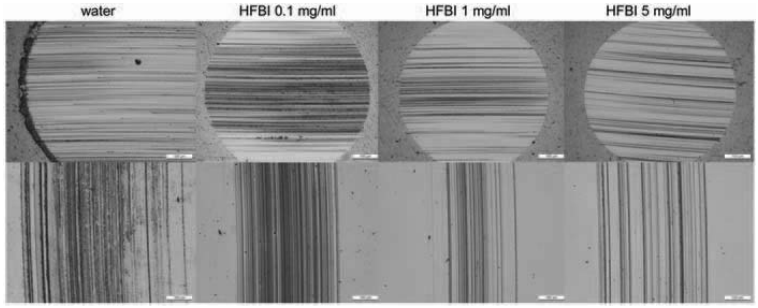

Fig. 4 Optical microscopy of the balls and discs after the water and HFBI tests
Note: The scale marker length is 100 μm

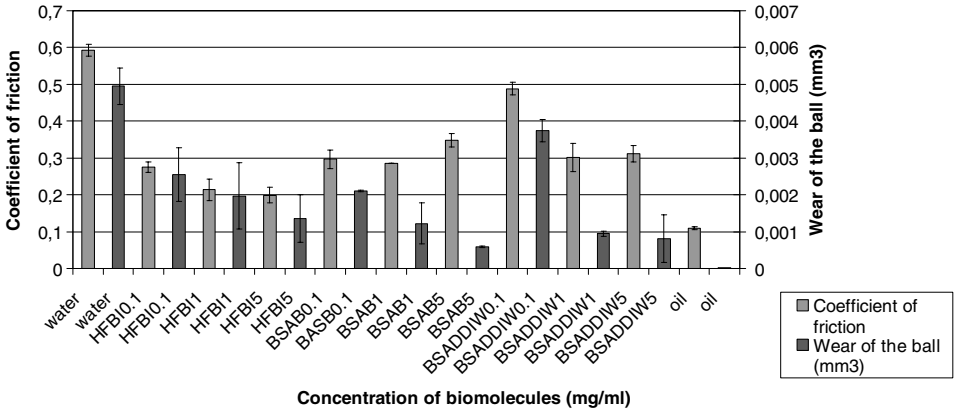

Fig. 5 The average friction coefficient values and wear of the balls in POD tests
Note: The lubricants from left to right: ion-exchanged water, HFBIs, BSAB, and BSADDIW all in three different concentrations of 0.1, 1, and 5 mg/mL, and mineral oil

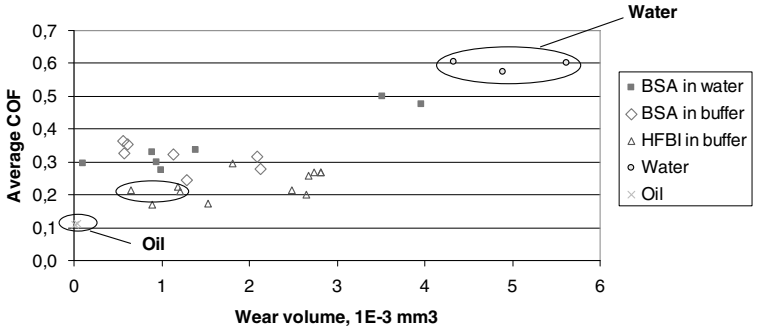

Fig. 6 The average COF versus wear volume of the ball in single tests
Note: HFBIs gave the best frictional behaviour of all the molecules tested. The lowest combination of average coefficient of friction and wear was obtained with the highest concentration, i.e. HFBI 5 mg/mL in buffer (in the circle). All values of HFBIs and BSA were between those of mineral oil and water

without rinsing, the surface was much more hydrophilic with HFBI in buffer. All contact angles are average values for three or more experiments.

4 DISCUSSION

4.1 POD measurements

During the POD tests, it was observed that initially clear HFBI solutions turned turbid. The solutions with the smallest concentration of HFBIs stayed clear longer than the higher concentrations that changed colour to white soon after the test started. Appearance of turbidity might be caused by the formation of large protein aggregates. It is known that above the critical micelle concentration, HFBI molecules begin to form dimers and tetramers, which may appear as cloudiness of the solutions [**20**]. There are no earlier observations on behaviour of HFBIs under shear, but the continuous rubbing motion of the test ball could possibly cause precipitation of the proteins. Changes taking place in the HFBIs during the tests may be one possible reason for the variation of their wear results although all the test specimens were worn in a similar way. BSA stayed clear during the tests. Biomolecules prevented rust formation, which was seen on the pure water tests. Pure water did not function properly as a lubricant but gave a friction coefficient of about 0.6 corresponding to dry friction in steel-on-steel contact. All the biomolecules resulted in a clear reduction of both the coefficient of friction (COF) and the volumetric

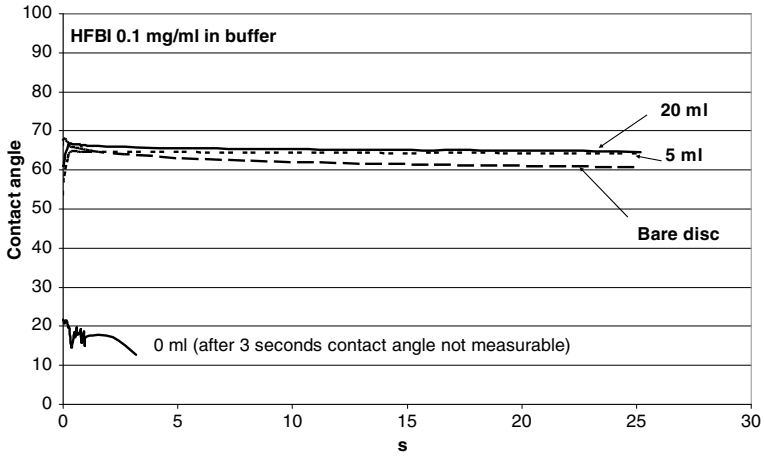

Fig. 7 Contact angles of water on stainless steel discs before and after exposing the surface to 0.1 mL/mL HFBI (in 50 mM sodium acetate buffer)
Note: Bare disc indicates the contact angle of clean disc. The amounts 0, 5, and 20 mL indicate the amount of water used for rinsing the disc after exposing to HFBI solution for 2 h. Great difference between the contact angle of water on rinsed discs and bare disc was not seen

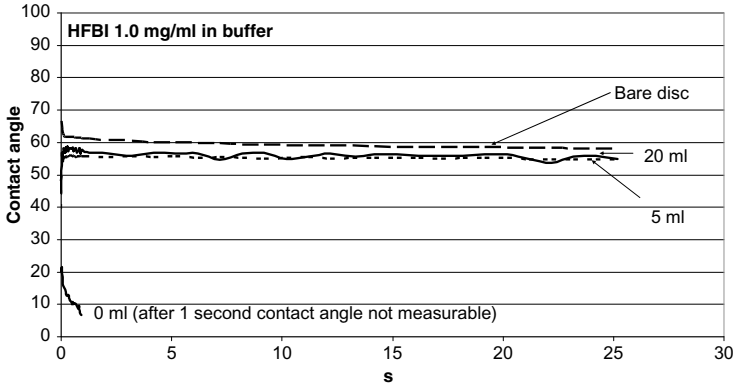

Fig. 8 Contact angles of water on stainless steel discs before and after exposing the surface to 1.0 mL/mL HFBI (in 50 mM sodium acetate buffer)
Note: Bare disc indicates the contact angle of clean disc. The amounts 0, 5, and 20 mL indicate the amount of water used for rinsing the disc after exposing to HFBI solution for 2 h. Great difference between the contact angle of water on rinsed discs and bare disc was not seen. That indicates that most of the HFBI solution was rinsed away

wear. The concentration did not show as clear correlation to the average friction coefficient as it did to wear. The presence of HFBIs in water significantly reduced both friction and wear of stainless steel compared with pure water. With the highest HFBI concentration 5 mg/mL in 50 mM sodium acetate buffer, the friction and wear values were only about 27–34 per cent of those with water. These results represented the lowest combination of average COF and wear of the molecules tested. The presence of albumin in buffer reduced the average friction coefficient to about 50 per cent of that obtained with water, whereas the average wear value with the highest concentration 5 mg/mL was only 12 per cent of that obtained with pure water. In the tests carried out with albumin in the lowest concentration 0.1 mg/mL in double deionized water, the highest friction and wear values of all the biomolecules were

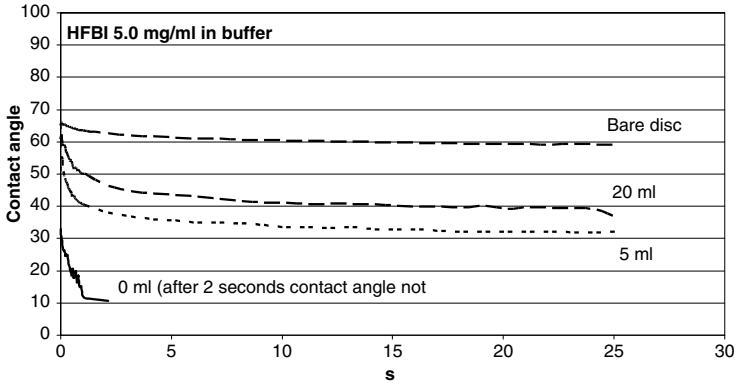

Fig. 9 Contact angles of water on stainless steel discs before and after exposing the surface to 5.0 mL/mL HFBI (in 50 mM sodium acetate buffer)
Note: Bare disc indicates the contact angle of clean disc. The amounts 0, 5, and 20 mL indicate the amount of water used for rinsing the disc after exposing to HFBI solution for 2 h. Difference between the contact angle of water on rinsed discs and bare disc was seen. That indicates that after rinsing there were still HFBI molecules on the steel surface

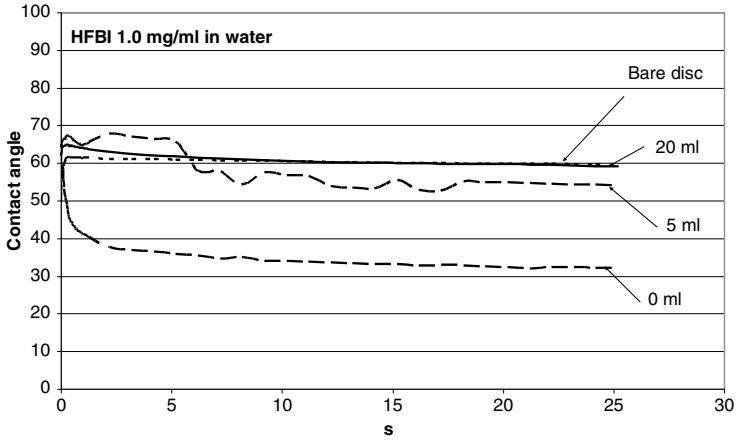

Fig. 10 Contact angles of water on stainless steel discs before and after exposing the surface to 1.0 mL/mL HFBI (in water)
Note: Bare disc indicates the contact angle of clean disc. The amounts 0, 5, and 20 mL indicate the amount of water used for rinsing the disc after exposing to HFBI solution for 2 h. Great difference between the contact angle of water on rinsed discs and bare disc was not seen. That indicates that most of the HFBI solution was rinsed away. Without rinsing, the contact angle of water was about 30°

observed. However, when the concentration was raised to 1 mg/mL, wear reduced dramatically by about 75 per cent and friction by about 39 per cent compared with friction and wear results of concentration 0.1 mg/mL. All the values of HFBIs and BSA were between those of mineral oil and water; thus, a significant enhancement to water lubrication was obtained with the biomolecules.

The POD tests were carried out at room temperature, but in comparison to many other proteins, HFBIs have excellent temperature stability because of their cross-linked globular structure. Thus, increasing the temperature (up to 100°C) would not affect the behaviour of HFBIs but may lead to less stable performance of other proteins, such as BSA. Temperature increase should lead to irreversible

denaturation of proteins in the solution and on the surface. This may not only lead to precipitation of a lubricative layer between the surfaces but also lower the amount of free proteins able to assemble at the surface after the layer wears out. It is obvious that the temperature near the steel-on-steel contact increases significantly even when the experiment is carried out at room temperature affecting some of the proteins in the above-described method.

4.2 Contact angle measurements

Contact angle measurements with highest concentration of HFBIs show that HFBIs can adsorb to the stainless steel surface. The explanation why contact angle after rinsing was not reduced in the case of the smallest concentrations may be related to the amount of HFBIs. HFBI was added on the steel disc, and on the top of the liquid, there was an air–water interface. It has been observed [**21**] that HFBIs can self-assemble on the air–water interfaces as monolayers. It might be so that the affinity to adhere on air–water interface is higher than that on steel. It is possible that after filling properly the air–water interface, only the rest of the molecules adsorb on the steel surface. When the liquid is between the contact of two solid surfaces, there is no air–water interface on the top and so molecules can adsorb on steel surface more efficiently also in smaller concentrations. In these tests, when O-rings were removed from steel surface after exposing the surface to the liquid, there was obvious film seen on them. That proves that there are surface-active molecules at the air–water interface.

It must be noticed that HFBI reduced the contact angle showing that the surface became more hydrophilic. It indicates that the hydrophilic part is upwards and hydrophobic part of the HFBI molecule adsorbs to the steel surface. The adsorption of the lubricant additives to the surface is one of the most important requirements in boundary lubrication.

5 CONCLUSIONS

In industrial machines and equipments, water lubrication needs smart compounds to enable adequate lubrication. The addition of biomolecules into water gave a clear reduction in friction, and the COF approached that of oil-lubricated sliding contacts. Biomolecules also reduced wear even by 75 per cent and more compared with water-lubricated contacts, and the reduction was larger with higher concentrations. HFBIs gave the best frictional behaviour of all the molecules tested. The lowest combination of average COF and wear was obtained with the highest concentration of HFBIs, i.e. 5 mg/mL in buffer and that is still relatively small concentration. Pure water did not function properly as a lubricant but gave a friction coefficient corresponding to dry friction in steel-on-steel contact.

Contact angle measurements showed that HFBI molecules adhere to the surface, and thus, they have a property to work as a lubricant additive in boundary lubrication regimes preventing the contact between two solid surfaces.

The results show that there is clear potential for moving from oil lubrication towards water lubrication using biomolecules as additives in water solution. However, more studies are needed to find and develop suitable molecules for different applications and the demanding operating conditions involved. Consideration must also be paid to the long-term stability of the new biomimetic lubricants.

ACKNOWLEDGEMENTS

The study was supported by the Academy of Finland (project Biomimetic water lubrication) and Tekes, the Finnish Funding Agency for Technology and Innovation (project New bioinspired and bio-based solutions for lubrication).

REFERENCES

1 **McFadden, C., Soto, C.,** and **Spencer, N. D.** Adsorption and surface chemistry in tribology. *Tribol. Int.*, 1997, **30**, 881–888.
2 **Dowson, D.** and **Neville, A.** Bio-tribology and biomimetics in the operating environment. *Proc. IMechE, Part J: J. Engineering Tribology*, 2006, **220**, 109–123.
3 **Neville, A., Morina, A., Liskiewicz, T.,** and **Yan, Y.** Synovial joint lubrication – does nature teach more effective engineering lubrication strategies? *Proc. IMechE, Part C: J. Mechanical Engineering Science*, 2007, **221**, 1223–1230.
4 **Holmberg, K.** *Elastohydrodynamic lubrication theory and its applications on machine elements*. Lic. Thesis, Helsinki University of Technology, 1980.
5 **Hills, B. A.** Boundary lubrication in vivo. *Proc. IMechE, Part H: J. Engineering in Medicine*, 2000, **214**, 83–94.
6 **Schwarz, I. M.** and **Hills, B. A.** Surface-active phospholipids as the lubricating component of lubricin. *Br. J. Rheumatology*, 1998, **37**, 21–26.
7 **Morina, A., Liskiewicz, T.,** and **Neville, A.** Designing new lubricant additives using biomimetics. *Design and Nature III: Comparing Design in Nature with Science and Engineering*, 2006, **87**, 157–166.
8 **Sarikaya, M., Tamerler, C., Jen, A. K.-Y., Schulten, K.,** and **Baneyx, F.** Molecular biomimetics: Nanotechnology through biology. *Nat. Mater.*, 2003, **2**, 577–585.

9 **Lim, G. H., Chua, P. S. K.,** and **He, Y. B.** Modern water hydraulics – the new energy-transmission technology in fluid power. *Appl. Energy*, 2003, **76**, 239–246.

10 **Masuko, M., Suzuki, A., Sagae, Y., Tokoro, M.,** and **Yamamoto, K.** Friction characteristics of inorganic or organic thin coatings on solid surfaces under water lubrication. *Tribol. Int.*, 2006, **39**, 1601–1608.

11 **Tomala, A., Karpinska, A., Werner, W. S. M., Olver, A.,** and **Störi, H.** Tribological properties of additives for water-based lubricants. *Wear*, 2010, **269**, 804–810.

12 **Santos, O., Nylander, T., Paulsson, M.,** and **Trägårdh, C.** Whey protein adsorption onto steel surfaces - effect of temperature, flow rate, residence time and aggregation. *J. Food Eng.*, 2006, **74**, 468–483.

13 **Claesson, P. M., Blomberg, E., Fröberg, J. C., Nylander, T.,** and **Arnebrant, T.** Protein interactions at solid surfaces. *Adv. Colloid Interface Sci.*, 1995, **57**, 161–227.

14 **Zappone, B., Ruths, M., Greene, G. W., Jay, G. D.,** and **Israelachvili, J. N.** Adsorption, lubrication, and wear of lubricin on model surfaces: polymer brush-like behavior of a glycoprotein. *Biophys. J.*, 2007, **92**, 1693–1708.

15 **Spencer, D. S., Xu, K., Logan, T. M.,** and **Zhou, H.-X.** Effects of pH, salt and macromolecular crowding on the stability of FK506-binding protein: an integrated experimental and theoretical study. *J. Mol. Biol.*, 2005, **351**, 219–232.

16 **Tanaka, N., Nishizawa, H.,** and **Kunugi, S.** Structure of pressure-induced denatured state of human serum albumin: a comparison with the intermediate in urea-induced denaturation. *Biochim. Biophys. Acta*, 1997, **1338**, 13–20.

17 **Farruggia, B.** and **Pico, G.** Thermodynamic features of the chemical and thermal denaturations of human serum albumin. *Int. J. Biol. Macromol.*, 1999, **26**, 317–323.

18 **Wang, Z., Huang, Y., Li, S., Xu, H., Linder, M. B.,** and **Qiao, M.** Hydrophilic modification of polystyrene with hydrophobin for time-resolved immunofluorometric assay. *Biosens. Bioelectron.*, 2010, **26**, 1074–1079.

19 **van der Vegt, W., van der Mei, H. C., Wösten, H. A. B., Wessels, J. G. H.,** and **Busscher, H. J.** A comparison of surface activity of the fungal hydrophobin SC3p with those of other proteins. *Biophys. Chem.*, 1996, **57**, 253–260.

20 **Linder, M., Szilvay, G., Nakari-Setälä, T.,** and **Penttilä, M.** Hydrophobins: the protein-amphiphiles of filamentous fungi. *FEMS Microbiol. Rev.*, 2005, **29**, 877–896.

21 **Linder, M. B.** Hydrophobins: proteins that self assemble at interfaces. *Curr. Opin. Colloid Interface Sci.*, 2009, **14**, 356–363.

22 **Coles, J. M., Chang, D. P.,** and **Zauscher, S.** Molecular mechanisms of aqueous boundary lubrication by mucinous glycoproteins. *Curr. Opin. Colloid Interface Sci.*, 2010, **15**, 406–416.

23 **Ahlroos, T., Linder, M., Helle, A., Holmberg, K., Nevanen, T.,** and **Varjus, S.** Biomimetic approach to boundary lubrication. In Proceedings of ECOTRIB09, the 2nd European Conference on *Tribology*, Pisa, Italy, 7–10 June 2009, pp. 473–478 (Edizioni ETS, Pisa).

24 **Roba, M., Naka, M., Gautier, E., Spencer, N. D.,** and **Crockett, R.** The adsorption and lubrication behavior of synovial fluid proteins and glycoproteins on the bearing-surface materials of hip replacements. *Biomaterials*, 2009, **30**, 2072–2078.

25 **Lee, S., Muller, M., Ratoi-Salagean, M., Vörös, J., Pasche, S., De Paul, S. M., Spikes, H. A., Textor, M.,** and **Spencer, N. D.** Boundary lubrication of oxide surfaces by poly(L-lysine)-g-poly(ethylene glycol) (PLL-g-PEG) in aqueous media. *Tribol. Lett.*, 2003, **15**, 231–239.

26 **Feiler, A. A., Sahlholm, A., Sandberg, T.,** and **Caldwell, K. D.** Adsorption and viscoelastic properties of fractionated mucin (BSM) and bovine serum albumin (BSA) studied with quartz crystal microbalance (QCM-D). *J. Colloid Interface Sci.*, 2007, **315**, 475–481.

27 **Lee, S., Müller, M., Rezwan, K.,** and **Spencer, N. D.** Porcine gastric mucin (PGM) at the water/poly(dimethylsiloxane) (PDMS) interface: influence of pH and ionic strength on its conformation, adsorption, and aqueous lubrication properties. *Langmuir*, 2005, **21**, 8344–8353.

28 **Stachowiak, G. W.** and **Batchelor, A. W.** *Engineering tribology*, 3rd edition, 2005, p. 801 (Elsevier, Amsterdam, The Netherlands).

II

Hakala, T.J., Laaksonen, P., Saikko, V., Ahlroos, T., Helle, A., Mahlberg, R., Hähl, H., Jacobs, K., Kuosmanen, P., Linder, M.B., Holmberg, K. (2012) Adhesion and tribological properties of hydrophobin proteins in aqueous lubrication on stainless steel surfaces. *RSC Advances,* 2 (26), 9867-9872.

View Article Online / Journal Homepage / Table of Contents for this issue
Dynamic Article Links

RSC Advances

Cite this: *RSC Advances*, 2012, **2**, 9867–9872

www.rsc.org/advances

PAPER

Adhesion and tribological properties of hydrophobin proteins in aqueous lubrication on stainless steel surfaces†

Timo J. Hakala,*[a] Päivi Laaksonen,[ab] Vesa Saikko,[c] Tiina Ahlroos,[a] Aino Helle,[a] Riitta Mahlberg,[a] Hendrik Hähl,[b] Karin Jacobs,[b] Petri Kuosmanen,[c] Markus B. Linder[a] and Kenneth Holmberg[a]

Received 23rd May 2012, Accepted 17th August 2012
DOI: 10.1039/c2ra21018e

Macroscale tribological properties of hydrophobin layers bound on stainless steel surfaces were investigated in an aqueous environment. Emphasis was on boundary lubrication because water easily fails in hydrodynamic lubrication due to its low viscosity. We studied the affinities of two different proteins, HFBI and FpHYD5, on stainless steel and their ability to bind water at the surface by combining quartz crystal microbalance (QCM-D) and ellipsometry. Both proteins contained an adhesive hydrophobic domain, but FpHYD5 also had a very strongly hydrating carbohydrate structure attached to it. The lubrication properties of the proteins were studied with two different methods, pin-on-disc (POD) (stainless steel *vs.* stainless steel) and circular translation pin-on-disc (CTPOD) (UHMWPE *vs.* stainless steel). It was observed that both hydrophobins could adhere to the stainless steel surface and form highly hydrated layers. Both proteins reduced friction and wear of the sliding contact between two stainless steel surfaces. With UHMWPE against stainless steel, the hydrophobins prevented the polyethylene transfer to the counterface. The lowest coefficient of friction (COF) 0.13 was observed when FpHYD5 hydrophobins were employed in pure water. On the other hand, the lowest wear was observed when FpHYD5 proteins were added in a 50 mM sodium acetate buffer. Increasing the water content and loosening the hydrophobin film structure on the stainless steel surface led to a reduction in friction and wear.

Introduction

Nature has developed effective means of water based lubrication—in synovial joints, for example—that have not been outperformed by synthetic approaches. As a lubricant, water is considered challenging due to its low viscosity. However, when compared to existing solutions that include the use of oil and additives, use of water as a lubricant in certain applications *e.g.* in the food industry is very attractive, while development of water-based lubrication systems is easily motivated by environmental and economic drivers. Proteins such as lubricin and mucin have been identified as important building blocks of the effective and complex lubrication system of cartilage, mucosa and other biological low friction surfaces.[1] Use of adhesive proteins as lubricant additives has thus gained interest among tribologists.[2]

The main principle in water lubrication with biomolecules is to create a water-containing layer between the surfaces.[3] Certain biomolecules, such as adhesive proteins, are known to be able to adhere to different surfaces and to form layers that decrease friction and wear when compared to plain surfaces.[1,4,5] When adsorbed to the surface, water molecules that hydrate proteins will be brought close to the target surface, thus enhancing formation of a stable and thin water film between the contacting surfaces.[6] Adsorption of the proteins on the surface is essential, and is often driven by the surface energies.[7] Typically, adsorption of proteins reduces surface energy, which in practice makes the surface more hydrophilic, meaning that water can easily form a lubricating film on the surface.

Since lubrication is a dynamic event, the dynamics and affinity of the adhesive molecules are very important. In order to prevent the direct contact of the surfaces and provide low friction and reduced wear, the molecules need to adhere strongly enough to the surface, and adsorb to the surface quickly to replace those that are sheared away during sliding contact.[1] It has been observed that a polymer structure combining a surface-attaching moiety with a water-binding moiety improves surface wettability and lubrication.[8] In general terms, adhesion of the biomolecules to surfaces is based on hydrophobic interactions, electrostatic interaction and van der Waals forces between molecules and the surface. Adsorption and adhesion properties are in addition

[a]*VTT Technical Research Centre of Finland, P.O. Box 1000, FI-02044, VTT, Finland. E-mail: timo.j.hakala@vtt.fi; Fax: +358 20 722 7069; Tel: +358 40 770 2369*
[b]*Saarland University, Experimental Physics, Campus E2 9, 66123 Saarbruecken, Germany*
[c]*Aalto University School of Engineering, P.O. Box 4300, 00076, Aalto, Finland*

† Electronic Supplementary Information (ESI) available: QCM, ellipsometry, FTIR and CTPOD data, as well as pictures of worn surfaces. See DOI: 10.1039/c2ra21018e

related to the conformation of the protein that can be affected by thermal and mechanical processes during tribological contact, as well as to changes in pH, ionic strength and temperature of the environment.[9–12] Furthermore, the environment may also affect the water content and swelling of the adsorbed layer and, thus, the lubrication.[11,13]

Fungal adhesion proteins, belonging to a class of proteins called hydrophobins, have strong interactions with certain surfaces, typically hydrophobic surfaces such as graphite and Si. Hydrophobins are small proteins (~ 3 nm in height) that have a strongly cross-linked fold containing four disulfide bridges, making them very stable against conformational changes. The most striking feature of these proteins is a patch of hydrophobic residues on one of the faces, leading to a structure resembling a surfactant with a hydrophilic and a hydrophobic part. In solution, hydrophobic interactions between individual proteins drive the formation of supramolecular dimers or tetramers. In the vicinity of interfaces, however, assembly of the protein at the interface is strongly preferred and the proteins adsorb, forming a monolayer. Lateral interactions between the proteins lead to strongly coherent surface films. Since amphiphilic hydrophobin forms a monolayer whose sides have significantly differing surface energies, these monolayers strongly modify the wetting properties of the target surface.

Here, a wild-type hydrophobin HFBI and a glycosylated hydrophobin FpHYD5 were studied as lubricant additives in aqueous environment on stainless steel. We investigated the affinity of the proteins to stainless steel and the amount of bound water in different conditions. The same conditions were applied in the tribological tests, performed on macroscopic scale.

Results

Adsorption of proteins on stainless steel

Binding of both proteins, HFBI and FpHYD5 on stainless steel (SS2343/AISI316) was studied by QCM-D and ellipsometry. QCM-D measures the additional mass bound on the sensor surface, including the solvent layer that is bound to the adsorbing molecules, whereas ellipsometry can only detect the so-called dry mass. Thus the combination of these methods allowed measurement of the amount of water in the protein layer. The bound masses of both proteins on stainless steel are presented in Fig. 1 and 2. The bound masses were calculated from the frequency changes measured by QCM-D by the Sauerbrey equation:[14]

$$\Delta m = -\frac{C\Delta f}{n} \quad (1)$$

where C is a constant 17.7 $ngHz^{-1}cm^{-2}$ arising from the properties of the quartz crystal, Δf is the frequency change and n is the overtone of the oscillations. This equation applies only for mass that is rigidly bound to the sensor surface, *i.e.* has similar acoustic properties as the quartz crystal. The validity of the above equation can be evaluated by measuring the dissipation signal caused by the adsorbed film. The Sauerbrey equation is considered valid when dissipation of the crystal does not increase significantly (several units) during the film formation. The measured dissipation values were rather low, less than 0.4×10^{-6}, and thus the Sauerbrey equation was considered valid for evaluation of bound mass.

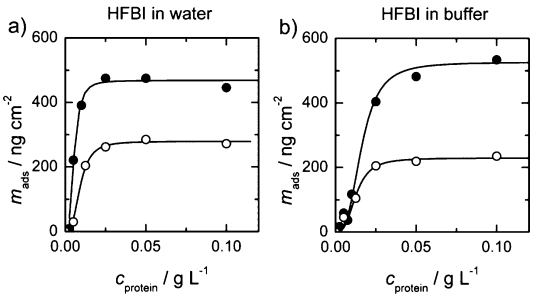

Fig. 1 Binding curves of HFBI in water and in a 50 mM acetate buffer. The closed symbols are the adsorbed masses measured by QCM, whereas the open symbols represent ellipsometry data. A simple one binding site curve was fitted to all data. With QCM, a significantly higher mass was measured in both conditions.

For the evaluation of the data recorded by ellipsometry, an optical box model consisting of stainless steel (n_{ss} = 2.157, k_{ss} = 3.323), the protein film (n_f = 1.460) and the water or buffer solution (n_s = 1.3367) was applied. The absolute amount of adsorbed protein Γ was determined with de Feijter's formula:

$$\Gamma = d_f \frac{n_f - n_s}{dn/ds} \quad (2)$$

The refractive index of the protein was assumed to be a linear function of its concentration. The increment of the refractive index, due to concentration increase with dn/dc, was taken from literature and assumed constant 0.183 cm^3g^{-1}.[15–17]

Fig. 1 and 2 show the measured amounts of adsorbed proteins from water and acetate buffer as a function of protein concentration. Saturation of the adsorbed amount for HFBI and FpHYD5 was achieved near concentrations 0.25 g L^{-1} and 0.1 g L^{-1} correspondingly. In Fig. 1 the x-axes were cut for clarity to 0.125 g L^{-1}. The data was modelled by a simple Langmuir adsorption isotherm, taking into account possible cooperativity of binding. The following equation was fitted to the measured adsorbed mass m_{ads} of the proteins.

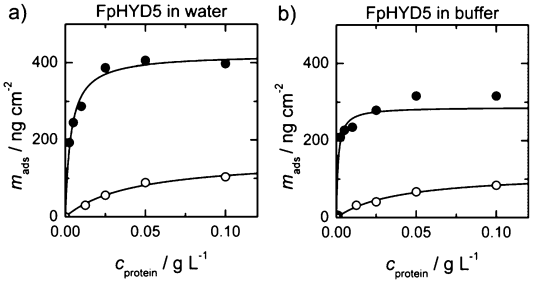

Fig. 2 Binding curves of FpHYD5 in water and in a 50 mM acetate buffer. The closed symbols are the adsorbed masses measured by QCM, whereas the open symbols represent ellipsometry data. A simple one binding site curve was fitted to all data. With QCM, a significantly higher mass was measured in both conditions.

$$m_{ads} = B_{max}\frac{(Kc)^{n'}}{1+(Kc)^{n'}} \quad (3)$$

Here, B_{max} denotes the maximum adsorbed amount of the protein, K is the equilibrium constant of adsorption, c the protein concentration and n' the number of co-operative binding sites. The results from the fitting of this equation to all the measurements, including both QCM-D and ellipsometry, are presented in Table 1. The equilibrium constant is given as the affinity constant K_d, which is the equilibrium constant of desorption and is often used as the measure of binding affinity of biomolecules.

In the case of HFBI (see Fig. 1), the binding curves have slightly sigmoidal shapes, thus the number of co-operative binding sites n' was greater than 1. The best fit to the data was obtained by assuming n' = 3 for HFBI. For FpHYD5, assumption n' = 1 fitted the data best and thus n was fixed as one.

The amount of proteins that bind on the stainless steel surface was obtained from the data measured by ellipsometry. The ionic strength of the protein solutions had only a minor effect on the protein coverage, showing slightly smaller amounts of bound protein from buffer. The most significant effect of buffer was obtained by QCM-D in the affinity of HFBI (Fig. 1), where the affinity increased significantly from 0.54 g L^{-1} to 1.61 g L^{-1} when adsorption occurred from buffer instead of water.

In every series of measurements, the amount of bound mass measured with QCM-D was significantly higher than the amount measured by ellipsometry. The difference between the corresponding two binding curves denotes the amount of water associated in the surface layer in each condition. The water content was reasonably high, as much as 64% of the total for FpHYD5 and between 40% and 56% for HFBI when comparing the B_{max} values. When adsorbed from buffer, the HFBI layer could bind a larger amount of water than in lower ionic strength in water. For FpHYD5 the situation was the opposite, and the absolute amount of bound water was higher in pure water.

Pin-on-disc (POD) experiments

The ability of hydrophobins to act as lubricant additives in water was studied by evaluating the coefficient of friction (COF) and wear amount of a stainless steel sphere in sliding contact against a stainless steel disc. It was observed that friction and wear measured for acetate buffer was much lower compared to ion exchanged water (Fig. 3). When 1.0 g L^{-1} of hydrophobins HFBI or FpHYD5 were added, friction and wear were reduced, regardless of whether water or sodium acetate buffer was used. The lowest coefficients of friction were measured for FpHYD5 in water, and lowest wear for FpHYD5 in buffer. The initial coefficient of friction was 0.2 when lubricated with HFBI in water, but this began to increase after a certain amount of sliding.

Dependence of the tribological properties of the hydrophobins concentration was studied by carrying out tests in a 50 mM acetate buffer solution with 2 N load and velocity of 50 mm s^{-1}, using protein concentrations of 0.1 g L^{-1}, 1.0 g L^{-1} and 5.0 g L^{-1}. The lowest concentration of both proteins did not reduce friction compared to the buffer solution, and sometimes even a small

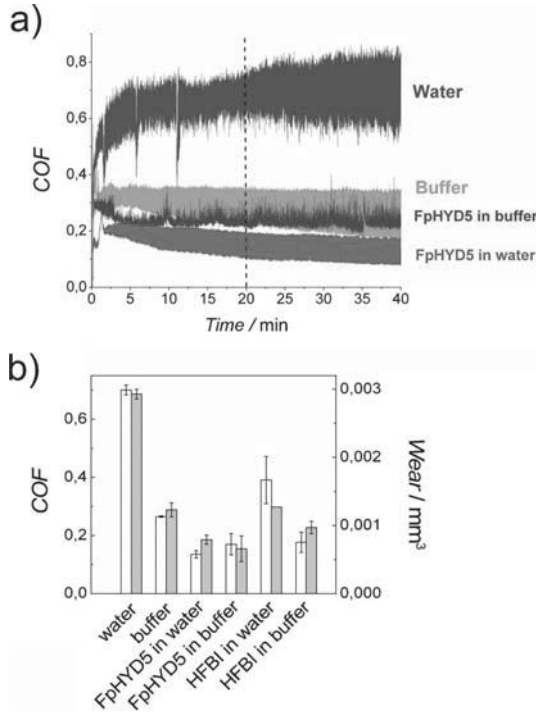

Fig. 3 a) Coefficient of friction *vs.* time curves and b) average coefficients of friction (white bars) and wear volumes (grey bars) of different lubricants in pin-on-disc experiments. HFBI and FpHYD5 concentrations were 1.0 g L^{-1}. The tests were carried with 2 N load, velocity 50 mm s^{-1}, and sliding distance 120 m. The coefficient of friction was determined as an average from 20 to 40 min, and scatter was determined as variation between the average coefficients of friction.

Table 1 Values for maximum bound amount (B_{max}) equilibrium constant (K) and affinity constant (K_d) for HFBI and FpHYD5 in water and in 50 mM NaAc buffer resulting from the data fitting. The number of co-operative sites and absolute mass of bound water in the layer based on the B_{max} values is also given

	B_{max},[a]/ng cm^{-2}	K_d[a]/10^2 g L^{-1}	B_{max} [b]/ng cm^{-2}	K_d[b]/10^2 g L^{-1}	n'	m_{water}/ng cm^{-2}
$HFBI^w$	468	0.54	279	0.92	3	189
$HFBI^b$	526	1.61	229	1.26	3	297
$FpHYD5^w$	422	2.00	153	0.17	1	269
$FpHYD5^b$	326	2.42	117	0.17	1	209

[a] Measured with QCM-D. [b] Measured with ellipsometry.

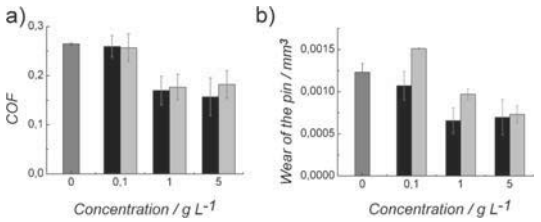

Fig. 4 a) The effect of protein concentration on coefficient of friction (COF) and b) on the wear volume of the stainless steel sphere in pin-on-disc experiments. Proteins were in 50 mM sodium acetate buffer. Both FpHYD5 (black columns) and HFBI (grey columns) showed decrease in friction and wear as a function of the concentration. Concentration 0 refers to 50 mM sodium acetate buffer pH 5. All lubricants were tested with 2 N load, sliding velocity 50 mm s^{-1} and sliding distance 120 m.

increase in friction and wear was observed when a steady state of friction was achieved (Fig. 4). Friction measured with 1.0 and 5.0 g L^{-1} protein solutions was very similar, thus it appeared that increasing the protein concentration above 1.0 g L^{-1} did not further reduce friction.

The wear volume of lubricated contacts was calculated by measuring the dimensions of the wear track of the stainless steel sphere after sliding on the stainless steel disc (see ESI, Fig. S1–S3†). The sliding distance of the sphere was 120 m. Surprisingly, an addition of a small amount of HFBI (0.1 g L^{-1}) in the buffer solution increased the wear of the sphere. For HFBI, the wear of the sphere was generally higher than for FpHYD5, and there was stronger dependency on the concentration. an increase of FpHYD5 concentration from 1.0 to 5.0 g L^{-1} in the buffer solution no longer reduced wear. However, the wear of the sphere reduced almost linearly as a function of concentration when lubricated with HFBI in buffer.

Circular translation pin-on-disc (CTPOD) experiments. With hydrophobin containing lubricants, the tests showed coefficients of friction within a narrow range of 0.08 to 0.18. The discs were not damaged in the tests. With water, the coefficient of friction was of the same order of magnitude (0.13) but the discs showed polyethylene transfer indicating that boundary lubrication was not effective. In dry sliding, the transfer was even heavier (see ESI Fig. S4†), and coefficient of friction was as high as 0.36. The 50 mM sodium acetate buffer gave varying results. When the discs remained undamaged, coefficient of friction values between 0.05 and 0.10 were measured and no transfer was detected with the FTIR analyses. Higher values of 0.16 and 0.18 were accompanied by transfer (see ESI Fig. S5†) and scratches on the disc. In these tests the standard contact pressure of 4.4 MPa was used. When the pressure was reduced to 2.3 MPa, the discs remained undamaged and coefficient of friction was between 0.13 and 0.16. It was common that the wear surface of the pin was markedly deformed (see ESI Fig. S6†).

Hydrophobins acted as boundary lubricants in CTPOD tests as they prevented polyethylene transfer to the stainless steel counterface. However, friction was not reduced compared to the acetate buffer or water (see ESI Fig. S7†).

Discussion

Adsorption of proteins on stainless steel surfaces

The adsorbed dry weight of both proteins on stainless steel was higher in water than in 50 mM buffer. In the case of HFBI, the amount of proteins bound from water corresponds to a rather densely packed monolayer of molecules, where each molecule occupies an area of $\sim$4.6 nm^2, which is close to the dimensions of a single HFBI molecule. When proteins are packed this closely there is less water bound within the molecules in the layer, which is observed as lower mass in QCM-D measurement when compared to the measurement in buffer. In the case of FpHYD5, being roughly the same size as HFBI, the bound molar amount of protein was lower and corresponded to a much lower density where, on average, there is one molecule in a 14.7 nm^2 area. Thus, FpHYD5 layers can contain a much larger fraction of water between the protein molecules. The water contents were especially large in the layer adsorbed from pure water, where the electrostatic interactions are more pronounced due to low ionic strength, and hydration of the proteins and glycans is stronger. Interestingly, the dissipation of all layers was very low; thus the water within the layers was tightly associated with the protein layers.

The formation of tightly bound films of HFBI was also reflected by the number of co-operative sites (n = 3), which, theoretically indicates that the protein binds to the surface in small clusters containing approximately three proteins. Although this cannot be taken as an absolute structure of the protein film, the co-operative nature of the binding indicates that the proteins interact strongly with each other when adsorbing to the surface. Strong lateral interactions are typical for hydrophobin films and have been observed earlier at an air/water interface.[18] No sign of co-operativity was observed for FpHYD5. A probable reason for this is the rather large carbohydrate structure (1.7 kDa) which may cause electrostatic repulsion and steric hindrance between the molecules, thus weakening the lateral interaction in the protein layer.

Besides the qualitative behaviour, there was a difference in the ability of the proteins to absorb water. The glycosylated FpHYD5 formed layers where most of the mass was water. We believe that this is due to the carbohydrate structures attached to the protein. Thus, a combination of an anchoring group (hydrophobin) and a water absorbing group (carbohydrate) enabled formation of reasonably thick layer of water on the surface. Hydration of proteins in aqueous solution is well known, but not always taken into account when analysing surface films of proteins. The significance of water that can be bound to an interface, such as stainless steel, can be of great importance when considering the behaviour of such interfaces.

Tribology

The results of friction measurements showed that friction and wear in water can be reduced when 50 mM sodium acetate is added. This may be due to the hydration lubrication by hydrated ions adsorbed on the stainless steel surface, or to change in environment (pH).[6,19]

At concentrations as low as 0.1 g L^{-1}, the proteins did not enhance lubrication compared to the buffer solution. However, a

decrease in friction and wear was observed when the protein concentration was increased to 1.0 g L^{-1}. Thus, even though a concentration of 0.1 g L^{-1} of FpHYD5 was enough to provide a saturation of proteins on the stainless steel surface in the binding studies, excess proteins were needed to gain a good lubrication in terms of both reduced friction and wear. This is most probably due to the dynamic situation during the tribological measurement, where the test surfaces were in constant motion and some of the protein sheared away. The adsorption rate of the proteins depended on their concentration (see ESI Fig. S8–S10†), which means that the recovery of the protein layer was faster with the higher concentrations. This could explain why the friction remained low with higher protein concentrations.

By combining the data from the adsorption measurements of Table 1 and the tribology measurements of Fig. 3b, an interesting dependency was observed: wear and friction decreased linearly as a function of the water contents of the protein layer. The data is presented in Fig. 5a, showing a clear decrease of wear and friction as the water percentage increased from 40% to nearly 65%. This shows that the water binding carbohydrate moiety improved the lubrication properties. It is known that many of the proteins essential in synovial lubrication are glycosylated by these kinds of carbohydrate moieties.[1] Curiously, the correlation of wear and friction with the bound mass of the proteins was positive, meaning the denser the protein layer, the higher friction and wear it caused (Fig. 5b). This indicates that the obtained decrease in friction was indeed caused by the thin water layer and not by the protein molecules themselves.

We have shown that both of the hydrophobins formed monolayers on the stainless steel surfaces. We found that the increase in water content on the layer attached to the surface reduces friction and wear. However, a higher amount of adsorbed proteins on the surface increases friction and wear. According to the results it can be assumed that the high amount of water associated with the protein layer and fast adhesion that guarantees rapid replacement of sheared molecules are beneficial for good lubrication.

Experimental

Production and purification of the proteins

HFBI and FpHYD5 were produced using recombinant strains of *T. reesei* and purified by a two-phase extraction and RP-HPLC as described previously.[20,21] The molar masses of HFBI and glycosylated FpHYD5 are 7.54 kDa and 9.21 kDa respectively. The mass of the glycan structure in FpHYD5 is ~1.7 kDa.

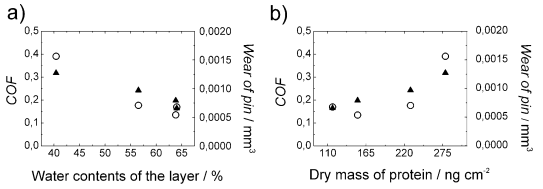

Fig. 5 a) Coefficient of friction (COF) (○) and wear (▲) as a function of water contents of the protein layer. b) Coefficient of friction (○) and wear (▲) as a function of the dry mass of protein adsorbed on a stainless steel surface. The data is combined from adsorption and tribology measurements of 1.0 g L^{-1} HFBI and FpHYD5 in water and 50 mM buffer solutions.

Adsorption measurements by QCM-D

A quartz crystal microbalance with dissipation monitoring (QCM-D) was used for simultaneous measurement of frequency and dissipation (D4-QCM system, Biolin Scientific, Sweden) to follow the binding of proteins on stainless steel sensors (SS2343, Biolin Scientific Sweden). First the sensor chips were cleaned in a standard UV/ozone chamber for 10 min and exposed to hot $H_2O/NH_3/H_2O_2$ mixture (1 : 1 : 5) for 10 min, followed by rinsing with Milli-Q water. The protein adsorption measurements were carried out by injecting 1 ml of protein solutions, in either milliQ water (Millipore, US) or 50 mM sodium acetate (Sigma-Aldrich, US) using a flow of ~ 0.1 mL min^{-1} to the chamber and following the frequency and dissipation responses.

Adsorption measurements by ellipsometry

Ellipsometric measurements were carried out using a multi-wavelength ellipsometer (EP3, Nanofilm, Göttingen, Germany) operated at a single wavelength of 532 nm. The device was set up in a PCSA (polarizer-compensator-sample-analyzer) configuration with an angle of incidence of 65° to the surface normal. A stainless steel QCM-D sensor was placed in a home-made liquid cell that was filled with the corresponding liquid. After equilibration of the surface, the protein solution was injected into the cell by hand with a syringe. Before performing the experiments the sensor was cleaned in a similar manner to the QCM-D experiments. The ellipsometric angles Δ and Ψ were recorded continuously over time *via* the nulling ellipsometry principle in two zones.[17]

Pin-on-disc experiments

The friction force was measured constantly in pin-on-disc experiments. The pin-on-disc device was designed and developed at VTT. The load used in the experiments was 2 N, sliding velocity 50 mm s^{-1} and sliding distance 120 m. Three parallel experiments (with HFBI in water two parallel experiments) were carried out.

The test specimens were stainless steel discs (AISI 440B) with a diameter of 40 mm (R_a value 0.05 μm or better) and stainless steel spheres (AISI 420) with a diameter of 10 mm. The same disc was used in several tests, and before each test was cleaned by ultrasonic washing in petroleum ether and in ethanol, 5 min each. A new sphere was used in every test.

The lubricant amount in each test was 0.6 ml, added as droplets on to disc by pipette. The lubricant covered the entire area of the wear track. The coefficient of friction was measured as an average value from 20 to 40 min (from 60 to 120 m of sliding). Contact pressures at the end of the experiments were between 4 and 22 MPa depending on the amount of wear of the stainless steel sphere.

Circular translation pin-on-disc experiments

The CTPOD device has been described in detail elsewhere.[22] Briefly, the pin translates along a circular track of 10 mm

diameter relative to the disc. The sliding speed is constant, 31.4 mm s^{-1}. Such low speed ensures that a boundary (or mixed) lubrication mechanism prevails. Because of the circular translation, the direction of sliding changes continually relative to the pin. Therefore, as there is no rotation, uniaxial grooving is avoided. The device is primarily designed for friction measurements with relatively high loads, up to 1 kN. The disc holder is supported by low-friction ball bearings. The rotation of the disc is prevented by a load cell and a lever arm. The frictional torque and coefficient of friction can be calculated from the load signal. In the present study, the pin was a flat-ended cylinder with a diameter of 9 mm and length of 12 mm. The pin was made from UHMWPE GUR 1050. The disc was made from austenitic stainless steel 316 (ASTM F 138), polished to a surface roughness R_a of 0.01 μm. Hardness of the disc is 200 HB. The contact was flat-on-flat and the nominal contact pressure 4.4 MPa. The test duration was 5 h with hydrophobins and 24 h with reference lubricants. The tests were run at room temperature. The reported COF value was the steady-state value at the end of the test. The specimens were surrounded by a chamber that contained the test lubricant of 3 to 5 ml volume. Due to the high wear resistance of UHMWPE, the test durations were not sufficient for meaningful gravimetric wear measurements. Optical microscopy was used to study the sliding surfaces with respect to possible damage, such as scratching or polyethylene transfer.

FTIR analyses of the CTPOD specimens

In order to determine whether any polyethylene transfer was formed on the CTPOD discs during the test, the discs were rinsed after the test with 5 ml of distilled water ($\sim$1 ml cm^{-2}), air-dried overnight, and analyzed with FTIR (Fourier transform infrared spectroscopy). The FTIR analyses of the discs were carried out using the reflectance mode. As a reference sample a UHMWPE sheet was used and analysed with a diamond micro-ATR. The instrument employed for the analyses was a BioRad FTS 6000 FTIR spectrometer interfaced with a UMA 500 IR-microscope equipped with an MCT detector. All the spectra were collected at 4 cm^{-1} spectral resolution. The background spectra were collected from the respective clean substrates.

Conclusions

It was shown that hydrophobin proteins adsorb and form a lubricating monolayer film on a stainless steel surface. The formation of the protein layer significantly reduced friction and wear of the stainless steel/stainless steel contact and reduced transfer of the polyethylene *vs.* stainless steel contact. Higher water content in the film and a lower amount of adsorbed proteins on the stainless steel surface decrease friction and wear on the studied steel qualities. The water content of the film was increased by attaching a carbohydrate moiety to a hydrophobin protein, and controlled by the conditions.

Acknowledgements

We thank Riitta Suihkonen for purification of the proteins, and for funding: Tekes—the Finnish Funding Agency for Technology and Innovation (project New bioinspired and bio-based solutions for lubrication), Academy of Finland (project Biomimetic water lubrication), VTT Technical Research Centre of Finland and Aalto University School of Engineering. PL, HH and KJ acknowledge partial funding by the German Research Foundation via GRK 1276.

References

1 J. M. Coles, D. P. Chang and S. Zauscher, *Curr. Opin. Colloid Interface Sci.*, 2010, **15**, 406–416.
2 T. Ahlroos, T. J. Hakala, A. Helle, M. B. Linder, K. Holmberg, R. Mahlberg, P. Laaksonen and S. Varjus, *Proc. Int. Mech. Eng. J*, 2011, **225**, 1013–1022.
3 M. P. Heuberger, M. R. Widmera, E. Zobeley, R. Glockshuber and N. D. Spencer, *Biomaterials*, 2005, **26**, 1165–1173.
4 G. E. Yakubov, J. McColl, J. H. H. Bongaerts and J. J. Ramsden, *Langmuir*, 2009, **25**, 2313–2321.
5 B. Zappone, M. Ruths, G. W. Greene, G. D. Jay and J. N. Israelachvili, *Biophys. J.*, 2007, **92**, 1693–1708.
6 U. Raviv and J. Klein, *Science*, 2002, **297**, 1540–1543.
7 M. B. Linder, *Curr. Opin. Colloid Interface Sci.*, 2009, **14**, 356–363.
8 K. Chawla, S. Lee, B. P. Lee, J. L. Dalsin, P. B. Messersmith and N. D. Spencer, *J. Biomed. Mater. Res., Part A*, 2009, **90A**, 742–749.
9 C.-B. Yang, H.-W. Fang, H.-L. Liu, C.-H. Chang, M.-C. Hsieh, W.-M. Lee and H.-T. Huang, *Chem. Phys. Lett.*, 2006, **431**, 380–384.
10 H.-W. Fang, M.-C. Hsieh, H.-T. Huang, C.-Y. Tsai and M.-H. Chang, *Colloids Surf., B*, 2009, **68**, 171–177.
11 L. Macakova, G. E. Yakubov, M. A. Plunkett and J. R. Stokes, *Tribol. Int.*, 2011, **44**, 956–962.
12 S. Lee, M. Müller, K. Rezwan and N. D. Spencer, *Langmuir*, 2005, **21**, 8344–8353.
13 R. Heeb, S. Lee, N. V. Venkataraman and N. D. Spencer, *ACS Appl. Mater. Interfaces*, 2009, **5**, 1105–1112.
14 G. Sauerbrey, *Z. Phys.*, 1959, **155**, 206–222.
15 J. A. de Feijter, J. Benjamins and F. A. Veer, *Biopolymers*, 1978, **17**, 1759.
16 V. Ball and J. J. Ramsden, *Biopolymers*, 1998, **46**, 489.
17 H. G. Tompkins and E. A. Irene, ed., *Handbook of Ellipsometry*, Heidelberg, Springer, 2005.
18 G. R. Szilvay, A. Paananen, K. Laurikainen, E. Vuorimaa, H. Lemmetyinen, J. Peltonen and M. B. Linder, *Biochemistry*, 2007, **46**, 2345–2354.
19 G. W. Stachowiak and A. W. Batchelor, *Engineering Tribology*, 3rd edition, Elsevier, Amsterdam, 2005.
20 M. B. Linder, M. Qiao, F. Laumen, K. Selber, T. Hyytiä, T. Nakari-Setälä and M. E. Penttilä, *Biochemistry*, 2004, **43**, 11873–11882.
21 T. Sarlin, T. Kivioja, N. Kalkkinen, M. B. Linder and T. Nakari-Setälä, *J. Basic Microbiol.*, 2011, **51**, 1–11.
22 V. Saikko, *Proc. Inst. Mech. Eng., Part H*, 2006, **220**, 723–731.

Electronic Supplementary Material (ESI) for RSC Advances

Electrical Supplementary Information for

Adhesion and tribological properties of hydrophobin proteins in aqueous lubrication on stainless steel surfaces

Timo J. Hakala*[a], Päivi Laaksonen[a,b], Vesa Saikko [c], Tiina Ahlroos[a], Aino Helle[a], Riitta Mahlberg[a], Hendrik Hähl[b], Karin Jacobs[b], Petri Kuosmanen[c], Markus B. Linder[a] and Kenneth Holmberg[a]

Wear in pin-on-disc (POD) experiments

Wear of the stainless steel sphere (diameter 10 mm) after sliding on a stainless steel disc was measured from the wear volume of the sphere. Figures S1-S3 present optical microscope images of the wear tracks. The dimensions of the worn area were used for calculation of the wear volume.

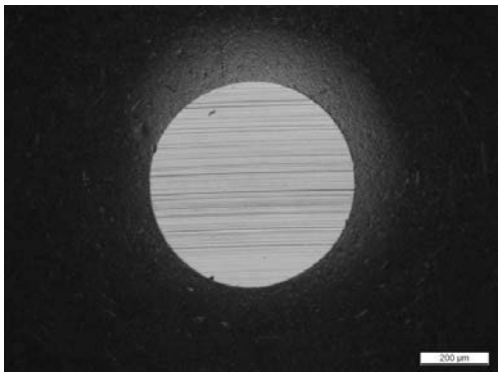

Figure S1. Wear track of the stainless steel sphere after 120 m of sliding on a stainless steel disc. The lubricant was 50 mM sodium acetate buffer pH 5. The scale bar is 200 µm.

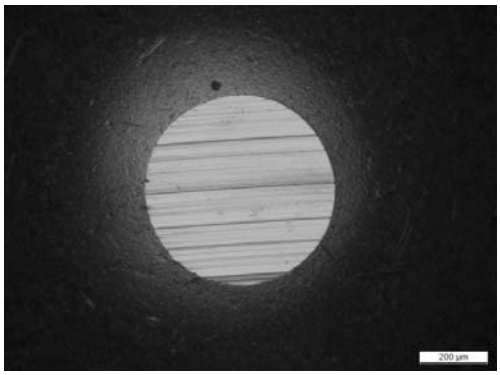

Figure S2. Wear track of the stainless steel sphere after 120 m of sliding on a stainless steel disc. The lubricant was HFBI 1.0 mg/ml in 50 mM sodium acetate buffer pH 5. The scale bar is 200 µm.

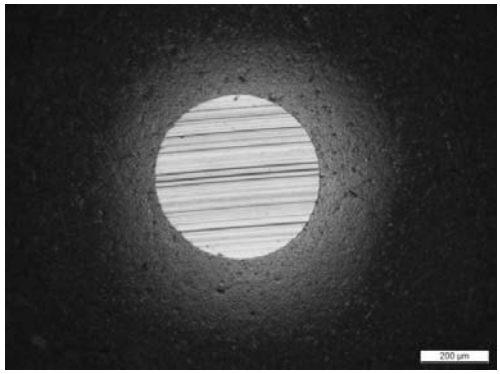

Figure S3. Wear track of the stainless steel sphere after 120 m of sliding on a stainless steel disc. The lubricant was FpHYD5 1.0 mg/ml in 50 mM sodium acetate buffer pH 5. The scale bar is 200 µm.

Transfer in tribological experiments by circular translation pin-on-disc (CTPOD)

In dry sliding, the transfer of polyethylene (UHMWPE) on the stainless steel disc was heavy and the COF was as high as 0.36. Transfer layers were tenacious and could only be removed by repolishing. A microscopy image of the stainless steel surface after a dry experiment is shown in Figure S4.

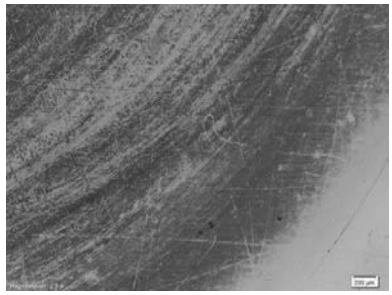

Figure S4. Optical micrograph from the stainless steel disc of a dry test showing the UHMWPE transfer layer. Edge of contact zone. Lower right corner shows original polished surface. The scale bar is 200 µm.

FTIR was used to investigate the polyethylene transfer on the stainless steel disc (Fig. S5). It was observed that hydrophobins were able to reduce transfer compared to plain buffer solution.

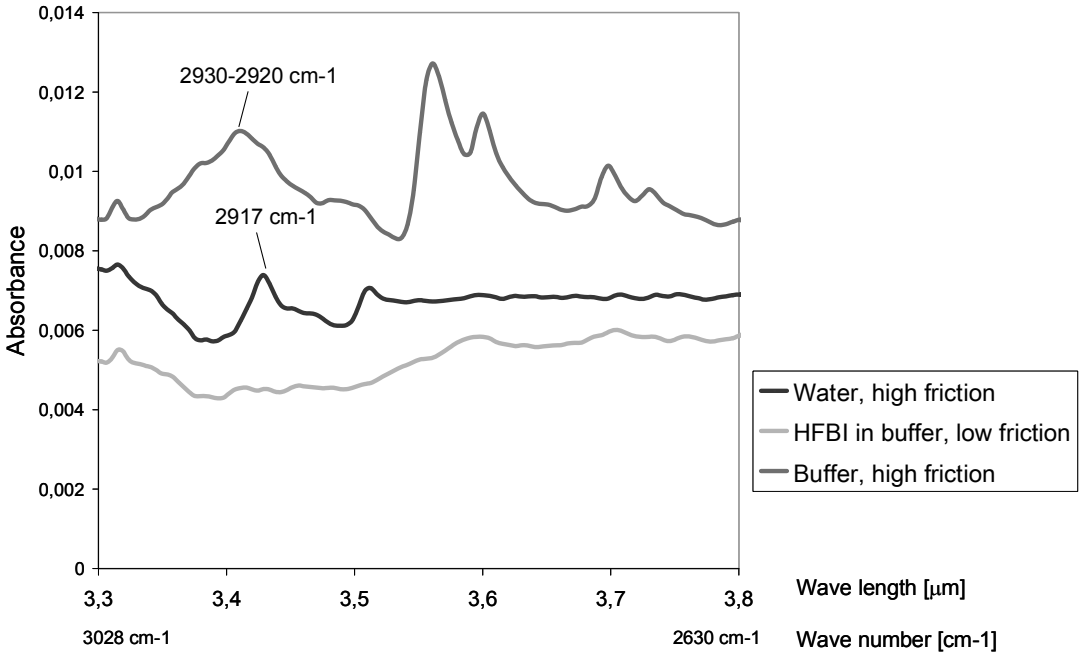

Figure S5. FTIR spectra (from top to bottom) of the CTPOD discs lubricated 1) with the sodium acetate buffer (high COF values), 2) with water (high COF values) and 3) with the 0.1 mg/ml HFBI in the buffer (low COF values). The absorbance bands at 2917-30 cm^{-1} are due to asymmetric CH_2 stretching and at 2849-50 cm^{-1} due to symmetric CH_2 stretching of polyethylene. Residues of the solid buffer were obtained on the disc lubricated with the buffer (additional absorption bands are seen in the top spectrum).

Marked deformation of the wear surface of the pin was common when UHMWPE vs. stainless steel contact was lubricated by the 50 mM sodium acetate buffer (Fig. S6).

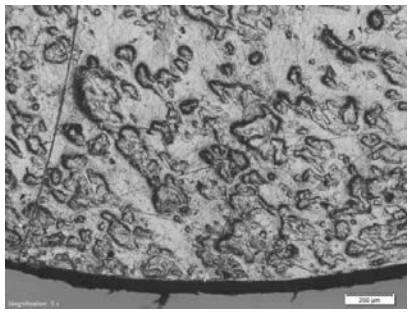

Figure S6. Optical micrograph from the edge of the UHMWPE pin worn in the sodium acetate buffer, showing typical protuberance formation caused by multidirectional motion, creep deformation, and possibly some thermal phenomena. The scale bar is 200 μm.

Friction in tribological experiments by circular translation pin-on-disc (CTPOD)

In UHMWPE vs. stainless steel contact the hydrophobins were not reducing the coefficient of friction compared to 50 mM sodium acetate buffer.

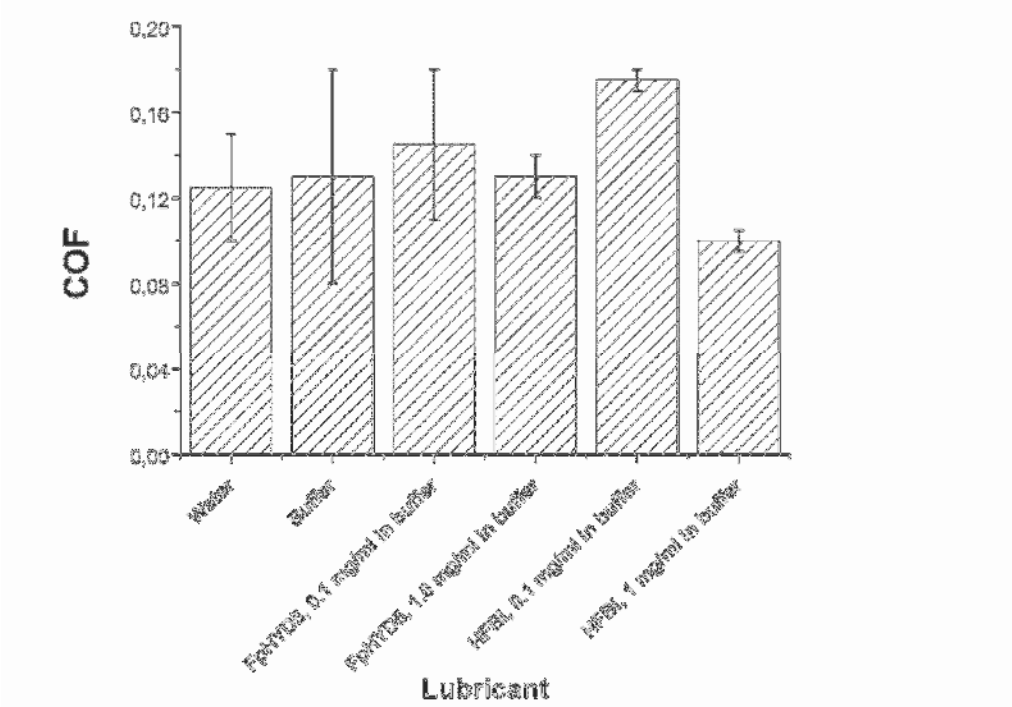

Figure S7. Coefficients of friction in lubricated UHMWPE vs. stainless steel contact. The buffer was 50 mM sodium acetate buffer pH 5. the coefficient of friction is presented as the average value of minimum and maximum. Scatter is presented as minimum and maximum.

Dynamics of protein adsorption on stainless steel

The dynamics of the protein adsorption was studied by analysing the binding of the proteins as a function of time. The binding curves measured by QCM are shown in Figure S8 and those measured by ellipsometry are shown in Figure S9. A simple Langmuir-type adsorption curve was fitted to the curves in order to extract a rate constant for the binding.

$$m_{\mathrm{ads}} = B_{\mathrm{max}}(1 - e^{-kt}) \qquad \text{(Eq. S1)}$$

Here B_{max} is the amount of bound protein in equilibrium and k is the rate constant of binding. The resulting rate constants as a function of concentration are presented in Figure S10. HFBI showed a more pronounced dependence on the protein concentration.

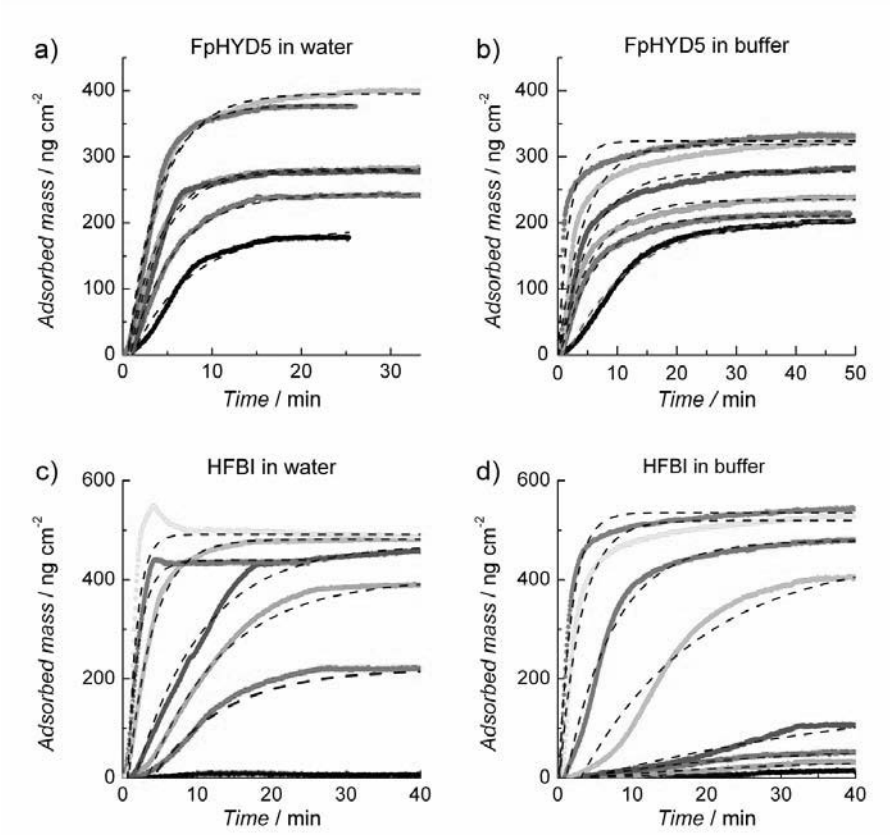

Figure S8: Adsorbed mass of FpHYD5 (a,b) and HFBI (c,d) on steel measured by QCM-D. Adsorption of FpHYD5 was measured in water (a) and in 50 mM NaAc buffer (b) at concentrations 0.1 (purple), 0.05 (cyan), 0.025 (blue), 0.01 (green), 0.005 (red) and 0.0025 g L^{-1} (black). Adsorption of HFBI was measured in water (c) at concentrations 0.25 (yellow), 0.1 (purple), 0.05 (cyan), 0.025 (blue), 0.01 (green), 0.005 (red) and 0.0025 L^{-1} (black) and in 50 mM NaAc buffer (d) at concentrations 0.25 (olive), 0.1 (yellow), 0.05 (purple), 0.025 (cyan), 0.01 (blue), 0.0075 (green), 0.005 (red) and 0.0025 g L^{-1} (black). The dashed curves show the curves fitted to the measured data.

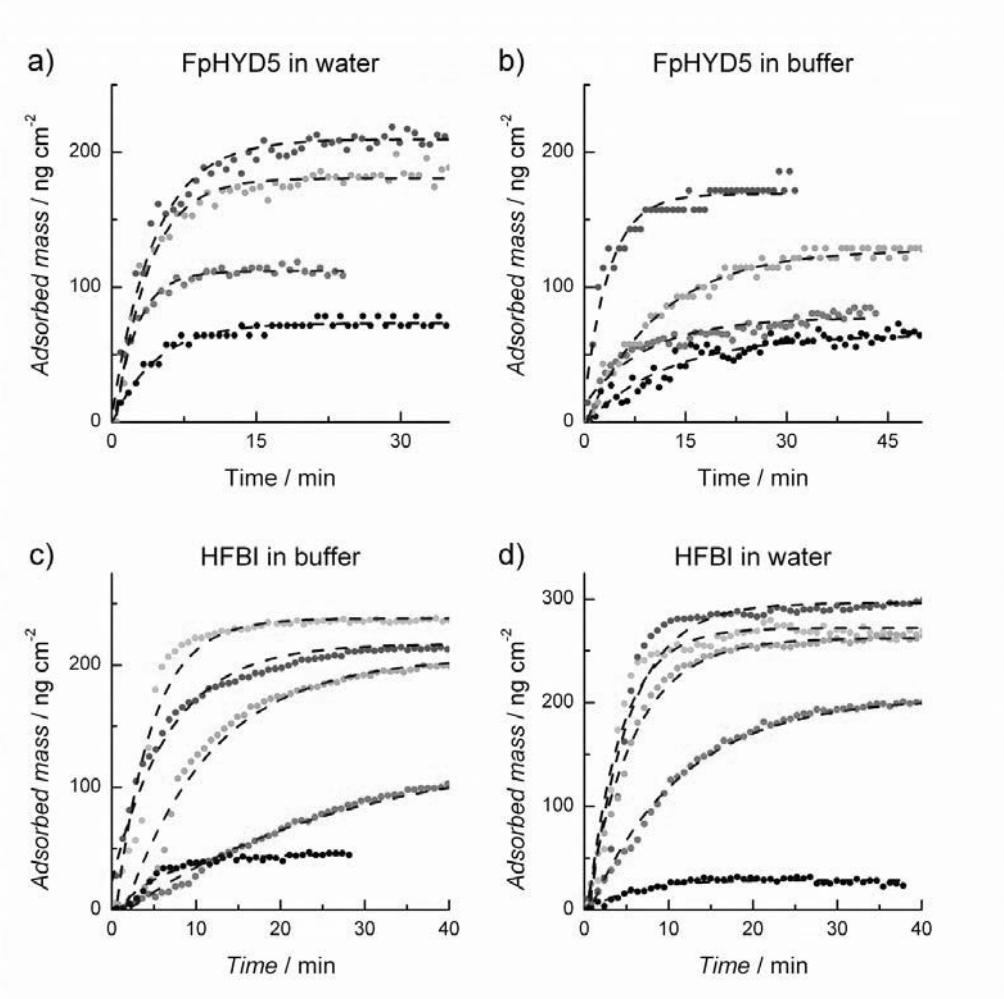

Figure S9. Adsorbed mass of FpHYD5 (a,b) and HFBI (c,d) on steel measured by ellipsometry. Adsorption of FpHYD5 was measured in water (a) and in 50 mM NaAc buffer (b) at concentrations 0.1 (blue), 0.025 (green), 0.0125 (red), 0.005 g L^{-1} (black). Adsorption of HFBI was measured in water (c) and in 50 mM NaAc buffer (d) at concentrations 0.1 (cyan), 0.05 (blue), 0.025 (green), 0.0125 (red) and 0.005 g L^{-1}(black). The dashed curves show the curves fitted to the measured data.

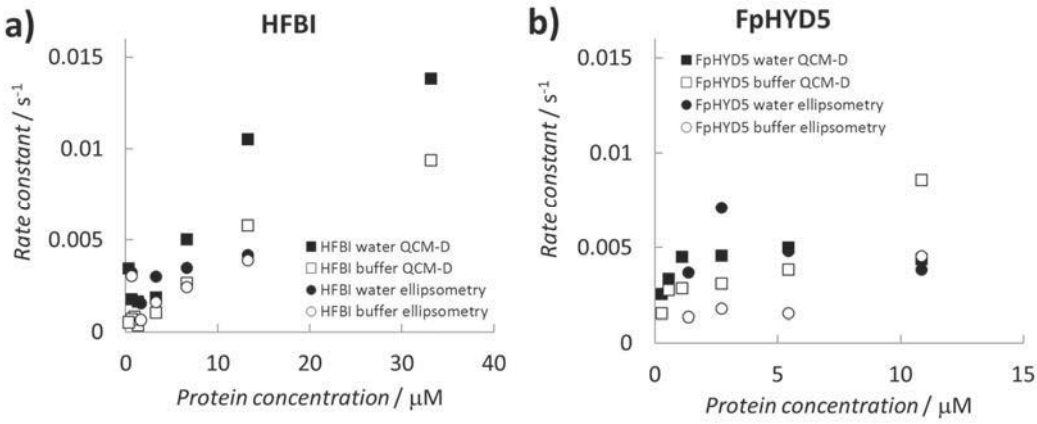

Figure S10. Rate constants extracted from the exponential decay fits.

III

Hakala, T.J., Saikko, V., Arola, S., Ahlroos, T., Helle, A., Kuosmanen, P., Holmberg, K., Linder, M.B., Laaksonen, P. (2014) Structural characterization and tribological evaluation of quince seed mucilage. *Tribology International*, 77, 24-31.

Tribology International 77 (2014) 24–31

Contents lists available at ScienceDirect

Tribology International

journal homepage: www.elsevier.com/locate/triboint

Structural characterization and tribological evaluation of quince seed mucilage

Timo J. Hakala [a], Vesa Saikko [b], Suvi Arola [a,b], Tiina Ahlroos [a], Aino Helle [a], Petri Kuosmanen [b], Kenneth Holmberg [a], Markus B. Linder [a,b], Päivi Laaksonen [a,b,*]

[a] VTT Technical Research Center of Finland, P.O. Box 1000, FI-02044 VTT, Finland
[b] Aalto University, P.O. Box 14300, 00076 Aalto, Finland

ARTICLE INFO

Article history:
Received 24 September 2013
Received in revised form
1 February 2014
Accepted 12 April 2014
Available online 23 April 2014

Keywords:
Biolubrication
Boundary lubrication
Macromolecules
Biomimetics

ABSTRACT

The mucilage, originating from the seeds of quince fruit was characterized as a potential bio-inspired water-based lubricant. The mucilage consists mainly of fine cellulose nanofibrils and charged hemicelluloses whose structure and properties were characterized here by atomic force microscopy (AFM) and tribological Pin-On-Disc (POD) experiments. The hemicellulose-decorated nanocellulose fibrils were 3.0 ± 0.7 nm in thickness, had a very large aspect ratio and also had a tendency to self-align when dried on mica surface. Macroscale tribological tests showed that the mucilage was able to reduce the coefficient of friction of polyethylene/stainless steel contact to values below 0.03. Thus, we show that quince mucilage is a native nanocellulose material with a notable ability to lower friction.

1. Introduction

Sustainability is a major driving force for development of better processes and more efficient utilization of the existing resources. Many processes and systems developed in Nature have been optimized to meet very specialized needs and their detailed study may also help in finding new solutions for present technological problems. For instance, impressive mechanical properties of mother of pearl, wood and bone have inspired many scientists in development of tough and light-weight materials using the same principles [1–3]. The natural material which inspired this work, is carbohydrate-containing mucilage extracted from the seeds of a quince fruit. We present the characterization of this strongly hydrating and self-aligned material that consists mainly of water, cellulose nanofibrils [1,4] and hemicelluloses such as glucoronoxylans [5–7]. The mucilage shows several beneficial properties such as strong swelling and slippery appearance, probably due to hydration of carbohydrate structures that has been observed to enhance lubrication of some other water-based systems [8,9]. The structure of the mucilage in its native state is fascinating; the cellulose nanofibrils stored on the epidermal layer of the seeds are readily dispersible in water, have a very narrow size distribution, and have a tendency to self-assemble into helicoidal organization, a true cholesteric liquid crystal state [10,11]. The reasons why these fibrils are packed into such strongly chiral assemblies into the cell walls remains yet unclear, but chirality of hemicellulose has been proposed as the cause for the assembly [12].

Quince fruit and especially the mucilage from its seeds, has raised interest among engineers and plant scientists. Since the late 19th century, there have been several suggestions for innovative uses of quince mucilage in applications varying all the way from hair tonic to metal polish [13–15]. Most of the recent interest in quince mucilage is however concentrated on the water-soluble polysaccharides it contains. There are several reports on separation and purification of the special glucuronoxylan from the quince seed mucilage [6,7]. The origin of the self-alignment of the fibrils and the interplay of cellulose and the glucuronoxylans has thus far been one of the most topical research areas related to quince mucilage. However, for cellulose research society, fruits have shown their potential also as a source of high quality nanofibrillar cellulosic materials [16] that combine exceptionally good mechanical properties and all the benefits of cellulose [17]. Materials based on nanofibrillated cellulose (NFC, also known as microfibrillated cellulose MFC) show especially great potential when the alignment of the nanofibrils can be controlled [18]. As a renewable material, NFC is extremely attractive as a building component for new materials and has been employed in many studies aiming at better composite structures [1,19].

Here, physicochemical and tribological characterization of quince mucilage is presented. The results from AFM studies show that the fibrils are very monodisperse and able to self-align in

* Corresponding author. Present address: Department of Materials Science and Engineering, Aalto University Vuorimiehentie 2 A, PO Box 16200 FI-00076 Aalto University, Finland. Tel.: +358 50 460 2611; fax: +358 9 863 2019.
E-mail address: paivi.laaksonen@aalto.fi (P. Laaksonen).

http://dx.doi.org/10.1016/j.triboint.2014.04.018
0301-679X/

native state (as-extracted), but also after mild purification. Slippery appearance being one of the natural properties of the mucilage, its lubrication abilities were studied by using macroscopic tribology measurements. The mucilage was able to reduce the friction of the polyethylene/stainless steel contact to a much lower level than pure water. Thus, quince seed mucilage and other nanomaterials like it, may provide a solution for efficient water-based lubrication in technologically relevant environment, which has thus far, been an unsolved problem. Many attempts to resolve the issue of water-based lubricants are based on characterization and mimicking of the synovial lubrication, which is one of the most long-lasting and versatile system for low friction found in Nature [20–22]. As a carbohydrate-based fibrillar material, quince mucilage may have similarities to the cartilage and other species found in the synovial joints, such as the water-absorbing proteoglycans and the hydrogel structure supported by the collagen fibrils. The lubrication of the synovial joint is a combination of mixed lubrication mechanisms involving several immobilized and soluble active species combined with self-healing abilities. Studies on certain individual species extracted from the synovial system or synthetic molecules mimicking their essential features including hyaluronan [23] and bottle-brush polymers [24] have shown promising results but the overall performance of the natural system has not been obtained. All of these features may appear impossible to capture in a synthetic system, but understanding the most essential ones that are responsible for the high performance may help us to solve technological problems and to replace oil-based lubrication systems.

2. Materials and methods

2.1. Lubricants

Quince seeds (*Cydonia oblonga*) were separated from fresh fruit, dried in ambient and stored in dry before use. Mucilage was extracted from quince seeds by immersing seeds into fresh water. A certain amount of seeds were weighed and kept in $\sim$40 mg mL^{-1} concentration in deionized water (Milli-Q Plus Pf/Milli RO 30 Plus, US) overnight. The solution was decanted and extraction was repeated once more. The extract contained some solid impurities originating from the seeds, which were removed by a gentle centrifugation and filtration through three layers of cotton gauze. The mucilage was stored in $+4$ °C. The dry mass of the mucilage, 0.55 m%, was determined by lyophilization. The mucilage could also be lyophilized and redispersed in deionized water to gain a higher concentration.

Washing of the mucilage was carried out by ethanol as described earlier [7]. Concentrated mucilage was dispersed in three volumes of ethanol and centrifuged. The excess ethanol was removed and the mucilage was dialyzed and freeze-dried. A part of the mucilage was freeze-dried without dialysis and used in the lubrication studies.

Reference measurements were carried out using deionized water (Merck Millipore, US) and 1 M sodium chloride (Sigma-Aldrich, US) solution as the lubricant.

2.2. Total enzymatic hydrolysis of quince seed mucilage and the analysis of sugar content

Hydrolysis of ethanol-washed and freeze-dried mucilage suspension was performed to determine its sugar contents [25]. A mixture of four different commercial enzyme was used (Econase (cellulase, Roehm Enzyme Finland) 20 mL, Ecopulp X-200 (xylanase, Roehm Enzyme Finland) 50 mL, Gamanase (mannanase, Novo, Denmark) 100 mL and Novozyme 188 (β-glucosidase, Novo, Denmark) 50 mL). Before use, the mixture was diluted with 200 mL of 50 mM sodium acetate buffer pH 5 and desalted using a Biogel P-6 gel (Bio-Rad, UK) column using the same buffer. The total activity of the mixture was 29.8 FPU (filter paper units) mL^{-1}. The load of enzyme used for total hydrolysis of 50 mg dried mucilage was 50 FPU g^{-1} and the reaction was allowed to proceed for 48 h at 40 °C (stirring 250 rpm), after which an additional 10 FPU g^{-1} amount of enzyme cocktail was added and the reaction continued for another 18 h to ensure total hydrolysis of the sample. The mixture was cleared by centrifugation (4000 rpm, 10 min, Eppendorf, Germany) and boiled for 5 min to inactivate enzymes. Monosaccarides were determined by chromatography (DIONEX ISC-5000, CarboPac PA20, Thermo Scientific, US). The dry weight of the first pellet from the total hydrolysis reaction was also determined.

2.3. Atomic force microscopy

Morphology of quince mucilage was studied by atomic force microscopy. A NanoScope IIIa Multimode (E-scanner, J-scanner, Bruker, Germany) AFM instrument was used with an NSCI5/AlBS cantilever with less than 10 nm tip radius (μMASCH, US). All images were recorded in tapping mode in air with scan rates of 0.5–1 Hz. The damping ratio was around 0.7–0.85. All images were flattened to remove possible tilts in the image data. Some images were further flattened by filtering out non-directional noise.

The samples were prepared by placing a droplet of diluted (<1 g L^{-1}) quince mucilage on a mica substrate (Electron Microscopy Sciences, US), which was then let dry in ambient conditions. Mica was cleaved just before sample preparation.

2.4. Epifluorescence microscopy

Surface of the quince seed was studied by an epifluorescence microscope (Olympus BX-50, Japan). Fluorescence imaging was carried out either based on samples autofluorescence or a fluorescent dye, Calcofluor (Scandinavian Brewery Laboratory Ltd., Denmark), which is specific towards cellulose.

2.5. Circular translation pin-on-disc tests

Tribological properties of quince mucilage in polyethylene (PE)/stainless steel contact were characterized in a flat-on-flat configuration by a high load friction circular translation pin-on-disc (CTPOD) device designed and constructed at TKK/Aalto University and described in detail elsewhere [26]. Briefly, in the HL-Friction CTPOD device the pin translates along a circular track of 10 mm diameter relative to the disc. The sliding speed is constant, 31.4 mm/s. Such a low speed ensures that a boundary lubrication mechanism prevails. In the CTPOD device, the pin translates along a circular track of 10 mm diameter relative to the disk. Neither the pin nor the disk rotates. In this way, the direction of sliding relative to the pin changes continually, and uniaxial grooving by wear can be avoided. The disc holder is supported by low-friction ball bearings. The rotation of the disc is prevented by a load cell and a lever arm. From the load signal, the frictional torque and coefficient of friction (COF) are calculated. In the present study, the pin was a flat-ended cylinder with a diameter of 9 mm and length of 12 mm. It was made from ultra-high molecular weight polyethylene (UHMWPE), type GUR 1050, which is a tough and chemically inert material. The disc was made from austenitic stainless steel 316 (ASTM F 138), polished to a surface roughness R_a of 0.01 μm. Its hardness is 200 HB. The contact was flat-on-flat and the nominal contact pressure was 4.4 MPa. The load was constant 277 N. The test duration varied from 5–24 h, and the tests were run at room temperature. The specimens were surrounded

by a chamber that contained the test lubricant, usually of 5 ml volume. 2–7 parallel tests were done. Due to the high wear resistance of UHMWPE, the test duration of 24 h was not sufficient for meaningful wear measurements.

2.6. Pin-on-disc tests

The pin-on-disc equipment was designed and built at VTT. The load used in the experiments was 50 N which corresponds to 4 MPa nominal contact pressure. The experiments were carried out at room temperature. During the experiment sliding velocities from 10 to 100 mm s^{-1} were used. The friction force was constantly measured during the pin-on-disc experiment. Each test was started with sliding velocity 50 mm s^{-1} for 10 min. After 10 min of sliding velocity was changed in every 3 min. Each sliding velocity (10, 50 and 100 mm s^{-1}) was used at least twice during each experiment. Coefficient of friction was determined as an average value at each step. Thus, at least two friction coefficient values were extracted for each velocity during one experiment. Two repeats of each experiments were carried out with both lubricant concentrations. The tests with stainless steel/stainless steel material pair were carried out by using sliding velocity 0.05 m/s and normal loads ranging between 2 and 10 N. Stainless steel vs. stainless steel experiments were not repeated.

The test specimens were stainless steel discs (AISI 440B) with a diameter of 40 mm (R_a value 0.05 μm or better) and conical shaped ultra-high molecular weight polyethylene pins (UHMWPE) with a flat contact area of 4 mm diameter. Stainless steel (AISI420) ball diameter was 10 mm. The same disc was used in several tests, and before each test, it was cleaned by ultrasonic washing in petroleum ether, ethanol and acetone, respectively, 5 min each. The sliding track diameter was varied between 20 and 34 mm. A new PE pin or stainless steel sphere was used in every test. The amount of lubricant in each test was 0.6 mL.

2.7. Rheological measurements

Steady-state viscosity of different lubricants was measured with Physica MCR 301 rheometer using cone and plate geometry. The experiments were carried out at 25 °C temperature using shear rate 15 s^{-1}.

3. Results and discussion

3.1. Extraction of mucilage from the seeds

Mucilage was extracted by immersing seeds in pure water. After removal of the solid particles, transparent, slightly yellowish gel was obtained (Fig. 1a). The seed surface before and during mucilage extraction was investigated by fluorescence microscopy (Fig. 1b–e). The dry seed surface was visible under the UV-light due to its autofluorescence and had tens of micrometers sized grain-like features in it. To observe the release of mucilage from the seed surface, solution of cellulose-specific dye (Calcofluor) was pipetted on the seed surface. Swelling of the mucilage started immediately after wetting and bright blue patterns following the grain structure appeared as shown in Fig. 1d. 20 min after wetting, a thick layer of stained gel was surrounding the seed surface. An image showing a side-view of the gel coating is shown in Fig. 1e.

A more detailed characterization of the seed surface was carried out by AFM. On high magnification, the surface of a seed, kept in ambient conditions, contained nanometer-sized granules showing even smaller porous patterns on them (Fig. 2a and b). The small features were especially well visible when imaged in the phase mode, as shown in Fig. 2b. AFM imaging was carried out also on a seed after swelling of the mucilage (Fig. 2c and d). The seed was dried before imaging. Again, nanometer sized features appeared on the surface, but in the case of the swollen mucilage the features were less compact and homogeneous as if the grain-like particles had been dissolved. On lower magnification, surface topography did not change when mucilage was extracted (Data not shown).

3.2. Composition and structure of quince mucilage

The composition of the ethanol-washed quince mucilage was analyzed based on the monosaccharide contents of the hydrolyzed samples. Table 1 summarizes the results of the enzyme hydrolysis determined against known standards. Based on the amount of glucose, the cellulose content of the mucilage was roughly 46% and the rest of the material consisted of other polysaccharides. As reported before, quince mucilage contains a large fraction of hemicelluloses consisting of charged uronic acids, the glucuronoxylans [6,7]. These are clearly present, as xylose and uronic acids are the major components after glucose, together about 38% of the dry weight. When comparing our result on monosaccharides to earlier studies on the contents of the quince mucilage, extracted by acid hydrolysis [6,7], the major difference is in the relative amount of glucose. In our case, where the hydrolysis was carried out by enzymes, the amount of glucose is higher (compare 46% to 32–34% reported earlier), most probably due to the more gentle and quantitative hydrolysis by enzymes instead of the harsh acid hydrolysis that may cause unspecific degradation of monosaccharides.

The morphology of quince mucilage was further analyzed by AFM. Diluted as-extracted mucilage was investigated by AFM on a mica surface. Mica was chosen as the substrate material due to its smooth surface which allows precise imaging of the fine details of the nanomaterial. AFM on stainless steel surface having much higher roughness was not attempted. Difference in the structure and behavior of the as-extracted mucilage was compared with mucilage after ultrasonic treatment and mucilage that had been washed with ethanol, dialyzed, freeze-dried and redispersed in water. Ethanol washing was done to reduce the amount of soluble material, such as hemicelluloses in the mixture. Thickness of the fibrils before and after ultrasonic treatment was analyzed from the AFM topography images (Fig. 3a–d). Sonication clearly shortened the fibril length, and also decreased the diameter of the fibrils from 3.0 to 2.7 nm. This was probably due to unwrapping of hemicellulose coating surrounding the native fibrils. Hemicelluloses were observed in the AFM images as a thin holey layer on the background of the sample, but also as slight variation in the thickness along a single fibril. Both as-extracted and ethanol washed mucilage organized into self-aligned long-range patterns on the mica surface. Similar behavior was not observed for the fibrils after ultrasonication (Fig. 3b). The thickness of the fibrils was not much affected by the ethanol wash (2.8 ± 0.5 nm) but was clearly decreased after dialysis (2.0 ± 0.4 nm).

Extraction of mucilage simply by incubating the seeds in water resulted in swelling of the tightly packed porous coating on the seed surfaces and release of cellulose nanofibrils and glucoronoxylan. The fibrils of the mucilage had the tendency to self-orientate into chiral continuous assembly when dried on mica surface, possibly due to the strong negative charge of the hemicelluloses bound to the surfaces of the fibrils and the underlying surface. The tendency to self-align did not diminish after ethanol wash, dialysis and redisperion to water, indicating that the assembly arises from the fibrils themselves or the hemicelluloses tightly attached to the fibrils.

In a previous study, the ζ-potential of quince fibrils and TEMPO-oxidized wood-based nanocellulose fibrils was measured

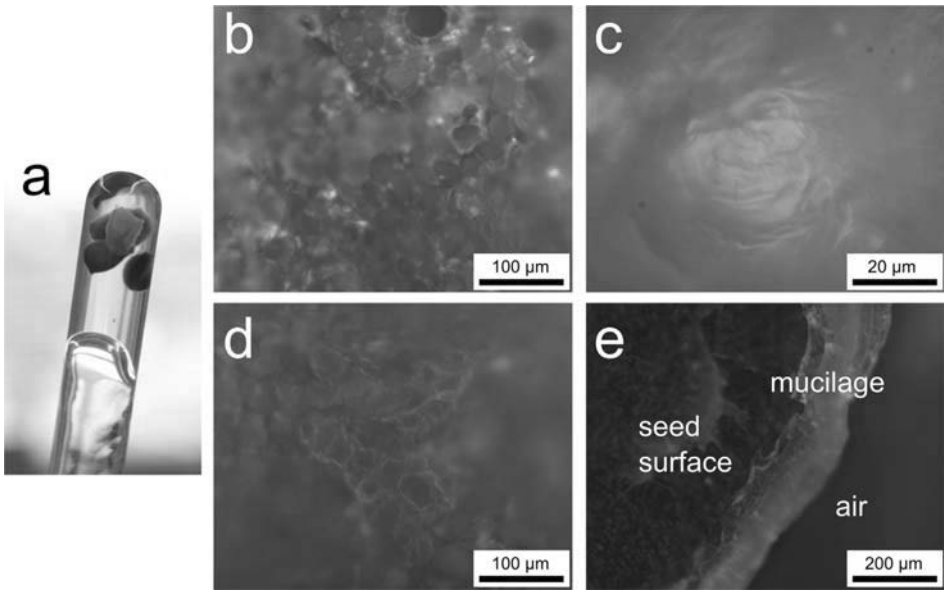

Fig. 1. (a) A photograph of gel-like quince mucilage extracted from seeds. (b–e) Fluorescence microscopy images of quince seed surface. Surface structure of a dry (ambient) seed (b) and high magnification (c) of the same surface, imaged by the autofluorescence. (d) Structure of the surface when moistened with a Calcofluor solution. (e) A gel-like layer formed on the seed surface after 20 min swelling with the Calcofluor solution.

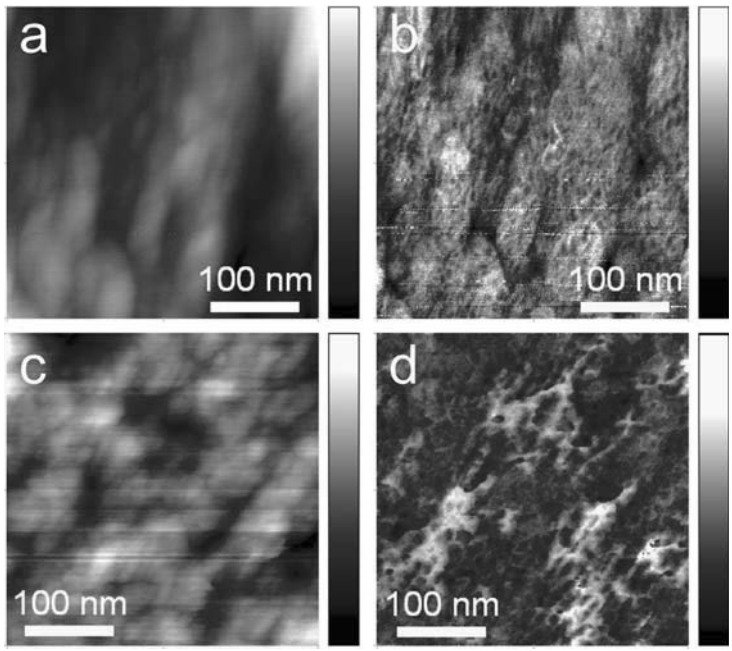

Fig. 2. AFM images of quince seed surface. (a) A topography image of a dry seed. *Z*-scale is 10 nm. (b) A phase image of a dry seed. *Z*-scale is 8 deg. (c) A topography image of a seed that is moistened with water and dried. *Z*-scale is 10 nm. (d) A phase image of a seed that is moistened with water and dried. *Z*-scale is 12 deg.

and rather similar characteristics for these materials with very different origins were observed [27]. The strong repulsion between the oxidized nanocellulose fibrils is believed to result in alignment of the fibrils and has been shown to result in enhanced properties of materials made from these fibrils. For instance, hydrogels with increased stiffness and films with extreme oxygen barrier properties and transparency have been prepared [18]. Thus, natural assembly and excellent monodispersity of the quince nanocellulose may be beneficial in design of novel bio-inspired materials.

3.3. Quince mucilage as lubricant

Tribological behavior of quince seed mucilage was studied using CTPOD and POD devices with a polyethylene (PE) pin sliding on a stainless steel surface. Stainless steel was chosen as the studied material due to its relevance in industrial uses. However, the harsh tribological conditions and the repulsion between the negatively charged quince mucilage and stainless steel surfaces lead to removal of the lubricant from the contact region when measurement was carried out by using a stainless steel/stainless steel material pair and sphere on flat configuration. Thus, milder conditions were created by replacing the stainless steel ball with a flat pin made of polyethylene. This clearly increased the stability of the experiment and allowed reliable measurement of the friction coefficient. The PE/stainless steel pair and the contact type (flat on flat) simulates the operation conditions of common industrial components such as sliding bearings. The chosen material pair is suitable for water lubrication because of its low friction and wear, and excellent corrosion and chemical resistance.

Table 1
The saccharide contents of quince mucilage as a percentage of the total amount of hydrolyzed sugars.

Saccharide	Content (%)
Arabinose	0.2
Galactose	3.2
Glucose	45.6
Xylose	10.7
Mannose	0.7
Fructose	7.4
Uronic acids	27.1
Non-determined oligosaccharides	5.1
Non-hydrolyzed solid material[a]	1.7

[a] The percentage of solid material that was not hydrolyzed by the enzymes compared to the total dry mass of quince mucilage.

The resulting coefficient of friction (COF) of the as-extracted mucilage as a function of mucilage concentration measured with CTPOD showed a reduction of friction when the concentration was increased above 4 g L^{-1}(Fig. 4a). The COF stabilized to values near 0.05 when the mucilage dry mass approached 10 g L^{-1}. Transfer of a visible PE layer on the stainless steel surface was observed only at the lowest mucilage concentration (0.4 g L^{-1}) used where the friction was also the highest and close to the friction level of pure water, which is indicated in Fig. 4a. The viscosity of the mucilage measured at different concentrations is presented in Fig. 4b and showed an exponential increase as a function of the concentration. Thus, a strong increase in viscosity and reduction of COF occur in the same concentration range. PE transfer at low concentration most probably occurred because of the insufficient surface coverage of the nanofibrils and low viscosity of the lubricant which together lead to situation where contact between the PE and stainless steel was possible. In concentrations higher than 4 g L^{-1},

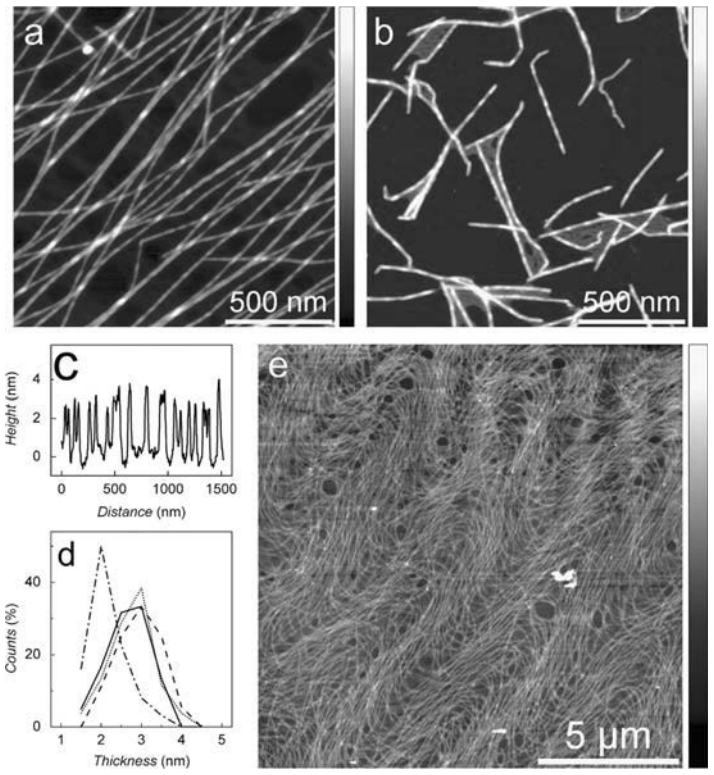

Fig. 3. AFM topography images of the quince mucilage. (a) Freshly extracted quince mucilage assembled on mica. A thin holey layer of hemicellulose has settled at the bottom of the sample. Height scale is 8 nm. (b) Quince mucilage after ultrasonic treatment. The fiber length and tendency to self-assemble have decreased. More unwrapped hemicellulose is seen between the fibrils. Height scale is 8 nm. (c) A cross section along the diagonal of Figure a. (d) Distribution of fibril thickness of as-extracted (dash), tip sonicated (solid), ethanol-washed (dot) and ethanol-washed and dialyzed (dash dot) mucilage. Washing and dialysis decreased the fibril thickness from initial 3.0 ± 0.7 nm to 2.0 ± 0.4 nm. (e) AFM topography image of a continuous assembly of as-extracted quince mucilage on mica.

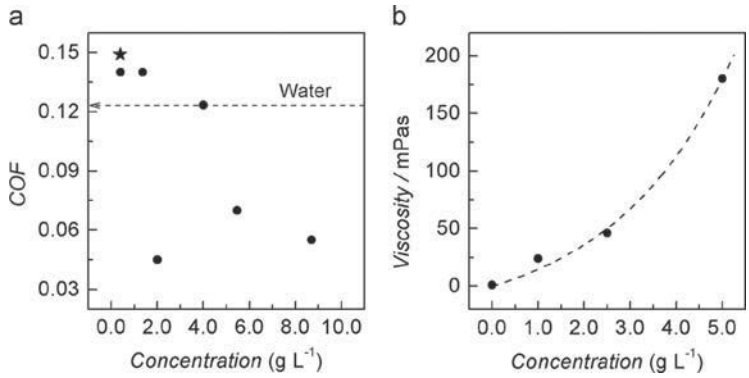

Fig. 4. (a) Friction coefficient of as-extracted quince mucilage as a function of concentration measured with CTPOD (4.4 MPa nominal contact pressure). A significant decrease in friction was observed near concentration range 2–4 g L^{-1}. PE transfer was observed at the lowest used concentration marked by a star symbol. The dashed line represents the friction measured for water. (b) Viscosity of as-extracted quince mucilage as a function of concentration showing an exponential increase of viscosity as a function of concentration. A value of 1.00 mPa s for viscosity of water was used as the concentration "zero g L^{-1}".

however, quince mucilage could act as an excellent lubricant for polyethylene/stainless steel pair. The low friction level indicates that the interaction between the quince mucilage and the PE surface is rather weak allowing slippage of mucilage on both stainless steel and PE interfaces. The low level of friction also indicates the absence of irreversible deformation of the nanocellulose fibrils or the hemicellulose molecules in the contact, since they would dissipate much energy, which would show up as high friction as discussed in earlier work describing tribological behavior of biomolecules [22].

The effect of the sliding speed on the friction of the as-extracted mucilage was tested with POD using a polyethylene pin and a stainless steel counter surface. A continuous experiment where the sliding speed was kept constant at a certain value for a few minutes at a time and then changed to another value was carried out. The resulting COF as a function of the sliding speed is presented in Fig. 5. Two different concentrations, 1 g L^{-1} and 5 g L^{-1} were used. The upper limit of the sliding speed was chosen by the fact that when it was increased above 0.1 m s^{-1}, the friction became unstable and began to increase in an unpredicted manner. The lowest speed 0.01 m s^{-1} was the lowest possible speed for the employed instrumentation. Similarly as in the CTPOD experiment, the COF at concentration higher than 4 g L^{-1} showed clearly lower friction than at 1 g L^{-1}. The dependence on the speed was rather similar for both concentrations. COF values smaller than 0.03 could be reached at high speeds.

The quince mucilage contains a large amount of soluble hemicelluloses that affect its viscoelastic behavior, thus the effect of washing the mucilage with ethanol was studied with the CTPOD setup. Data showing COF values at different contact pressures for both as-extracted and ethanol washed mucilage (~2 g L^{-1}) are presented in Fig. 6. There was no clear dependence of COF on the contact pressure, but the COF values for the ethanol-washed mucilage were systematically higher in each experiment. Although extraction of ethanol-soluble components from the mucilage showed no effect on the assembly of the cellulose nanofibrils when dried on mica surface (data not shown), the removal of these water-absorbing components from the continuous phase increased the friction of the mucilage. Thus, instead of a single component such as the cellulose nanofibrils or the bound hemicelluloses, being responsible for the good shearing properties of the as-extracted mucilage, the lowering of the friction was most probably caused by co-operative effect between several components. Visible transfer of PE from the pin to the stainless steel

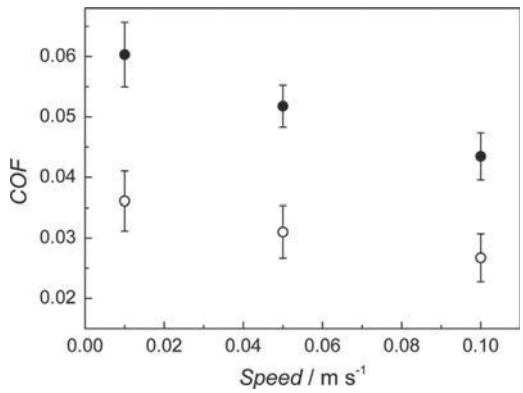

Fig. 5. Friction coefficients of as-extracted quince mucilage as a function of sliding speed measured with POD with a 50 N normal load corresponding to contact pressure of 4 MPa. The concentration of quince seed mucilage was 1 g L^{-1} (closed circles) and 5 g L^{-1} (open circles).

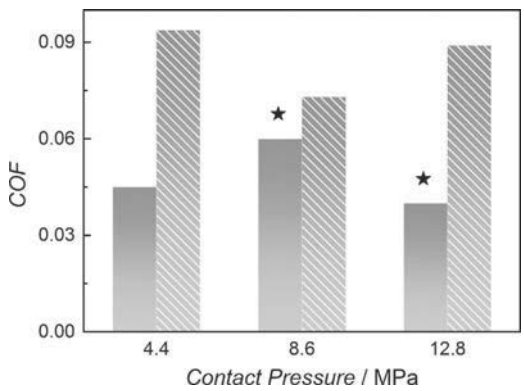

Fig. 6. Friction coefficient of 2.0 g L^{-1} as-extracted quince mucilage (grey bars) and 1.9 g L^{-1} ethanol-washed quince mucilage (dashed bars) measured with CTPOD using different nominal contact pressures. The ethanol wash showed a clear increase in friction of the mucilage. The star symbols denote experiments were PE transfer was observed.

counter surface was observed for the as-extracted mucilage at loads 8.6 and 12.8 but not for the ethanol-washed mucilage in any of the studied circumstances. The polyethylene transfer indicates adhesive wear, and means that the as-extracted mucilage had lower lubricating capability compared to the ethanol-washed mucilage. On the other hand, the presence of soluble macromolecules probably both increase the stability of the gel structure but also increase the viscosity of the continuous phase thus enhancing the elasticity of the gel that would explain the lower friction levels of the as-extracted mucilage. Earlier observations have shown that disturbing the structure of nanocellulose hydrogel by partial removal of the hemicelluloses that stabilize the NFC dispersion can lead to dramatic decrease of the elasticity of the gel [28]. This supports the role of the soluble hemicelluloses of quince mucilage in stabilizing the gel.

Another experiment to prove the essential nature of the stable gel structure in the performance of the quince mucilage as a lubricant was carried out by measuring the friction of the as-extracted mucilage in high ionic strength. For mucilage having concentration of 5.5 g L^{-1}, a 36% increase in friction coefficient measured with the CTPOD using 4.4 MPa nominal contact pressure, from 0.07–0.11 was observed when 1 M NaCl was added to it. The observation was expected since the high salinity should reduce the level of hydration of the charged hemicellulose molecules leading to partial collapse of the hydrogel structure, thus increasing the level of friction. A similar observation on the reduction of the lubrication ability due to decreased level of hydration has been observed previously for water-based lubrication of ethylene glycol-based molecules [29]. This result also supports the hypothesis that hydration of the carbohydrates in quince mucilage stabilizes the gel structure, which has a major role in lubrication.

The lubrication properties of quince mucilage were dependent on the concentration of the mucilage, the sliding speed and the stability of the gel structure as well as material pair lubricated. However, no clear dependence on the contact pressure could be observed (Fig. 6). Increasing the viscosity to a sufficient level (~200 mPas), clearly helped to prevent the direct contact between the polyethylene pin and the stainless steel surface thus maintaining the friction low between them, indicating to the formation of a loosely bound boundary layer [30]. The lowest COF values were obtained with highest speed and load, which are the conditions where the shear stress that directed to the gel is the highest. The high shear may cause alignment of the cellulose nanofibrils showing up as shear thinning behavior of the gel. This has been observed earlier for the highly charged TEMPO-oxidized nanocellulose gels [31], which share similar characteristics with quince mucilage, including fibril thickness and surface charge [27], which could explain the similarities in their behavior. Shear thinning has been proposed to be one of the key reasons for the ultralow friction coefficient (0.005) reported for another plant-based mucilage (*Brasenia schreberi*) [32]. However, the employed method differs so much from the one presented here that direct comparison of the values obtained here and in the earlier work is difficult.

4. Conclusions

We have shown that quince mucilage is able to form self-aligned cellulose/hemicellulose nanostructures on mica. Washing the mucilage with ethanol, dialyzing it and freeze-drying it did not affect the self-assembly abilities. Lubrication of a polyethylene/stainless steel contact with the water-based mucilage was studied by varying several parameters and resulted in coefficient of friction as low as 0.03 in the CTPOD experiments. Quince mucilage is thus an interesting natural nanomaterial showing a robust self-alignment that most probably is essential for its high performance as a water-based lubricant. We believe that identification of the key features of naturally occurring systems with exceptional abilities, may result in findings that enable design and fabrication of better and more sustainable materials.

Acknowledgments

Annaleena Kokko is thanked for technical assistance. Hérve Bizot from INRA is kindly thanked for giving the quince seeds. Tekes – the Finnish Funding Agency for Innovation (New bioinspired and bio-based solutions for lubrication, 41202), Academy of Finland (Biomimetic water lubrication, Composite Materials Based on Novel Biomolecules), VTT Technical Research Center of Finland and Aalto University School of Engineering are thanked for funding.

References

[1] Eichhorn SJ, Dufresne A, Aranguren M, Marcovich NE, Capadona JR, Rowan SJ, et al. Review: current international research into cellulose nanofibres and nanocomposites. J Mater Sci 2010;45:1–33.
[2] Tang Z, Kotov NA, Magonov S, Ozturk B. Nanostructured artificial nacre. Nat Mater 2003;2:413–8.
[3] Antonietti M, Fratzl P. Biomimetic principles in polymer and material science. Macromol Chem Phys 2010;211:166–70.
[4] Ha M-A, Apperley DC, Evans BW, Huxham IM, Jardine WG, Vietor RJ, et al. Fine structure in cellulose microfibrils: NMR evidence from onion and quince. Plant J 1998;16:183–90.
[5] Renfrew AG, Cretcher LH. Quince-seed mucilage. J Biol Chem 1932;97:503–10.
[6] Lindberg B, Mosihuzzaman M, Nahar N, Abeysekera RM, Brown RG. Willison JHM. An unusual (4-O-methyl-D-glucurono)-D-xylan isolated from the mucilage of seeds of the quince tree (Cydonia oblonga). Carbohydr Res 1990;207:307–10.
[7] Vignon MR, Gey C. Isolation, 1H and 13C NMR studies of (4-O-methyl-D-glucurono)-D-xylans from luffa fruit fibers, jute bast fibers and mucilage of quince tree seeds. Carbohydr Res 1998;307:107–11.
[8] Roba M, Naka M, Gautier E, Spencer ND, Crockett R. The adsorption and lubrication behavior of synovial fluid proteins and glycoproteins on the bearing-surface materials of hip replacements. Biomaterials 2009;30:2072–8.
[9] Hakala T, Laaksonen P, Saikko V, Ahlroos T, Helle A, Mahlberg R, et al. Adhesion and tribological properties of hydrophobin proteins in aqueous lubrication on stainless steel surfaces. RSC Adv 2012;2:9867–72.
[10] Reis D, Vian B, Chanzy H, Roland JC. Liquid crystal-type assembly of native cellulose-glucuronoxylans extracted from plant-cell wall. Biol Cell 1991;73:173–8.
[11] Reis D, Vian B. Helicoidal pattern in secondary cell walls and possible role of xylans in their construction. C R Biol 2004;327:785–90.
[12] Reis D, Vian B, Roland J-C. Cellulose–Glucuronoxylans and plant cell wall structure. Micron 1994;25:171–87.
[13] Newcom A, Newcom J. Hair tonic, US885073, 1908.
[14] Feix R. Cheese, GB424305, 1935.
[15] Rust EG. Metal-polish, US580225A, 1897.
[16] Kuga S, Matsumoto Y, Niimura H. Cellulose from fruit tissues. Cell Commun 2010;17:116–20.
[17] Ioelovich M. Nanostructured cellulose and its properties. Curr Trends Polym Sci 2008;12:43–8.
[18] Saito T, Uematsu T, Kimura S, Enomae T, Isogai A. Self-aligned integration of native cellulose nanofibrils towards producing diverse bulk materials. Soft Matter 2011;7:8804–9.
[19] Laaksonen P, Walther A, Malho J-M, Kainlauri M, Ikkala O, Linder MB. Genetic engineering of biomimetic nanocomposites: diblock proteins, graphene, and nanofibrillated cellulose. Angew Chem Int Ed 2011;50:8688–91.
[20] Klein J. Molecular mechanisms of synovial joint lubrication. Proc Inst Mech Eng J J Eng 2006;220:691–710.
[21] Neville A, Morina A, Liskiewicz T, Yan Y. Synovial joint lubrication—does nature teach more effective engineering lubrication strategies? Proc Inst Mech Eng C J Eng 2007;221:1223–30.
[22] Dedinaite A. Biomimetic lubrication. Soft Matter 2012;8:273–84.
[23] Tadmor R, Chen N, Israelachvili J. Normal and shear forces between mica and model membrane surfaces with adsorbed hyaluronan. Macromolecules 2003;36:9519–26.
[24] Krivorotova T, Makuska R, Naderi A, Claesson PM, Dedinaite A. Synthesis and interfacial properties of novel cationic polyelectrolytes with brush-on-brush structure of poly(ethylene oxide) side chains. Eur Polym J 2010;46:171–80.

[25] Tenkanen M, Gellerstedt G, Vuorinen T, Teleman A, Perttula M, Li J, et al. Determination of hexenuronic acid in softwood kraft pulps by three different methods. J Pulp Pap Sci 1999;25:306–11.
[26] Saikko V. Effect of contact pressure on wear and friction of ultra-high molecular weight polyethylene in multi-directional sliding. Proc Inst Mech Eng H J Eng Med 2006;220:723–31.
[27] Valo H, Arola S, Laaksonen P, Torkkeli M, Peltonen L, Linder MB, et al. Drug release from nanoparticles embedded in four different nanofibrillar cellulose cryogels. Eur J Pharm Sci 2013;50:69–77.
[28] Arola S, Malho J-M, Laaksonen P, Lille M, Linder MB. The role of hemicellulose in nanofibrillated cellulose networks. Soft Matter 2013;9:1319–26.
[29] Heeb R, Lee S, Venkataraman NV, Spencer ND. Influence of salt on the aqueous lubrication properties of end-grafted, ethylene glycol-based self-assembled monolayer. ACS Appl Mater Interfaces 2009;5:1105–12.
[30] Yakubov GE, McColl J, Bongaerts JHH, Ramsden JJ. Viscous boundary lubrication of hydrophobic surfaces by mucin. Langmuir 2009;25:2313–21.
[31] Lasseuguette E, Roux D, Nishiyama Y. Rheological properties of microfibrillar suspension of TEMPO-oxidized pulp. Cellulose 2008;15:425–33.
[32] Li J, Liu Y, Luo J, Liu P, Zhang C. Excellent lubricating behavior of brasenia schreberi mucilage. Langmuir 2012;28:7797–802.

IV

Hakala, T.J., Laaksonen, P., Helle, A., Linder, M.B., Holmberg, K. (2014)
Effect of operational conditions and environment on lubricity of hydrophobins in water based lubrication systems. *Tribology - Materials, Surfaces and Interfaces*, 8 (4), 241-247.
DOI 10.1179/1751584X14Y.0000000084

The effect of operational conditions and environment on lubricity of hydrophobins in water-based lubrication systems

T.J. Hakala[1]*, P. Laaksonen[1,2], A. Helle[1], M. B. Linder[1,3] and K. Holmberg[1]

[1]*VTT Technical Research Centre of Finland, Metallimiehenkuja 8, Espoo, P.O. Box 1000, FI-02044, Finland.*
[2]*Aalto University, Department of Materials Science and Engineering, Nanostructures and Materials, PO. Box 16200 FI-00076 Aalto, Finland.*
[3]*Aalto University, Department of Biotechnology and Chemical Technology, Kemistintie 1, FI-00076, Espoo, Finland*

*Corresponding author: Timo J. Hakala (timo.j.hakala@vtt.fi), *Metallimiehenkuja 8, Espoo, P.O. Box 1000, FI-02044, Finland, +358407702369.*

Abstract

In this study, the effect of operational conditions (normal load, sliding velocity) and environment (pH and ionic strength) on the lubrication properties of two different hydrophobin proteins were investigated using pin-on-disc tribometry and ellipsometry. The studied proteins were wild-type HFBI and the glycosylated hydrophobin FpHYD5. It was observed that the friction of a stainless steel vs. stainless steel contact lubricated with either of the hydrophobins did not depend on the normal load. However, increased sliding velocity occasionally led to a decrease in friction when the surfaces were lubricated with the glycosylated FpHYD5. The tribological behaviour of FpHYD5 was studied at pH values ranging from 3 to 9 and generally lowered friction by 31-38% and wear by 40-65% compared to the corresponding buffer solutions. An exception was pH 9, where FpHYD5 increased friction and wear compared to the buffer solution. Ionic strength affected both the amount of protein that was adsorbed and the lubrication properties of glycosylated hydrophobins.

Keywords: Water-based lubrication, Hydrophobins, Biolubrication, Tribology

1. INTRODUCTION

Water is conventionally used as lubricant in forming processes such as deep drawing, cutting and rolling, as well as in water hydraulics. [1] However, the usability of water is limited due

to being a poor lubricant in boundary and mixed lubrication regimes. This is because, unlike oils, which can form a solid-like phase under high pressures, water lacks the ability to increase viscosity under increased pressure. Moreover, water has no lubricity because it cannot form lubricating molecular layers on sliding surfaces, as oil does. However, employing water as a lubricant is preferred in certain applications, and thus attempts have been made to enhance the boundary lubrication properties of water-based systems by means of nanoparticle additives [2], polymers [3], polar end-group containing molecules [4] and ionic liquids [5,6]. In addition, there are some materials, such as diamond-like carbon, that are well lubricated by water and are often used as thin films [7,8]. Another reason for water's limited use as a lubricant is its corrosiveness to some commonly used engineering materials, such as steel. This corrosion problem has been overcome for some materials, such as stainless steel, but their lubricity must be improved with coatings or lubricant additive molecules. The benefits of water as a lubricant are its purity, availability, price and thermal conductivity. It is expected that the use of water as lubricant will increase in the future due to the development in materials engineering and water-based lubricant additives.

Boundary lubrication is considered most challenging lubrication regime because only thin molecular layers are used to prevent contact between surface asperities. New low-viscosity lubricants and applications where boundary lubrication conditions prevail, such as new-generation engines in the car industry, will set high demands for new boundary lubricant additives. Based on temperature and load, boundary lubrication regimes can be divided into four main categories; [9] 1) low load and low temperature, 2) high load and low temperature, 3) medium load and high temperature and 4) high load and high temperature. In each regime, friction and wear are reduced by the different lubrication mechanisms of the lubricant additives. This study focuses on the high load and low temperature regime, also known as the adsorption lubrication regime, where the lubricant additives are physically adsorbed onto the

surface, effectively reducing friction and wear. At higher temperatures and loads the lubricant additive molecules may react with the surface and form soapy, amorphous, or sacrificial layers [9, 10].

Due to the limited temperature range (from 0 to 100 °C) in which water can be used as a lubricant the prevailing solutions used for improving lubrication properties are low-temperature mechanisms, especially adsorption lubrication where thin molecular layers are formed on the surface to reduce friction and wear. One additive type that can be used to enhance the lubrication properties of water is biomolecules [11,12,13,14]. In nature, biomolecules, such as proteins, phospholipids and carbohydrates, are used to form lubricating systems with friction coefficients as low as 0.001 [15]. Some of these molecules have been successfully applied as lubricants on artificial surfaces and engineering materials [16, 17] under relatively low contact pressures. Biomolecules are often bound to the surface by physisorption.

The use of adhesive fungal hydrophobin proteins in lubricating stainless steel has yielded promising results [12, 14]. It has been observed that hydrophobins are able to reduce friction and wear of stainless steel surfaces when compared to water or buffer solutions without any additive molecules. Hydrophobins are small globular (diameter ~3 nm) amphiphilic proteins that are known to have a high tendency to adhere to surfaces and interfaces [18]. The hydrophobin structure includes four sulphur bridges at the core of the protein, making them very stable against environmental changes, such as temperature and ionic strength, which often cause denaturation of proteins. It has been shown that certain hydrophobins can survive at 90 ˚C without losing their original conformation [19]. Hydrophobins' ability to adhere to surfaces and to bind water is similar to that of lubricating glycoproteins, such as mucin and lubricin, which has motivated research into hydrophobins as potential water-based lubricant

additives [12,14,20]. Several studies on class II hydrophobins, such as HFBI and HFBII, have shown strong adhesion to hydrophobic interfaces [21, 22] but also to hydrophilic, polarised surfaces [23,24]. The ability to form well-defined protein monolayers can be beneficial when attempting to enhance the lubrication of materials such as stainless steel in water. The layers formed by hydrophobins are stable against shear due to their ability to form highly elastic films [18]. Forming stable films with strong cohesion is an important parameter when choosing lubricating layers for tribological contacts. To evaluate the positive effect of surface hydration [16,25] we have also studied a glycosylated variant of a hydrophobin, FpHYD5 [26], which has previously shown slightly better performance as a lubricant as well as higher ability to bind water [14]. This paper presents a study of the lubricating effects of hydrophobin layers under different loads and sliding velocities and the effect of ionic strength and pH on the adsorption and lubrication properties of the glycosylated hydrophobin FpHYD5.

2. MATERIALS AND METHODS

2.1 Production and purification of the proteins

HFBI and FpHYD5 hydrophobins were produced using recombinant strains of *T. reesei* and purified by two-phase extraction and RP-HPLC as described previously [26, 27]. The proteins were dissolved in different buffer solutions and water for the experiments. Buffers are listed in Table 1. Purified mQ water was used in the experiments.

Table 1. Buffer solutions

pH	**Ionic Strength**	**Buffer solution**	**Feedstock, purity, manufacturer**
pH 3	50 mM	50 mM citric acid – sodium citrate	Citric acid monohydrate, p.a., SIGMA ALDRICH Sodium citrate tribasic dihydrate, p.a. , SIGMA-ALDRICH
pH 5	50 mM	50 mM sodium acetate	Sodium acetate anhydrous, Ultra; ≥99.0%, Fluka BioChemika (71179)
pH 7	50 mM	50 mM tris(hydroxymethyl)aminomethane - HCl	Tris, Ultra Pure, MP Biomedicals, LLC (Cat. no. 819638) HCl, ≥37% , p.a. , SIGMA-ALDRICH
pH 9	50 mM	50 mM glycine-sodium hydroxide	Glycine, p.a. , Merck Sodium hydroxide, p.a., Riedel-deHaën
pH 5	500 mM	500 mM sodium acetate, pH 5	Sodium acetate anhydrous, Ultra; ≥99.0%, Fluka BioChemika (71179)

2.2 Pin-on-disc (POD) tribometer

Test specimens for the POD experiments were made of stainless steel. A 10 mm diameter sphere (AISI420) was employed against a disc (AISI440B, hardness 54 HRC and surface roughness 0.05 μm or lower) in the tests. Tests were performed for loads ranging from 2 N to

100 N and sliding velocities from 0.01 m s^{-1} to 0.1 m s^{-1}. The test duration was limited to 40 minutes to avoid excessive evaporation of the lubricant. The sliding distance ranged between 24 to 240 metres, depending on the sliding velocity. The lubricant quantity was 0.6 ml, and was added onto the disc by pipette. The lubricant covered the entire wear track during the experiment. At least two experiments under identical conditions were carried out.

The presented numerical values of the friction coefficients were determined as an average value of the friction coefficient between 20 to 40 minutes of sliding. Wear volumes were calculated from the dimensions of the wear track on the stainless steel sphere after the experiment. The disc wear was minimal and unmeasurable with the stylus profilometer. The temperature of the lubricant could not been measured during the test due to its low volume. However, the amount of liquid did not change significantly during the experiment, indicating negligible evaporation of the solvent. All tests were carried out under controlled temperature of 22 ± 1 ˚C and relative humidity of 50 ± 2 %.

2.3 Scanning electron microscopy (SEM)

SEM images were obtained with a Philips XL 30 with LaB_6 filament. The images were taken using 20 kV acceleration voltage, 4.5 spot and 10 mm working distance.

2.4 UV Resonance Raman spectrometer (Renishaw 1000 UV)

The Raman spectrum was obtained with a spectrometer equipped with a microscope with 15X and 40X objectives. The laser was an Innova 300C FreDTM frequency-doubled Ar+ ion laser (Coherent, Inc., California), which was operated at 244 nm wavelength. A CCD camera was used for detecting the scattered light. The system was controlled and the data was processed with Grams32 software.

2.5 Ellipsometry

The adsorbed amount of protein was estimated by measuring the effective film thickness using a multi-wavelength ellipsometer (EP3, Nanofilm, Göttingen, Germany) operated at a single wavelength of 532 nm. A polarizer-compensator-sample-analyser configuration was employed. Data was collected between the angle of incidence from 45° to 83° reflected from a polished stainless steel surface that had been immersed in the liquid of interest for 60 minutes, rinsed and dried. The experiments were carried out at 40-45 % relative humidity and temperature of 20.4 ºC.

The film thickness results were obtained by fitting the measured data to an optical box model consisting of stainless steel and the protein film. The complex refractive index for the stainless steel was measured from a clean surface and a constant refractive index n = 1.460 was assumed for the protein film. **[28]** The absolute amount of adsorbed protein where the effective thickness was calculated was determined with de Feijter's formula. **[29]**

3. RESULTS

3.1 Effect of normal load on friction and wear

The friction of stainless steel vs. stainless steel contact lubricated with 1.0 g L^{-1} hydrophobins dissolved in 50 mM sodium acetate buffer was measured at different loads between 2 N and 100 N in sliding conditions. The friction did not remarkably change at different normal loads, but the friction coefficient remained roughly constant near the value 0.175 (Fig. 1 a). However, it was observed that HFBI hydrophobins could prevent wearing more effectively than FpHYD5 hydrophobins when the normal loads exceeded 10 N (Fig. 1 b). There was

significant variation in the wear volumes of the stainless steel spheres between experiments under nominally identical conditions.

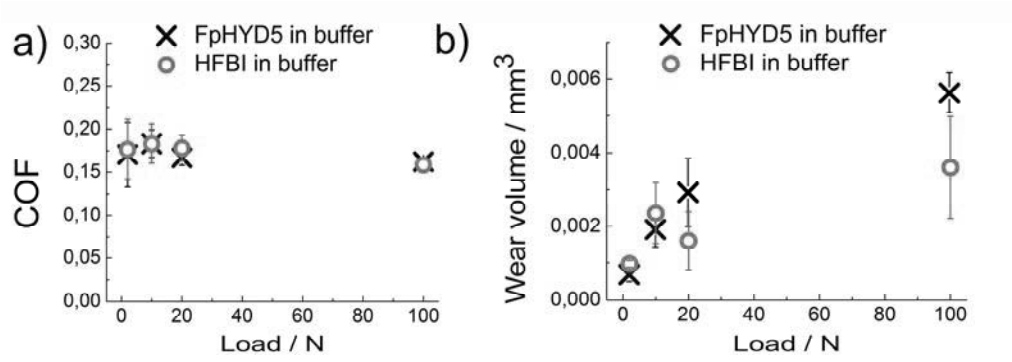

Figure 1: a) Friction coefficients (COF) and b) wear volumes of the stainless steel sphere as a function of normal load in hydrophobin-lubricated stainless steel vs. stainless steel contacts. The sliding velocity was 0.05 m s^{-1} and sliding distance 120 m. In all experiments the proteins were dissolved in 50 mM sodium acetate buffer (pH 5).

3.2 Effect of sliding velocity on friction and wear

While the two hydrophobins HFBI and FpHYD5 exhibited no significant difference in friction when the load was increased, their frictional response differed when the sliding velocity was increased while keeping the load constant (10 N). The coefficient of friction is presented as a function of the sliding speed in Figure 2a, showing a negative dependence for FpHYD5 and constant friction for HFBI. At a sliding velocity of 0.1 m s^{-1}, a significant decrease in the friction coefficients from 0.15-0.20 to below 0.05 was occasionally observed when lubricated with glycosylated hydrophobins FpHYD5 (Fig 2b). However, the occurrence of this drop in friction varied between experiments started under identical conditions. No such friction drop was observed when lubricating with HFBI hydrophobins or bare buffer

solution. The long-term development of friction coefficients indicates differences in stability between FpHYD5 and HFBI hydrophobins in sliding contacts.

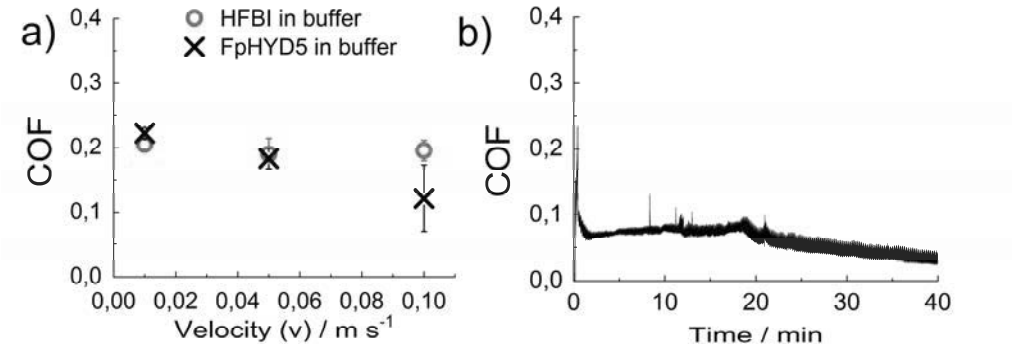

Figure 2. a) Friction coefficient vs. sliding velocity in stainless steel vs. stainless steel contact lubricated with HFBI and FpHYD5 hydrophobins in 50 nM sodium acetate buffer (pH 5) b) Friction curve of FpHYD5 lubricated contact where the friction coefficient dropped below 0.05 at 0.1 m/s sliding velocity. Experiments were carried out with 10 N normal load.

The wear tracks after the experiments were investigated by optical microscopy. A tribofilm was observed on the wear track of the stainless steel sphere after an experiment with FpHYD5 showing a sudden drop in friction coefficient (Fig. 3 a). No comparable formation of such tribofilm was observed in the experiments with HFBI or with FpHYD5 without a sudden drop in friction (Fig. 3 b). The tribofilm appeared as scale-like patterns formed on the sliding surface. The film was studied by Raman spectrometry (Fig 3 inset), which showed the presence of protein. The spectrum was deconvoluted into separate bands that were identified as amide II and III bands and a c_{α}-H amide bending vibration band that were comparable with those reported in the literature for proteins having β-sheet and random coil secondary structures**.[30]**

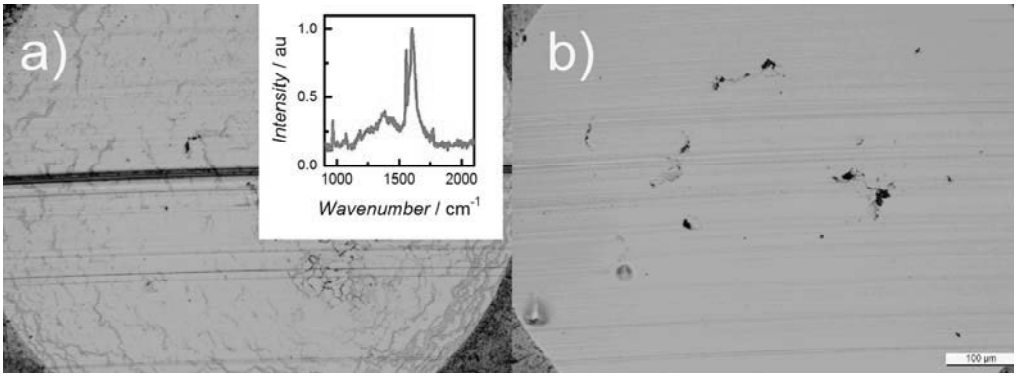

Figure 3: a) Optical microscopy image of the tribofilm on the wear track on a stainless steel sphere after sliding in a contact lubricated with FpHYD5 in 50 mM sodium acetate buffer . Inset: Raman spectrum measured at the wear track after formation of the tribofilm. b) No comparable tribofilm formation was observed on the wear track on a stainless steel sphere after sliding in a HFBI-lubricated contact. Test parameters were 0.1 m/s velocity, 10 N load and a sliding distance of 240 m. The scale bar indicates 100 µm.

3.3 Effect of pH on friction and wear

The friction coefficients and wear volumes of 1.0 g L^{-1} FpHYD5 were measured at different pHs from pH 3 to pH 9 (Figure 4 a-b) and at a constant load of 10 N and constant sliding velocity of 0.05 m s^{-1}. The respective buffer solutions were studied as a reference system. At lower pH values the friction and wear of the stainless steel vs. stainless steel contact remained constant, but increasing the pH to 7 caused a small increase both in friction and wear in contacts lubricated with either buffer solution or buffer solution containing hydrophobins. When the pH was increased to 9, the friction coefficient and wear of the buffer solution lubricated contacts decreased slightly, whereas the FpHYD5 solution caused an increase in both friction and wear.

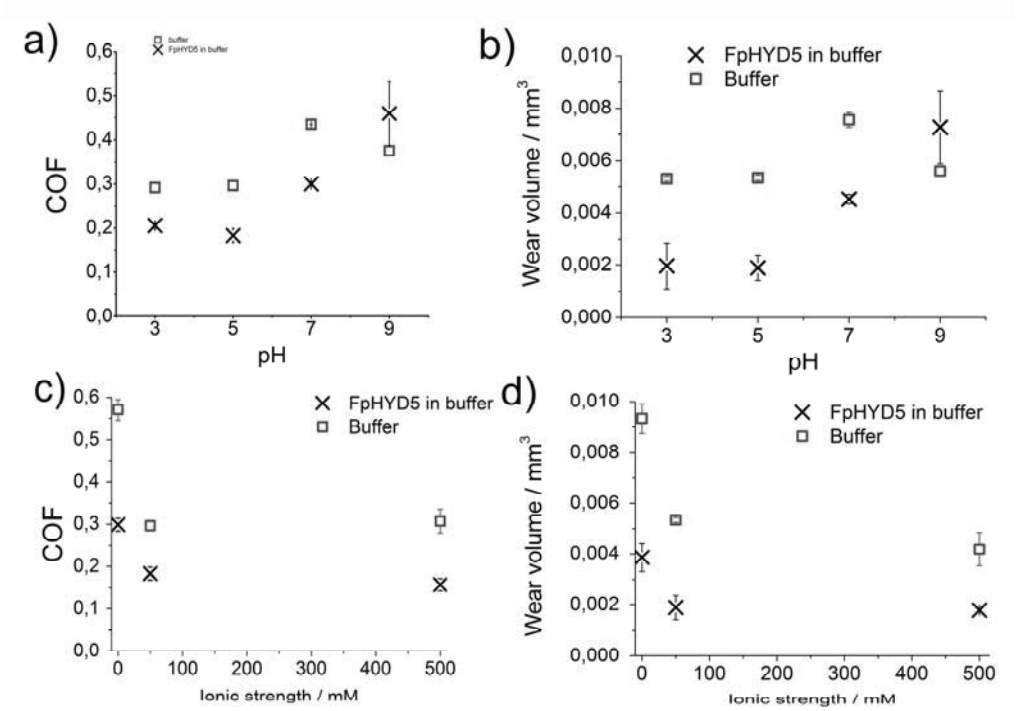

Figure 4. a) Friction coefficient and b) wear volume of the sphere in stainless steel vs. stainless steel contacts lubricated by buffer solutions and glycosylated hydrophobins (FpHYD5) in buffer solutions at different pH values. c) Friction coefficient and d) wear volume of the spheres in stainless steel vs. stainless steel contacts lubricated by buffer solutions and glycosylated hydrophobins (FpHYD5) in sodium acetate buffer solutions with different ionic strength. Sliding velocity was 0.05 m s^{-1} and normal load 10 N. Sliding distance was 120 m.

3.4 Effect of ionic strength on friction and wear

When the ionic strength was increased from 0 (mQ water) to 50 mM (sodium acetate buffer, pH 5) the friction coefficient was decreased in glycosylated hydrophobin-lubricated contacts from 0.3 to below 0.2 (Fig. 4 c). Notably, friction and wear decreased significantly also for

the 50 mM sodium acetate buffer lubricated contact when compared to pure mQ water. This indicates that ions added to water enhance lubricity by adsorbing tightly to the stainless steel surface. Increased ionic strength from 50 mM to 500 mM did not, however, have a significant effect on the lubrication properties of the buffer solution nor the glycosylated hydrophobins.

The wear track on the stainless steel disc was studied by SEM. The wear track that was lubricated by mQ water contained corrosion products and signs of abrasive wear, as shown in Fig 5a. In the contact lubricated by the 500 mM sodium acetate buffer, no corrosion products were observed and there were fewer wear grooves than in the mQ lubricated surface [Fig 5b]. It was observed that FpHYD5 hydrophobins in mQ water also reduced corrosion [Fig 5c].

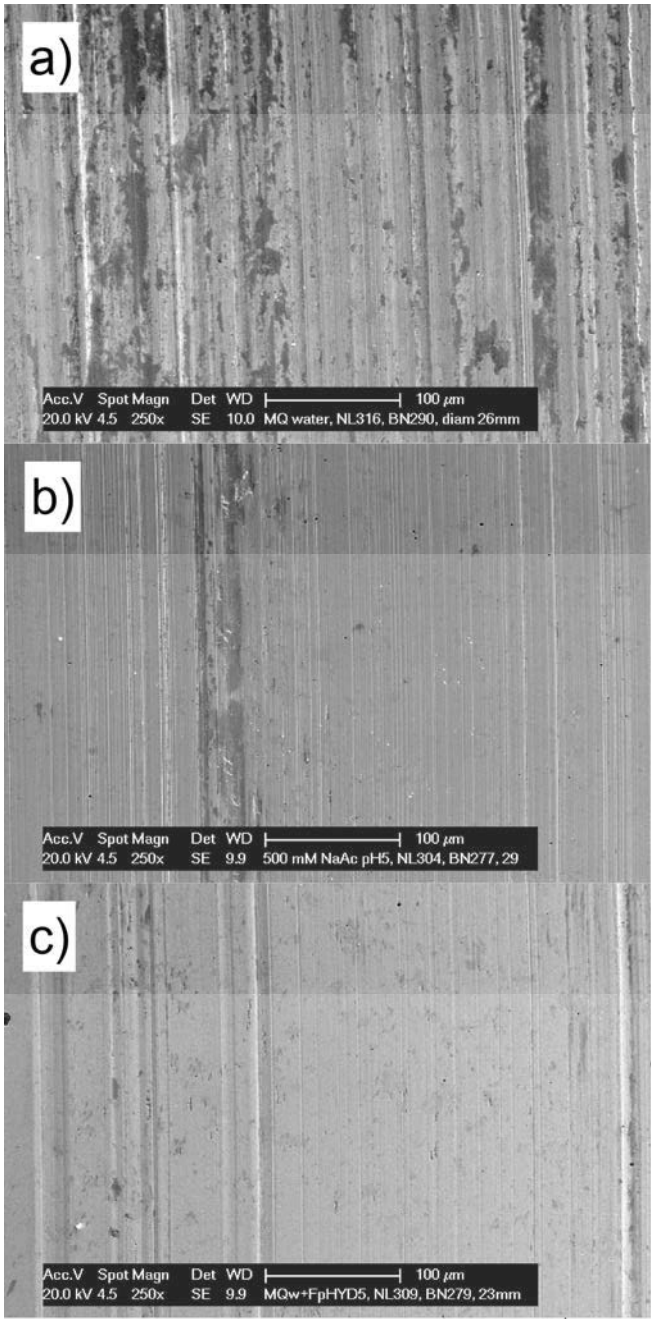

Figure 5. Wear track of the stainless steel disc after lubrication by a) mQ water, b) 500 mM sodium acetate buffer solution and c) FpHYD5 hydrophobins in mQ water.

The ellipsometry measurements gave the effective height of a dried FpHYD5 protein layer on stainless steel surface. The height is proportional to the density of the adsorbed layer, thus for sparse layers the height may be smaller than the apparent height of the studied molecule, which was close to 3 nm for the studied proteins. Two different factors affecting adsorption were studied; the ionic strength of the buffer and the pH. The resulting layer thicknesses are presented in Figure 6. Increasing the ionic strength clearly decreased the amount of bound protein, whereas an increase in pH from 5 to 9 more than doubled the thickness of the bound protein layer.

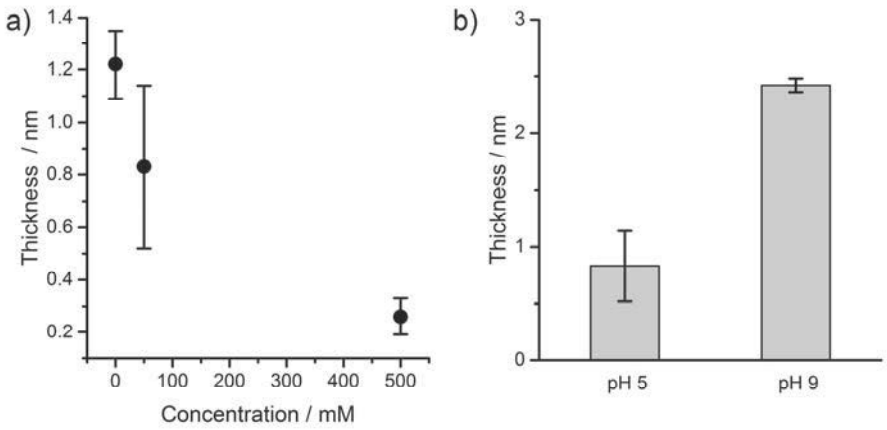

Figure 6. Thicknesses of the adsorbed FpHYD5 layers after drying. a) At pH 5, increasing the ionic strength of the solution by using acetate buffer at different concentrations clearly decreased the amount of adsorbed protein. b) The effective thickness of the protein layer adsorbed from 50 mM buffers was clearly higher at pH 9. The error bars represent the statistical error between several repeated measurements.

4. DISCUSSION

Both of the studied hydrophobins, as additives in water-lubricated systems, reduced friction and wear in the stainless steel vs. stainless steel contacts compared to plain buffer solutions. Although the hydrophobins were able to reduce friction compared to water and the buffer, friction coefficients were relatively high compared, for example, to mucin-lubricated contacts found in the literature. However, those are typically measured in nanoscale or soft vs. soft types of contacts [15,16,17] and the difference can be explained by different lubrication mechanisms at the nano and microscale. In the stainless steel vs. stainless steel contact, both sliding surfaces undergo wear, and thus no stable molecule layers can exist on the contact from the beginning until the end of the experiment. Here, the upper surface moves in relation to the lower surface and is thus constantly in contact, which affects the reorganization of the lubricating film. It can be assumed that lubrication occurs due to a self-assembled molecular layer on the stainless steel disc surface.

The average friction coefficients were observed not to depend on load within the load regime from 2 N to 100 N. Thus, within this load range, the prevailing lubrication mechanism did not depend on the load. However, HFBI hydrophobins prevented wear more effectively than FpHYD5 hydrophobins under high normal loads. This difference in wear could be explained by a more densely packed layer of HFBI hydrophobins, which has been measured in an earlier study [14]. Based on this observation, a densely packed protein layer may be able to prevent contact between the stainless steel surfaces under relatively high loads. Because hydrophobins form monolayers on surfaces, a more densely packed surface layer results in

higher coverage of the surface by proteins and thus the area of direct contact between surface asperities is decreased.

An interesting observation was made when the sliding velocity was increased from 0.01 m s^{-1} to 0.1 m s^{-1}. While the increase in velocity did not affect the friction coefficients of HFBI-lubricated contacts, a pronounced drop in friction was occasionally observed in FpHYD5-lubricated contacts. This reduction in friction coefficients to values below 0.05 was observed together with the formation of a tribofilm on the wear surface of the sphere. It is known that an increase in sliding velocity increases the surface temperature in sliding contacts [10] and may promote chemical reactions and changes in lubricating film structure, thus causing the formation of the observed tribofilm. It might also be that the structure of the more sparsely adsorbed FpHYD5 protein film could have been beneficial for lubricating the sliding contact compared to the more dense and possibly rigid layer formed by HFBI hydrophobins.

Biomolecules are considered to be sensitive to changes in their environment. The lubricating properties of protein layers may be affected by changes in pH and ionic strength brought about by changes in water content, adhesion and molecular alignment [17,31]. It is known that anions can also bind water and form hydrated structures that increase local viscosity between sliding surfaces, thus increasing lubricity [32]. The buffer solutions used in the present study thus had a degree of lubricity. No significant difference in lubrication properties of the different buffer solutions was observed between pH 3 and 7. However, at pH 9 the buffer solutions lubricated better without the addition of hydrophobins. The reason for this unexpected result may be related to the increased level of friction due to a more densely packed FpHYD5 layer on the surface. The ellipsometer experiments showed that at pH 9 more hydrophobins were adsorbed onto the stainless steel surface compared to pH 5. This is in line with earlier work carried out with similar proteins, where the more sparsely bound

layers acted as better lubricants due to the large amount of water associated with the proteins. [14]

Increasing the ionic strength increased the lubrication properties of FpHYD5 solutions, but only up to 50 mM buffer concentration, whereas increasing the ionic strength further led to an even lower degree of protein binding. Thus, the very sparse protein layer achieved at 500 mM acetate buffer concentration, having an effective thickness of only one tenth of the height of the protein (0.26 nm vs. ~3 nm), was still effective in achieving low friction. Sodium acetate buffer solution as well as hydrophobins in water were able to reduce abrasive wear and corrosion in stainless steel vs. stainless steel sliding contacts compared to water-lubricated contacts as observed by SEM (Fig.5).

When combining the results of the POD experiments and ellipsometry carried out at different pH values it was observed that the height of adsorbed protein layer and friction coefficient (COF) had almost linear correlation (Figure 7). Similar correlation has been observed previously for HFBI and FpHYD5 hydrophobins in water and 50 mM sodium acetate buffer [14]. Although the hydrophobins can reduce friction significantly compared to the plain water and the buffer solution, the increased amount of adsorbed proteins will cause increased friction. Possible explanations for the increase in friction are the increased energy dissipation related to deformation of the protein film, which is held together by relatively strong lateral interactions. Another possible reason is the better flow of water in the more sparse layers, which also contain high fractions of water.

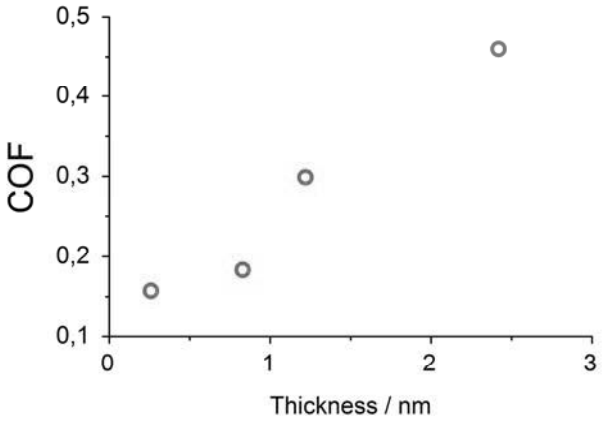

Figure 7. Friction coefficient in FpHYD5-lubricated experiments vs. effective thickness of adsorbed protein layer (nm).

5. CONCLUSION

We have shown that the studied HFBI hydrophobins were able to reduce (by 36-45%) stainless steel vs. stainless steel contact wear more effectively than FpHYD5 hydrophobins under high normal loads (>20 N), possibly due to more densely packed protein film. Increasing the sliding velocity occasionally caused a drop in friction coefficient from ~0.2 to values as low as 0.05 in the FpHYD5-lubricated contacts. Such low friction was related to a tribofilm formation on the worn surface. The amount of adsorbed molecules and lubrication properties were dependent on the ionic strength and pH of the buffer solutions. An increase in ionic strength from 0 to 50 mM decreased the friction coefficients from ~0.3 to below 0.2.

ACKNOWLEDGEMENTS

Sincere thanks to Riitta Suihkonen for purification of the proteins, to Jarkko Metsäjoki for the SEM analysis, Mikko Salomäki and University of Turku for the ellipsometer experiments and to the Finnish Funding Agency for Technology and Innovation (Tekes; New Bio-inspired and Bio-based Solutions for Lubrication project), the Academy of Finland (Biomimetic Water Lubrication project) and VTT Technical Research Centre of Finland for funding.

REFERENCES

[1] R.M. Mortier and S.T. Orszulik: 'Chemistry and Technology of Lubricants', 2nd ed., Great Britain, Chapman & Hall, 1997.

[2] C. Zhang, S. Zhang, L. Yu, Z. Zhang, Z. Wu and P. Zhang: 'Preparation and tribological properties of water-soluble copper/silica nanocomposite as a water-based lubricant additive', *Applied Surface Science*, 2012, **259**, 824– 830

[3] Y. Li, O.J. Rojas and J.P. Hinestroza: 'Boundary Lubrication of PEO-PPO-PEO Triblock Copolymer Physisorbed on Polypropylene, Polyethylene, and Cellulose Surfaces', *Ind. Eng. Chem. Res*., 2012, **51**, 2931−2940

[4] W.H. Briscoe, S. Titmuss, F. Tiberg, R.K. Thomas, D.J. McGillivray and J. Klein: 'Boundary lubrication under water', *Nature Letters*, 2006, **444**, 191-194

[5] B.S. Phillips and J.S. Zabinski: 'Ionic liquid lubrication effects on ceramics in a water environment', *Tribology Letters*, 2004, **17**, 533-541

[6] B.A. Omotowa, B.S. Phillips, J.S. Zabinski and J.M. Shreeve: 'Phosphazene-based ionic liquids: Synthesis, temperature-dependent viscosity, and effects as additives in water lubrication of silicon nitride ceramics', *Inorganic Chemistry*, 2004, **43**, 5466-5471

[7] H. Ronkainen, S. Varjus and K. Holmberg: 'Friction and wear properties in dry, water- and oil-lubricated DLC against alumina and DLC against steel contacts', *Wear*, 1998, **222**, 120–128

[8] F. Zhao, H.X. Li, L. Ji, Y.F. Mo, W.L. Quan, W. Du, H.D. Zhou and J.M. Chen: 'Superlow friction behavior of Si-doped hydrogenated amorphous carbon film in water environment', *Surface & Coatings Technology*, 2009, **203**, 981–985

[9] G.W. Stachowiak and A.W. Batchelor: 'Engineering Tribology', 3rd ed. Amsterdam, Elsevier, 2005.

[10] F.P. Bowden and D. Tabor: 'The Friction and Lubrication of Solids', Great Britain, Clarendon Press, Oxford, 1986.

[11] B.A. Hills: 'Remarkable anti-wear properties of joint surfactant', *Annals of Biomedical Engineering*, 1995, **23**, 112-115

[12] T. Ahlroos, T.J. Hakala, A. Helle, M.B. Linder, K. Holmberg, R. Mahlberg, P. Laaksonen and S. Varjus: 'Biomimetic approach to water lubrication with biomolecular additives', *Proceedings of the Institution of Mechanical Engineers, Part J: Journal of Engineering*, 2011, **225**, 1013-1022.

[13] A. Neville, A. Morina, T. Liskiewicz and Y. Yan: 'Synovial joint lubrication - Does nature teach more effective engineering lubrication strategies?. *Proceedings of the Institution of Mechanical Engineers, Part C: Journal of Mechanical Engineering Science*', 2007, **221**, 1223-1230

[14] T.J. Hakala, P. Laaksonen, V. Saikko, T. Ahlroos, A. Helle, R. Mahlberg, H. Hähl, K. Jacobs, P. Kuosmanen, M.B. Linder and K. Holmberg: 'Adhesion and tribological properties of hydrophobin proteins in aqueous lubrication on stainless steel surfaces', *RSC Advances*, 2012, **2**, 9867–9872

[15] J. Seror, Y. Merkher, N. Kampf, L. Collinson, A.J. Day, A. Maroudas and J. Klein: 'Articular Cartilage Proteoglycans as Boundary Lubricants: Structure and Frictional Interaction of Surface-Attached Hyaluronan and Hyaluronan-Aggrecan Complexes', *Biomacromolecules*, 2011, **12**, 3432–3443

[16] N.M. Harvey, G.E. Yakubov, J.R. Stokes and J. Klein: 'Normal and Shear Forces between Surfaces Bearing Porcine Gastric Mucin, a High-Molecular-Weight Glycoprotein', *Biomacromolecules*, 2011, **12**, 1041-1050.

[17] S. Lee, M. Müller, K. Rezwan and N.D. Spencer: 'Porcine Gastric Mucin (PGM) at the Water/Poly(Dimethylsiloxane) (PDMS) Interface: Influence of pH and Ionic Strength on its Conformation, Adsorption, and Aqueous Lubrication Properties', *Langmuir*, 2005, **21**, 8344-8353.

[18] M.B. Linder, G.R. Szilvay, T. Nakari-Setälä and M.E. Penttilä: 'Hydrophobins: the protein-amphiphiles of filamentous fungi', *FEMS Microbiol Rev*, 2005, **29**, 877-896.

[19] S. Askolin, M. Linder, K. Scholtmeijer, M. Tenkanen, M. Penttilä, M.L. de Vocht and H.A.B. Wösten: 'Interaction and Comparison of a Class I Hydrophobin from Schizophyllum commune and Class II Hydrophobins from Trichoderma reesei', *Biomacromolecules*, 2006, **7**, 1295-1301

[20] R. Misra, J. Li, G.C. Cannon and S.E. Morgan: 'Nanoscale reduction in surface friction of polymer surfaces modified with Sc3 hydrophobin from Schizophyllum commune', *Biomacromolecules*, 2006, **7**, 1463-1470.

[21] H.K. Valo, P.H. Laaksonen, L.J. Peltonen, M.B. Linder, J.T. Hirvonen and T.J. Laaksonen: 'Multifunctional Hydrophobin: Toward Functional Coatings for Drug Nanoparticles', *ACS Nano*, 2010, **4**, 1750-1758.

[22] S. Varjonen, P. Laaksonen, A. Paananen, H. Valo, H. Hähl, T. Laaksonen and M.B. Linder: 'Self-assembly of cellulose nanofibrils by genetically engineered fusion proteins', *Soft Matter*, 2011, **7**, 2402-2411.

[23] M.S. Grunér, G.R. Szilvay, M. Berglin, M. Lienemann and P. Laaksonen: 'Self-assembly of Class II Hydrophobins on Polar Surfaces', *Langmuir*, 2012, **28**, 4293-4300.

[24] Z. Wang, M. Lienemann, M. Qiau and M.B. Linder: 'Mechanisms of Protein Adhesion on Surface Films of Hydrophobin', *Langmuir*, 2010, **26**, 8491-8496.

[25] K. Chawla, S. Lee, B.P. Lee, J.L. Dalsin, P.B. Messersmith and N.D. Spencer: A novel low-friction surface for biomedical applications: Modification of poly(dimethylsiloxane) (PDMS) with polyethylene glycol(PEG)-DOPA-lysine. *Journal of Biomedical Materials Research Part* A, 2009, **90A**, 742-749.

[26] T. Sarlin, T. Kivioja, N. Kalkkinen, M.B. Linder and T. Nakari-Setälä: 'Identification and characterization of gushing-active hydrophobins from Fusarium graminearum and related species', *J Basic Microbiol*, 2012, **52**,184-194.

[27] M.B. Linder, M. Qiao, F. Laumen, K. Selber, T. Hyytiä, T. Nakari-Setälä and M.E. Penttilä: 'Efficient Purification of Recombinant Proteins Using Hydrophobins as Tags in Surfactant-Based Two-Phase Systems', *Biochemistry*, 2004, **43**, 11873-11882.

[28] H. Arwin: 'Spectroscopic ellipsometry and biology: Recent developments and challenges', *Thin Solid Films*, 1998, **313–314**, 764-774

[29] J.A. de Feijter, J. Benjamins and F.A. Veer: 'Ellipsometry as a tool to study the adsorption behavior of synthetic and biopolymers at the air–water interface', *Biopolymers*, 1978, **17**, 1759-1772

[30] Z. Chi, X.G. Chen, J.S.W. Holtz and S.A. Asher: 'Uv resonance raman-selective amide vibrational enhancement: Quantitative methodology for determining protein secondary structure', *Biochemistry,* 1998, **37**, 2854-2864

[31] L. Macakova, G.E. Yakubov, M.A. Plunkett and J.R. Stokes: 'Influence of ionic strength on the tribological properties of pre-adsorbed salivary films'. *Tribology International*, 2011, **8**, 956-962.

[32] D.A. Garrec and I.T. Norton: 'Boundary lubrication by sodium salts: A Hofmeister series effect'. *Journal of Colloid and Interface Science,* 2012, **379**, 33–40

V

Hakala, T.J., Metsäjoki, J., Granqvist, N., Milani, R., Szilvay, G.R., Elomaa, O., Deng, M., Zhang, J., Li, F. (2015) Adsorption and lubricating properties of HFBII hydrophobins and diblock copolymer poly(methyl methacrylate-b-sodium acrylate) additives in water-lubricated copper vs. a-C:H contacts. *Tribology International*, 90, 60-66.

Tribology International 90 (2015) 60–66

Contents lists available at ScienceDirect

Tribology International

journal homepage: www.elsevier.com/locate/triboint

Adsorption and lubricating properties of HFBII hydrophobins and diblock copolymer poly(methyl methacrylate-b-sodium acrylate) additives in water-lubricated copper vs. a-C:H contacts

Timo J. Hakala [a,*], Jarkko Metsäjoki [a], Niko Granqvist [b], Roberto Milani [a], Géza R. Szilvay [a], Oskari Elomaa [c], Mengmeng Deng [d], Jianjun Zhang [d], Feng Li [d]

[a] VTT Technical Research Centre of Finland Ltd, P.O. Box 1000, FI-02044, Finland
[b] Bionavis Ltd, Elopellontie 3C, 33470 Ylöjärvi, Finland
[c] Aalto University, School of Chemical Technology, Department of Materials Science and Engineering, Vuorimiehentie 2A, FI-02150 Espoo, Finland
[d] Suzhou Institute of Nano-Tech and Nano-Bionics, Chinese Academy of Sciences, Suzhou 215123, China

ARTICLE INFO

Article history:
Received 13 January 2015
Received in revised form
19 March 2015
Accepted 3 April 2015
Available online 14 April 2015

Keywords:
DLC
Water lubrication
Hydrophobins
Tribology

ABSTRACT

In a metal forming process the adhesion between the workpiece and the tool needs to be minimised, which can be achieved by use of lubricants and coatings. Here adsorption and lubrication properties of HFBII hydrophobins and diblock copolymer poly(methyl methacrylate-b-sodium acrylate) in water-lubricated copper vs. a-C:H coating contacts were studied by Surface Plasmon Resonance (SPR) and by a pin-on-disc (POD) tribometer. Hydrophobins formed a dense monolayer film on a-C:H surface and reduced friction by 13–30% but increased the wear of copper compared to pure water lubrication. Poly (methyl methacrylate-b-sodium acrylate) formed a sparse lubricating layer compared to HFBII lubricated contacts, but the friction coefficient was lower. HFBII molecules prevented copper oxide tribofilm formation on the copper pin.

1. Introduction

In cold forming processes of copper such as forging, lubricating emulsions, mineral oil or soaps are used to increase the surface quality of the workpiece and the lifetime of tools. The yield strengths and tensile stresses of copper and copper alloys vary greatly. The lowest yield strengths are typically at range 60–80 MPa. In cold forming of copper the main challenges are related to extreme pressure (EP) additives, which are generally based on the chemical reactions between sulphur, phosphorus or chlorine and the steel surface. EP additives enhance lubrication in boundary lubrication regime where they react with the contact surfaces and form thin, low shear strength layer. These types of additives cannot form lubricating layers on a copper surface and may contain sulphur that causes staining [1]. Most EP additives are also environmentally hazardous and may cause human health risks. By using environmentally friendly water-based lubricants and coatings, these problems could be avoided [2]. In addition, low viscosity and good thermal conductivity of water are beneficial properties for a lubricant in the forming process. However, the use of water as a lubricant in industrial applications is fairly limited due to its poor boundary lubrication properties and corrosiveness. In order to prevent corrosion and reduce friction, different kinds of additives can be added into water [3,4].

In water-based lubrication systems, polymers and biomolecules have been found to reduce friction and the wear of sliding surfaces. These lubricating molecules adhere to surfaces and bind large amounts of water into the contact zone [5,6]. The adsorption of the molecules to the surfaces can occur via electrostatic forces, van der Waals forces, covalent bonding or hydrophobic interaction. With polymer brushes, low friction coefficient (below 0.05) and wear rate can be achieved up to few hundreds of MPa's [7–9]. Amphiphilic diblock copolymers are an interesting option for water-based lubrication additives. They form lubricating layers by self-assembly. The experimental results are promising and friction coefficients below 0.001 [10] have been reported. However, the friction in polymer-lubricated contacts increases under increasing contact pressures because the shear force caused by tribostress exceeds the adhesion force between molecules and substrate [7].

Biomolecules are known to be part of water-based lubrication systems in nature. Their properties are fascinating from the industrial point of view [11]. However, few studies of biomolecules as additives in lubrication for industrial applications have been made so far [6,12,13]. In nature, biomolecules lubricate under relatively low loads and contact pressures, while in industrial applications the contact pressures are up to several gigapascals. Friction coefficients below

* Corresponding author. Tel.: +358 40 7702369.
E-mail address: timo.j.hakala@vtt.fi (T.J. Hakala).

http://dx.doi.org/10.1016/j.triboint.2015.04.006
0301-679X/

0.1 have not been achieved with traditional oil-based lubricants in a boundary lubrication regime. Thus, there is a great interest in biomolecules as lubricant additives because friction coefficients below 0.05 [14] have been measured with biomolecule additives in the laboratory. By increasing the adhesion between lubricating molecules and substrate, the low friction can be retained under the relatively high contact pressures that has been demonstrated with polymer brushes attached to the surface by covalent bonding [15]. Lubricating biomolecules thus need strong adhesion to the surface and a good water binding ability.

Hydrophobins are water soluble proteins produced by filamentous fungi. In nature, they control the interfacial adhesion of fungus and are known to form elastic films both on the air-water interface and on solid surfaces [16,17]. Due to their ampliphilic structure, hydrophobins are able to bind large amounts of water with their hydrophilic moiety [6]. In addition, hydrophobin structure is very stable due to sulphide bridges inside the protein, and the structure can survive high temperatures (over 90 °C) without irreversible changes in their structure [18]. Due to these properties, hydrophobins are an attractive choice as a lubricant additive in water-based lubrication systems. Previously, it was observed that hydrophobins can form highly hydrated layers and reduce friction from 0.7 to 0.1 in water-lubricated stainless steel vs. stainless steel contacts [6]. The friction performance on mica surfaces was at the same level ~0.1–0.3 [19]. Lower friction coefficients (below 0.05) have been measured in stainless steel vs. stainless steel contacts with increased sliding velocities [13] and in PDMS vs. PDMS contacts [20].

Low friction in water-based systems where polymers and biomolecules lubricate the surfaces is related to hydration lubrication mechanism where amphiphilic molecules are adsorbed onto the surfaces, and sliding occurs between their hydrophilic moieties (Fig. 1) [9,19]. The water content of the molecule layer plays an important role both in polymer- [5,8] and biomolecule-lubricated contacts [6,21,22].

In cold forming processes the contact pressures can reach levels (hundreds of MPa's) where biomolecules are not able to provide lubrication. Thus thin hard coatings, such as diamond-like carbon (DLC), can be applied. The DLC coatings have excellent tribological properties under high contact pressures including low friction coefficient (0.05–0.2) in water-lubricated contacts and high wear resistance [23–26]. DLC is a general term used for a wide number of coatings with varying properties, ranging from tetrahedral amorphous carbon (ta-C) to hydrogenated amorphous carbon (a-C:H). The friction and wear performance of DLC films in water lubrication can be modified by controlling the hydrogen content of the coatings or by the addition of dopants, such as silicon [23]. The lubricity of DLC films in humid conditions originates from both graphitization of the top layer of sliding surfaces and formation of water molecules that interacts with the DLC surface [27]. Hydrogenated a-C:H coatings are known to have low friction and wear in dry contact, but both wear and friction are increased in humid conditions [26].

In this paper, we have studied the adsorption and tribological behaviour (friction and wear) of HFBII hydrophobins protein and diblock copolymer poly(methyl methacrylate-b-sodium acrylate) in water on copper vs a-C:H contacts.

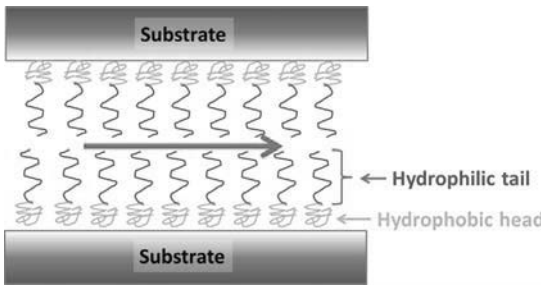

Fig. 1. In hydration lubrication, ampliphilic molecules are adsorbed onto the sliding surfaces and sliding occurs between the hydrophilic moieties.

2. Materials and methods

2.1. a-C:H film deposition

The a-C:H films were deposited using an ICP-PECVD system (Oxford Plasmalab 100) with both ICP and RF generators operating at a frequency of 13.56 MHz. Prior to film deposition, all substrates were cleaned in an ultrasonic bath with acetone, isopropyl alcohol, deionised water, and finally dried by nitrogen blowing. Before the film deposition, the process chamber was evacuated to a base pressure of 2×10^{-4} Pa. During the deposition processes, the power of the ICP generator and RF generator were set at 1000 W and 250 W, respectively. The flow rates of the precursor CH_4 and the dilution gas Ar were kept at 30 sccm and 10 sccm, respectively.

For Surface Plasmon Resonance measurements a 10–20 nm a-C:H coating was deposited on sensors; glass substrates with an Au layer of a few nanometres. The process time was 1 min at 75 °C. The corresponding deposition rate was 12.5 nm/min.

For tribological experiments, a-C:H coatings with R_a value below 0.05 μm and hardness of 20.3 GPa were deposited onto stainless steel (AISI440B) substrates. The process time was 1 h at 75 °C. The coating thickness was about 1 μm including a 300 nm thick SiN_x adhesion layer which was deposited by using SiH_4 (40 sccm) and N_2 (40 sccm) precursor gases, RF power 150 W, ICP power 2400 W, pressure 10 mTorr at 75 °C temperature. The process time for SiN_x layer was 9 min.

2.2. Preparation of lubricants

Following the approach described by Klein [10], a diblock copolymer poly(methyl methacrylate-b-sodium acrylate), molecular weight: PMMA(4300)-b-PANa(17500), was used (Fig. 2a). The polymer contains a short hydrophobic segment to favour adhesion to a hydrophobic DLC surface in an aqueous environment, and a long hydrophilic, ionic segment which enables good water lubrication properties. The polymer solutions were prepared at a 1.0 mg/mL concentration in milli-Q water. The solutions were perfectly transparent by visual inspection.

HFBII hydrophobins (Fig. 2b) were produced in a recombinant *Trichoderma reesei* strain VTT-D-99745 using a bioreactor. The molecular mass of the HFBII is 7200 g/mol [28] and it consists of 71 amino acids. The amino acid sequence of HFBII hydrophobin is presented elsewhere [29]. The HFBII was extracted from a culture supernatant using an aqueous two-phase system [30] and further purified using a Bio-Gel P-6DG size exclusion chromatography column (Bio-Rad) in a 20 mM ammonium acetate buffer pH 8. HFBII containing fractions were adjusted with acetic acid to about pH 5.5, and subsequently pooled and freeze-dried. For friction tests, HFBII powder was dissolved in Milli-Q (mQ) water (resistivity 18.2 MΩ cm) and 50 mM sodium acetate buffer (pH 5). In all tribological experiments, the HFBII concentration was 1.0 mg/ml. For contact angle measurements and SPR experiments, lower HFBII concentrations were used, because hydrophobins form a monolayer on solid surfaces and full coverage of the surface is achieved with lower concentrations than 1.0 mg/ml [6].

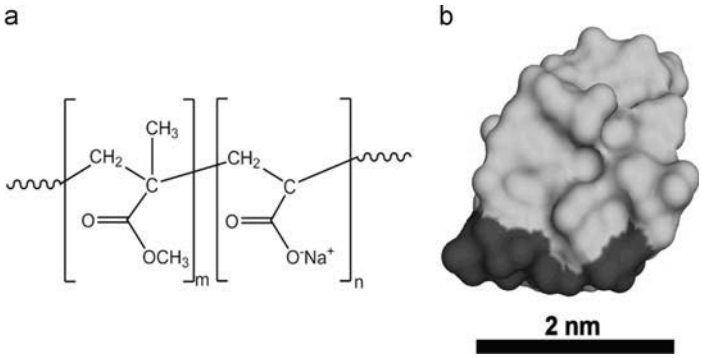

Fig. 2. (a) Molecular formula of diblock copolymer poly(methyl methacrylate-b-sodium acrylate) and (b) structure of HFBII hydrophobin protein. Green colour indicates the hydrophilic exposed surface and dark grey colour at the bottom indicates the hydrophobic patch. The diameter of hydrophobic patch is approximately 2.2 nm. (Structure from Protein Data Bank entry 1R2M) [29]. (For interpretation of the references to colour in this figure legend, the reader is referred to the web version of this article.)

2.3. Surface plasmon resonance

Surface Plasmon Resonance (SPR) is a surface-bound optical phenomenon that can be used to study interactions and optical layer properties, such as the refractive index (RI) and thickness (d) of materials. While commonly applied in biomolecular screening [31], new methods such as the now utilised Multi-Parametric surface plasmon resonance (MP-SPR) allow us to characterise interactions between biomolecules and surfactants with different coatings [32,33].

MP-SPR instrument SPR Navi 220A (BioNavis Ltd, Ylöjärvi Finland) together with gold and copper-coated sensors were used in the measurements. The a-C:H coating was deposited on the gold sensor as described in 2.1. The measurements were performed at 20 °C using flow rate of 30 μL/min. HFBII interaction with a-C:H and Cu surfaces was studied in pure water (milliQ) and in an acetate buffer (50 mM sodium acetate, pH 5.0). Each interaction experiment consisted of a series of HFBII or polymer injections with concentrations of 3.9, 15.6 or 62.5 μg/mL. An exception to this was a polymer interaction with a Cu surface, which was performed with a single injection of 250 μg/mL. The amount of HFBII was calculated from the SPR signal level after all the injections, and the initial slope of the first HFBII sample injection was used to calculate the relative interaction rate. a-C:H coating thickness was determined using SPR Navi LayerSolver v.1.0.2.2.4.

2.4. Contact angle measurements

For the contact angle measurements, an Attension Theta optical tensiometer (from Biolin Scientific) was used at 22.5 °C and 50% relative humidity (RH). The sessile drop method was used to measure the contact angles of water on surfaces. The Young–Laplace equation was used for fitting the drop profiles. The size of the water droplet was 5 μl and the contact angle of the water was determined as an average from 5 parallel experiments. For the contact angle, measurements concentration of HFBII solutions was 0.1 mg/ml. The HFBII layer was formed by an addition of 0.5 ml solution on the a-C:H surface, and after 30 min of adsorption, the excess of solution was washed away with 1.0 ml of MQ water. After washing, the a-C:H surface was dried by air blowing.

2.5. Tribology

Tribological tests were carried out on a pin-on-disc tribometer (POD) designed and manufactured at VTT. A stationary, spherical counterbody (Cu, ∅50 mm) was used against rotating a-C:H coated stainless steel disc. The hardness of the copper was 96.0 ± 1.1 HV1, and initial surface roughness R_a value was 0.44 ± 0.03 μm which decreased below 0.10 μm due to wear as measured with a stylus profilometer. The water contact angle was about 80°, indicating a moderately hydrophobic surface. The friction force was constantly measured during the experiments and friction coefficient was determined as an average value between 30 and 40 min. A sliding velocity of 0.05 m/s and a normal load of 2 N were applied and test duration was kept at 40 min so as to avoid excess evaporation of the lubricant. The initial Hertzian contact pressure was approximately 100 MPa, but it decreased to the level of 0.35–1.65 MPa due to the wear of the sliding bodies that increased the contact area. Contact pressures in the tribotests correspond to the adsorption lubrication regime where physically adsorbed molecules are able to lubricate [34]. A small amount of lubricant (0.6 ml) was added to the disc before the experiment and the lubricant covered the entire wear track during the experiment. Three parallel experiments were carried out for each coating/lubricant pair. All the tests were carried out at room temperature (22 ± 1 °C). After the tests, the discs were ultrasonically cleaned in ethanol and the wear tracks were characterised by optical microscopy, scanning electron microscopy + energy dispersive spectroscopy (EDS) (Zeiss Ultraplus + Thermo Fisher Scientific Ultradry EDS detector) and Raman spectroscopy (Horiba Jobin-Yvon Labram HR Raman, 488 nm). The wear volume of the counterbody was calculated using wear track micrographs and spherical cap approximation.

3. Experimental results

3.1. MP-SPR experiments and contact angle measurements

The binding sensograms of HFBII hydrophobins and polymer poly(methyl methacrylate-b-sodium acrylate) on a-C:H surfaces are presented in Fig. 3. The HFBII was found to bind well to the a-C:H surface, and the binding was significantly larger in pure water than in an acetate buffer (Table 1). Similar results were measured with HFBI and FpHYD5 hydrophobins on stainless steel surface [6]. The polymer poly(methyl methacrylate-b-sodium acrylate) was found to bind significantly more weakly to the a-C:H surface. The HFBII in acetate buffer seems to exhibit faster relative binding than the HFBII in water, seen from the initial binding slope at time = 0 of the binding sensogram. Between injections of HFBII or polymer molecules there was a flow of water or acetate buffer depending on which solution molecules

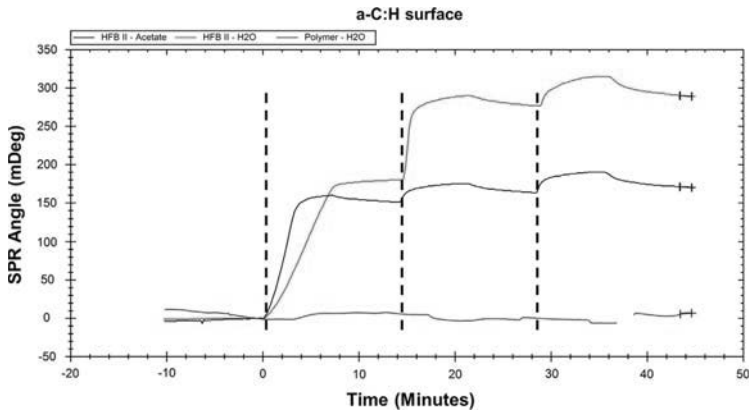

Fig. 3. Binding of HFBII in water (red) and in acetate (black) and binding of the polymer (blue) to a-C:H surface. Each interaction experiment consisted of a series of HFBII or polymer injections with concentrations of 3.9, 15.6 or 62.5 μg/mL. Dashed lines represent the HFBII injections. (For interpretation of the references to colour in this figure legend, the reader is referred to the web version of this article.)

Table 1
Mass of bound molecules on a-C:H coating measured with MP-SPR and calculated average area per molecule.

Solution	Bound mass (ng/cm^2)	Area per molecule (nm^2)
HFBII in water	290	4.1
HFBII in 50 mM sodium acetate	171	7.0
Polymer in water	7	517

were dissolved. However, it can be seen that there is no significant desorption of the molecule layers from the a-C:H surface.

The copper coated sensors gave anomalous binding with HFBII. There are both mass adding and removing processes present (supplementary information, Fig. 1S).

The contact angle of water on the dried HFBII films on a-C:H surfaces was 61°, regardless of whether they were formed in water or an acetate buffer. The contact angle was significantly lower compared to a clean a-C:H surface which has a contact angle of approximately 77°.

3.2. Friction and wear tests

In tribological experiments, it was observed that both polymer and hydrophobins reduced the friction coefficient in comparison to pure mQ water (Fig. 4a). For polymer additives, the friction coefficient did not reach a stable state, but fell continuously throughout the tests (Fig. 2S). The value of the friction coefficient for polymers in mQ water at the end of the tests was lower than for hydrophobins. For hydrophobins, the friction coefficient was relatively stable throughout the test time. The friction coefficients were at the same level for hydrophobins both in water and a 50 mM sodium acetate buffer.

The wear volume of the copper counterbody was larger in polymer and hydrophobin-lubricated experiments compared to pure mQ water-lubricated experiments (Fig. 4b). The largest wear volume was observed for HFBII in buffer-lubricated experiments. No delamination of a-C:H coating occurred during the tribotests. The thicker tribofilm was formed onto the copper surface because it is constantly in contact. The possible tribolayer on DLC surface is so thin that EDS cannot detect the chemical elements accurately.

3.3. Surface analysis

In water-lubricated experiments, a blue coloured tribofilm was formed on the copper surface. No similar tribofilm formation was observed in other experiments (Fig. 5). EDS analyses (Table 2) showed oxygen enrichment on the wear tracks on the copper surface. The highest oxygen concentration was observed in the wear tracks with water-lubricated experiments (Fig. 3S). Traces of sulphur were observed on wear tracks on a copper surface lubricated with hydrophobins in a water and buffer solution (Fig. 4S). Sulphur was not found on the wear track of the copper surface after the polymer and water-lubricated experiments. Lubricant residue observed on the copper surfaces outside the wear track after HFBII-lubricated tests showed indication of C, N, O and S respectively (Fig. 5S). This indicates that they originate from hydrophobin proteins.

The wear tracks on a-C:H coated discs were not observed by optical microscopy due to limited resolution, and the track depth was smaller than the resolution of a stylus profilometer. However, the wear tracks could be observed by SEM. EDS measurements showed no indication of copper on the a-C:H surfaces.

EDS analysis was supported by Raman experiments where copper oxide was found on the wear track of a copper pin after water-lubricated experiment. Raman spectra (Fig. 6) show peaks at 108 and 154 cm^{-1} that correspond to inactive Raman mode and an only infrared allowed Raman mode of Cu_2O peaks that have been observed to be formed by chemomechanical polishing of copper [35]. No Cu_2O was detected on a copper pin with Raman after HFBII in water-lubricated experiments.

4. Discussion

According to the SPR experiments, hydrophobin coverage on a-C:H is almost perfect in water if they form monolayer structure. The measured area that one HFBII molecule takes is approximately 4 nm^2 which corresponds to the calculated average area of one molecule (4.1 nm^2) in an SPR experiment. It is interesting that the HFBII hydrophobins do not fill the whole surface when adsorbed in a 50 mM sodium acetate buffer. The reason may be associated with differences in surface charges of HFBII in the different pHs, that may affect lateral interactions between HFBII molecules and interactions with the coating layer as observed earlier for SAM coatings [17]. In water the net electric charge of HFBII molecule is more close to 0 than in pH 5 because the isoelectric point of HFBII

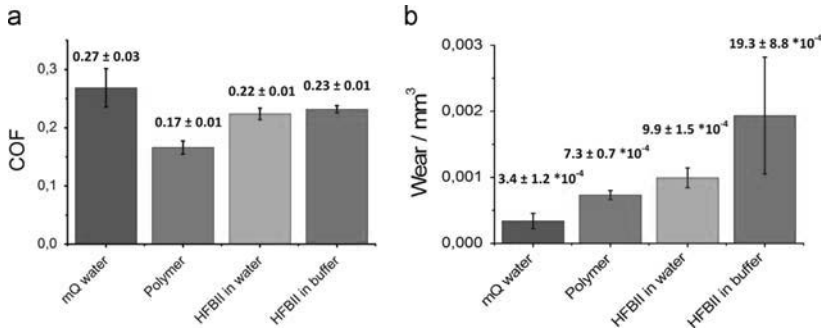

Fig. 4. (a) Friction coefficient and (b) wear volume of the copper pin after sliding against a-C:H coating. Both polymer and hydrophobins were dissolved in mQ water. Test parameters: normal load 2 N, sliding velocity of 0.05 m/s and sliding distance 120 m.

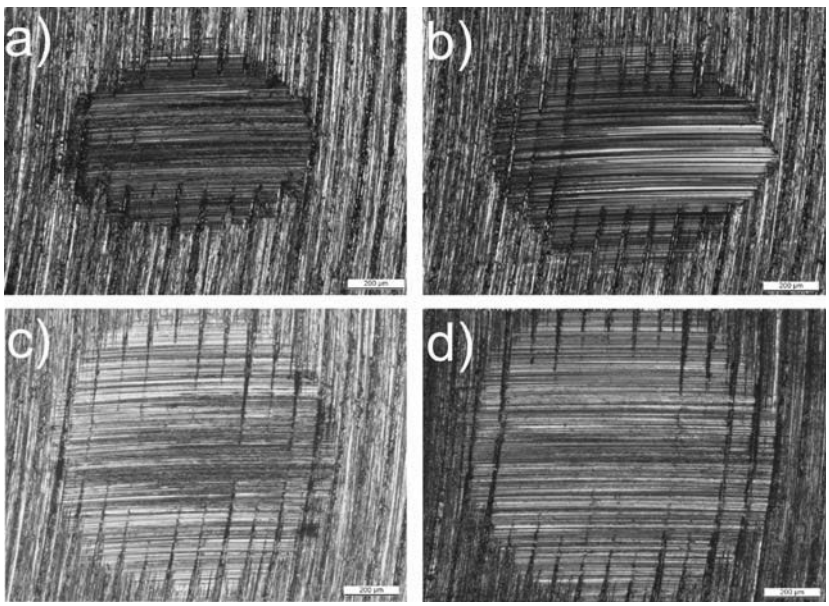

Fig. 5. Optical microscopy images of worn copper surfaces after sliding against a-C:H coatings lubricated with (a) water, (b) polymer in water, (c) HFBII in water and (d) HFBII in buffer. Scale bar 200 μm.

Table 2
Chemical elements observed outside wear track and on the wear track of copper pin by EDS (+ = chemical elements found, − = chemical elements not found).

Lubricant	Chemical elements					
	Outside wear track			Wear track		
	C	O	S	C	O	S
Water	+	+	−	+	+	−
HFBII in water	+	+	−	+	+	+
HFBII in buffer	+	+	−	+	+	+
Polymer in water	+	+	−	+	+	−

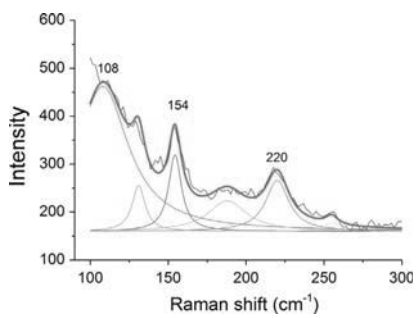

Fig. 6. Raman data from 100 to 300 cm^{-1} of tribofilm formed on a copper pin in water-lubricated experiments. Peaks at 108 and 154 cm^{-1} revealed Cu_2O.

molecule is at 6.7. [36] There is no removal of the HFBII layer when there is a water flow between HFBII injections which supports the monolayer existence without a weakly bonded second layer. The contact angle measurements support monolayer formation as well, because no difference in contact angles between HFBII layers formed in water and acetate buffer was observed. The contact angle of approximately 60° shows that the alignment of the molecule layer might not be perfect. Gruner et al. found out that

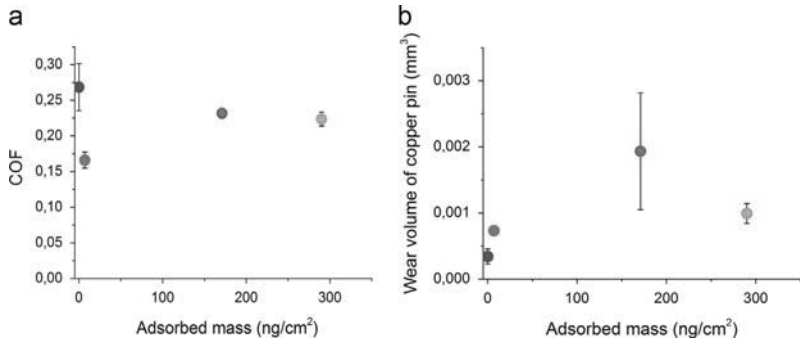

Fig. 7. Adsorbed mass of lubricant molecules on a-C:H surface vs. (a) friction coefficient and (b) wear volume of a copper pin.

HFBII molecules reduce the contact angle of water to 40° when adsorbed on a hydrophobic surface [17].

The SPR results show that the HFBII in an acetate buffer binds less in terms of mass to a-C:H than in water, but the kinetics of the binding are faster. The larger amount of bound hydrophobins in water may be caused by the higher pH of water compared to a 50 mM sodium acetate buffer which has a pH of 5 [13,17]. The faster adsorption of hydrophobins in the buffer may be caused by differences in molecule rearrangements on a-C:H surface.

The lowest friction coefficient was measured in a poly(methyl methacrylate-b-sodium acrylate)-lubricated contact, where the adsorbed mass on DLC surface was the smallest measured with SPR. These results are supported by previous studies by Hakala et al. [6,13] where an increase in adsorbed mass increased friction and wear. However, when comparing HFBII-lubricated experiments the better surface coverage formed in water reduces the amount of surface asperity contacts, and thus reduces wear (Fig. 7).

The friction coefficients in hydrophobin- and polymer-lubricated experiments were between 0.20 and 0.25. Similar results have been reported for contacts where the lubrication through hydration lubrication mechanism was not possible due to high contact pressures. As shown by Klein [7], in hydration lubrication the friction coefficients can reach values well below 0.05. However, high contact pressures may disturb low friction mechanisms by causing the entanglement of molecule layers adsorbed to both sliding surfaces [7,14], removal of surface adhered molecules [10] and bridging where molecules are adhered on both sliding surfaces [14,37]. Previously, it has been observed that hydrophobins do not withstand contact pressures of 0.36 MPa without shearing away from the surface [20], and in our experiments on copper vs. a-C:H contact the contact pressure is usually higher than 0.36 MPa even at the end of the experiments.

It is known that hydrophobins are able to lubricate soft hydrophobic surfaces with friction coefficients as low as 0.01–0.02 [20] although higher friction coefficients were measured at nanoscale with surface force apparatus (SFA) [19]. In hydration lubrication, the perfect alignment of the molecules is important as well (Fig. 1). As mentioned above, in the case of hydrophobins on a DLC surface it might be possible for a small portion of the proteins to still expose their hydrophobic sides after adhesion to the surface [17], thus reducing somewhat the water-based lubricating properties of the film.

In POD experiments, it was seen that friction in water-lubricated Cu vs. a-C:H contact increased with time. This is probably due to a tribofilm, which is gradually formed on the copper surface. It also indicates that the copper oxide vs. a-C:H contact formed is not well lubricated by water. Additives, such as HFBII hydrophobins and a diblock copolymer poly(methyl methacrylate-b-sodium acrylate), can prevent the formation of copper oxide tribofilm and reduce friction compared to water-lubricated contact. The reason why copper oxide film is not formed on the copper pin in a HFBII-lubricated contact may be the reactions between HFBII molecules and the copper surface. EDS analysis showed a small amount of sulphur on the sliding surfaces of the copper pin. Thus, it can be expected that the hydrophobins react with the copper surface in the contact area. It is known that inside the hydrophobin molecule there are four disulphide bridges. The HFBII molecule may be stretched or broken down in tribocontact, which can allow reactions between the copper surface and sulphur. The reactions between copper and HFBII molecules were also supported by SPR experiments where the anomalous binding response of HBFII was observed. The optical change induced by the removal of the oxides can be the cause of the heavily drifting signal in the experiment. The earlier works by Sheardown et al. and Torres Bautista et al. describe similar behaviour with copper surfaces and proteins [38,39].

Based on the results, it could be possible to use hydrophobin proteins and polymer additives in cold forming or polishing processes of copper to prevent the oxide film formation. Hydrophobins increase the wear of copper more than polymer additives and remove oxides from the copper surface without causing undesirable increase in friction. Polymer additives are able to reduce friction more than hydrophobins. DLC coating is needed to prevent wear of the tool.

5. Conclusion

Polymer additives and HFBII hydrophobins in water reduced the friction coefficient in copper vs. a-C:H sliding contacts compared to pure water. The main mechanism observed was the prevention of copper oxide tribofilm formation. The wear volume of the copper counter body increased when no copper oxide film was formed. Hydrophobins adsorbed to a-C:H surfaces and formed a monolayer, which reduced the contact angle of water from 77° to approximately 60° compared to a clean a-C:H surface. Hydration lubrication did not take place in copper vs. a-C:H contact possibly due to the alignment of HFBII molecules and high contact pressures. The adsorption of HFBII hydrophobins on copper surfaces was more complicated compared to adsorption on a-C:H surfaces, because both removal and addition of material on a copper surface occurred during SPR measurement. The reasons for this behaviour are the chemical reactions between HFBII molecules and the copper surface.

Acknowledgements

The authors want to thank Riitta Suihkonen for purification of proteins, Ajai Iyer (Aalto University, School of chemical technology, Department of Materials Science and Engineering) for Raman

measurements and the technical personnel from Suzhou Institute of Nano-Tech and Nano-bionics (SINANO) for their technical support on Thin Film Coating equipment. This research work is financially supported by the China (Jiangsu) and Finland International R&D Programme (BZ2013009), Academy of Finland, the Finnish Funding Agency for Technology and Innovation (Project VTT Finland-China Innovation Alliance in Nanotechnology) and VTT Technical Research Centre of Finland Ltd.

Appendix A. Supporting information

Supplementary data associated with this article can be found in the online version at http://dx.doi.org/10.1016/j.triboint.2015.04.006.

References

[1] Altan T, Ngaile G, Shen G. Cold and hot forging: fundamentals and applications. 1st ed. USA: ASM International; 2005.
[2] Gariety M, Ngaile G, Altan T. Evaluation of new cold forging lubricants without zinc phosphate precoat. Int J Mach Tools Manuf 2007;47:673–81.
[3] Tomala A, Naveira-Suarez A, Pasaribu R, Doerr N, Werner WSM, Stoeri H. Behaviour of corrosion inhibitors under different tribological contact. Tribol Lett 2012;45:397–409.
[4] Elomaa O, Singh VK, Iyer A, Hakala TJ, Koskinen J. Graphene oxide in water lubrication on diamond-like carbon vs. stainless steel high-load contacts. Diam Relat Mater 2015;52:43–8.
[5] Chawla K, Lee S, Lee BP, Dalsin JL, Messersmith PB, Spencer ND. A novel low-friction surface for biomedical applications: modification of poly(dimethylsiloxane) (PDMS) with polyethylene glycol(PEG)-DOPA-lysine. J Biomed Mater Res Part A 2009;90:742–9.
[6] Hakala TJ, Laaksonen P, Saikko V, Ahlroos T, Helle A, Mahlberg R, et al. Adhesion and tribological properties of hydrophobin proteins in aqueous lubrication on stainless steel surfaces. RSC Adv 2012;2:9867–72.
[7] Klein J. Polymers in living systems: from biological lubrication to tissue engineering and biomedical devices. Polym Adv Technol 2012;23:729–35.
[8] Müller MT, Yan X, Lee S, Perry SS, Spencer ND. Lubrication properties of a brushlike copolymer as a function of the amount of solvent absorbed within the brush. Macromolecules 2005;38:5706–13.
[9] Yan X, Perry SS, Spencer ND, Pasche S, De Paul SM, Textor M, et al. Reduction of friction at oxide interfaces upon polymer adsorption from aqueous solutions. Langmuir 2004;20:423–8.
[10] Raviv U, Giasson S, Kampf N, Gohy J-F, Jerome R, Klein J. Lubrication by charged polymers. Nature 2003;425:163–5.
[11] Neville A, Morina A, Liskiewicz T, Yan Y. Synovial joint lubrication – does nature teach more effective engineering lubrication strategies? Proc IMechE Part C: J Mech Eng Sci 2007;221:1223–30.
[12] Ahlroos T, Hakala TJ, Helle A, Linder MB, Holmberg K, Mahlberg R, et al. Biomimetic approach to water lubrication with biomolecular additives. Proc Inst Mech Eng, Part J: J Eng Tribol 2011;225:1013–22.
[13] Hakala TJ, Laaksonen P, Helle A, Linder MB, Holmberg K. Effect of operational conditions and environment on lubricity of hydrophobins in water based lubrication systems. Tribology 2014;8(4):241–7.
[14] Harvey NM, Yakubov GE, Stokes JR, Klein J. Normal and shear forces between surfaces bearing porcine gastric mucin, a high-molecular-weight glycoprotein. Biomacromolecules 2011;12:1041–50.
[15] Chen M, Briscoe WH, Armes SP, Klein J. Lubrication at physiological pressures by polyzwitterionic brushes. Science 2009;323:1698–701.
[16] Szilvay GR, Paananen A, Laurikainen K, Vuorimaa E, Lemmetyinen H, Peltonen J, et al. Self-assembled hydrophobin protein films at the air-water interface: structural analysis and molecular engineering. Biochemistry 2007;46:2345–54.
[17] Grunér MS, Szilvay GR, Berglin M, Lienemann M, Laaksonen P, Linder MB. Self-assembly of class II hydrophobins on polar surfaces. Langmuir 2012;28:4293–300.
[18] Askolin S, Linder M, Scholtmeijer K, Tenkanen M, Penttila M, de Vocht ML, et al. Interaction and comparison of a class I hydrophobin from schizophyllum commune and class II hydrophobins from *Trichoderma reesei*. Biomacromolecules 2006;7:1295–301.
[19] Goldian I, Jahn S, Laaksonen P, Linder M, Kampf N, Klein J. Modification of interfacial forces by hydrophobin HFBI. Soft Matter 2013;9:10627–39.
[20] Lee S, Røn T, Pakkanen KI, Linder M. Hydrophobins as aqueous lubricant additive for a soft sliding contact. Colloids Surf B: Biointerfaces 2015:264–9.
[21] Heuberger MP, Widmer MR, Zobeley E, Glockshuber R, Spencer ND. Protein-mediated boundary lubrication in arthroplasty. Biomaterials 2005;26:1165–73.
[22] Hakala TJ, Saikko V, Arola S, Ahlroos T, Helle A, Kuosmanen P, et al. Structural characterization and tribological evaluation of quince seed mucilage. Tribol Int 2014;77:24–31.
[23] Zhao F, Li HX, Ji L, Mo YF, Quan WL, Du W, et al. Superlow friction behavior of Si-doped hydrogenated amorphous carbon film in water environment. Surf Coat Technol 2009;203:981–5.
[24] Ronkainen H, Varjus S, Holmberg K. Tribological performance of different DLC coatings in water-lubricated conditions. Wear 2001;249:267–71.
[25] Holmberg K, Matthews A. Coatings Tribology. 2nd ed.. Oxford, Great Britain: Elsevier; 2009.
[26] Donnet C, Erdemir A. Tribology of Diamond-like Carbon Films – Fundamentals and Applications. New York, USA: Springer Science+Business Media, LLC; 2010.
[27] Martin J-M, De Barros Bouchet M-I, Matta C, Zhang Q, Goddard III WA, Okuda S, et al. Gas-phase lubrication of ta-C by glycerol and hydrogen peroxide. Exp Comput Model J Phys Chem C 2010;114:5003–11.
[28] Stanimirova RD, Gurkov TD, Kralchevsky PA, Balashev KT, Stoyanov SD, Pelan EG. Surface pressure and elasticity of hydrophobin HFBII layers on the air−water interface: rheology versus structure detected by AFM imaging. Langmuir 2013;29:6053–67.
[29] Hakanpää J, Paananen A, Askolin S, Nakari-Setälä T, Parkkinen T, Penttilä M, et al. Atomic resolution structure of the HFBII hydrophobin, a self-assembling amphiphile. J Biol Chem 2004;279:534–9.
[30] Linder MB, Qiao M, Laumen F, Selber K, Hyytiä T, Nakari-Setälä T, et al. Efficient purification of recombinant proteins using hydrophobins as tags in surfactant-based two-phase systems. Biochemistry 2004;43:11873–82.
[31] Rich R, Myszka D. Grading the commercial optical biosensor literature-Class of 2008: 'The Mighty Binders'. J mol recognit. 2009;23:1–64.
[32] Granqvist N, Liang H, Laurila T, Sadowski J, Yliperttula M, Viitala T. Characterizing ultrathin and thick organic layers by surface plasmon resonance three-wavelength and waveguide mode analysis. Langmuir 2013;29:8561–71.
[33] Orelma H, Filpponen I, Johansson L-S, Laine J, Rojas O. Modification of cellulose films by adsorption of CMC and chitosan for controlled attachment of biomolecules. Biomacromolecules 2011;12:4311–8.
[34] Stachowiak GW, Batchelor AW. Engineering Tribology. 3rd ed.. USA: Elsevier Inc; 2005.
[35] Solache-Carranco H, Juarez-Dıaz G, Esparza-Garcıa A, Briseno-Garcıa M, Galvan-Arellano M, Martınez-Juarez J, et al. Photoluminescence and X-ray diffraction studies on Cu_2O. J Lumin. 2009;129:1483–7.
[36] Kisko K, Szilvay GR, Vainio U, Linder MB, Serimaa R. Interactions of hydrophobin proteins in solution studied by small-angle x-ray scattering. BiophysJ 2008;94:198–206.
[37] Carapeto AP, Serro AP, Nunes BMF, Martins MCL, Todorovic S, Duarte MT, et al. Characterization of two DLC coatings for joint prosthesis: the role of albumin on the tribological behavior. Surf Coat Technol 2010;204:3451–8.
[38] Sheardown H, Cornelius RM, Brash JL. Measurement of protein adsorption to metals using radioiodination methods: a caveat. Colloids Surf B: Biointerfaces 1997;10:29–33.
[39] Torres Bautista BE, Carvalho ML, Seyeux A, Zanna S, Cristiani P, Tribollet B, et al. Effect of protein adsorption on the corrosion behavior of 70Cu–30Ni alloy in artificial seawater. Bioelectrochemistry 2014;97:34–42.

Supplementary information for

Adsorption and lubricating properties of HFBII hydrophobins and diblock copolymer poly(methyl methacrylate-b-sodium acrylate) additives in water-lubricated copper vs. a-C:H contacts

Timo J. Hakala[a]*, Jarkko Metsäjoki[a], Niko Granqvist[b], Roberto Milani[a], Geza Szilvay[a], Oskari Elomaa[c], Mengmeng Deng[d], Jianjun Zhang[d] and Feng Li[d]

[a]*VTT Technical Research Centre of Finland Ltd, P.O. Box 1000, FI-02044, Finland.*

[b]*Bionavis Ltd, Elopellontie 3C, 33470, Ylöjärvi, Finland*

[c]*Aalto University, School of Chemical Technology, Department of Materials Science and Engineering, Vuorimiehentie 2A , FI-02150 Espoo, Finland*

[d]*Suzhou Institute of Nano-Tech and Nano-Bionics, Chinese Academy of Sciences, Suzhou 215123, China.*

*Corresponding author. Tel.: +358 40 7702369

E-mail address: timo.j.hakala@vtt.fi

SPR measurements with the copper coated sensors gave anomalous binding with HFBII. There are both mass adding and removing processes present.

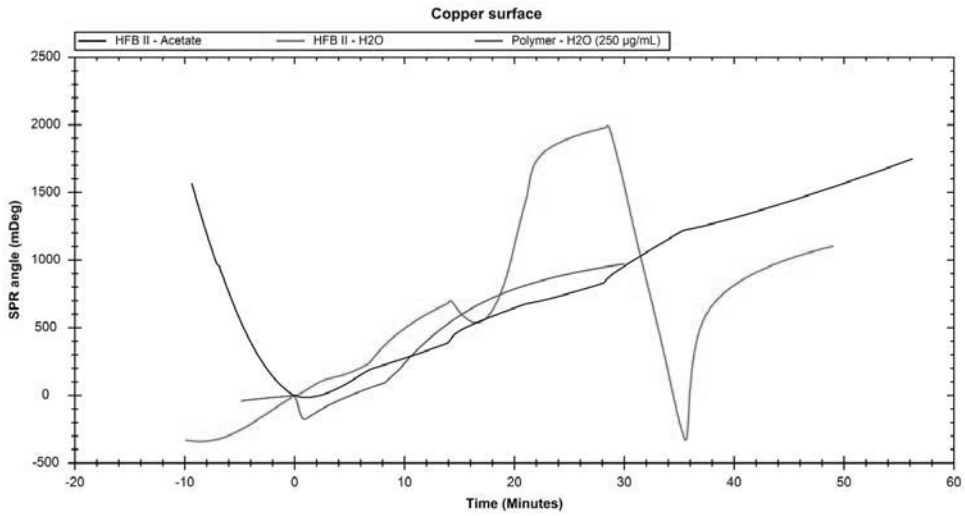

Figure 1S. Binding of HFB-II in water (red) and in acetate (black) and binding of the polymer (blue) to copper surface.

The friction coefficient did not reach a stable state in copper vs. a-C:H contact lubricated with poly(methyl methacrylate-b-sodium acrylate) additives but fell continuously throughout the tests.

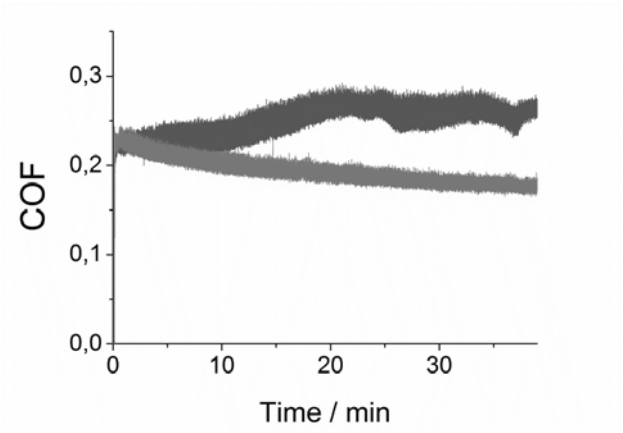

Figure 2S. Friction coefficient curves in mQ water (blue) and polymer (pink)-lubricated copper vs. a-C:H coating contacts. Test parameters: normal load 2 N, sliding velocity of 0.05 m/s and sliding distance 120 m.

The EDS analyses were performed using acceleration voltage of 15 kV. The signal comes from a volume that may be deeper than thin layer(s) on the surface.

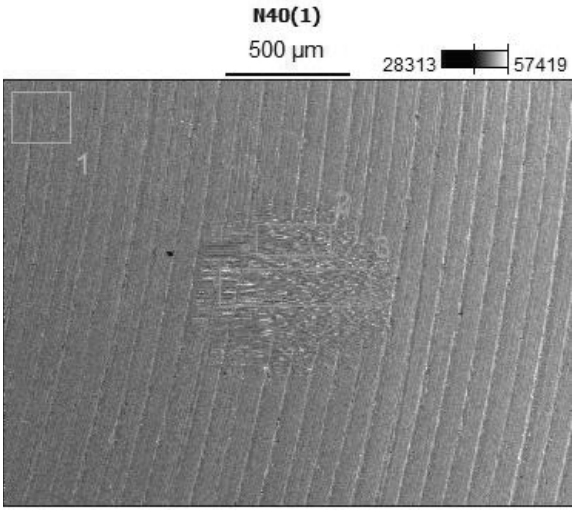

Figure 3S. EDS analysis locations on a water-lubricated copper pin. On the wear track the amount of oxygen is higher compared to location 1 outside the wear track. Result tables and graphs below.

Weight %

	C-K	O-K	Cu-K
N40(1)_pt1	6.3	1.2	92.5
N40(1)_pt2	6.9	6.2	86.9
N40(1)_pt3	6.9	5.1	88.0

Atom %

	C-K	O-K	Cu-K
N40(1)_pt1	25.7	3.5	70.8
N40(1)_pt2	24.8	16.6	58.6
N40(1)_pt3	25.3	14.0	60.7

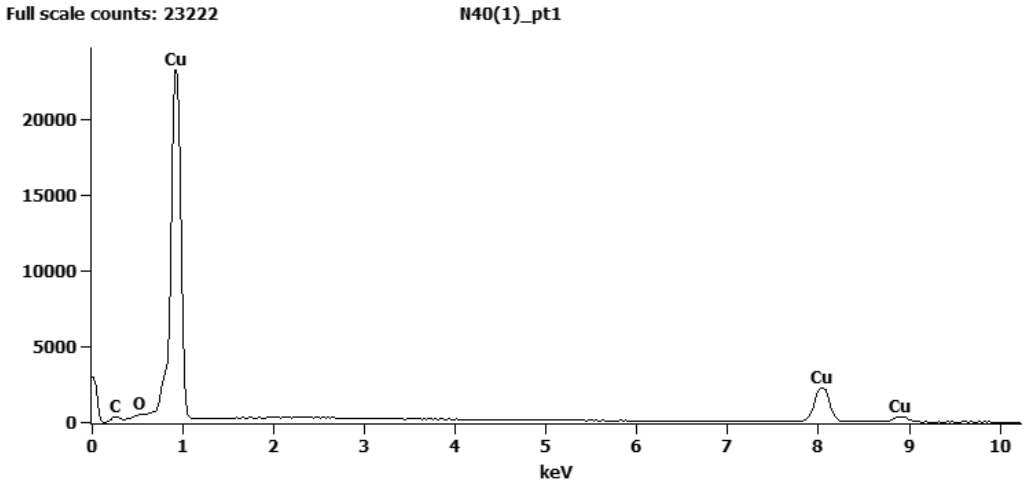

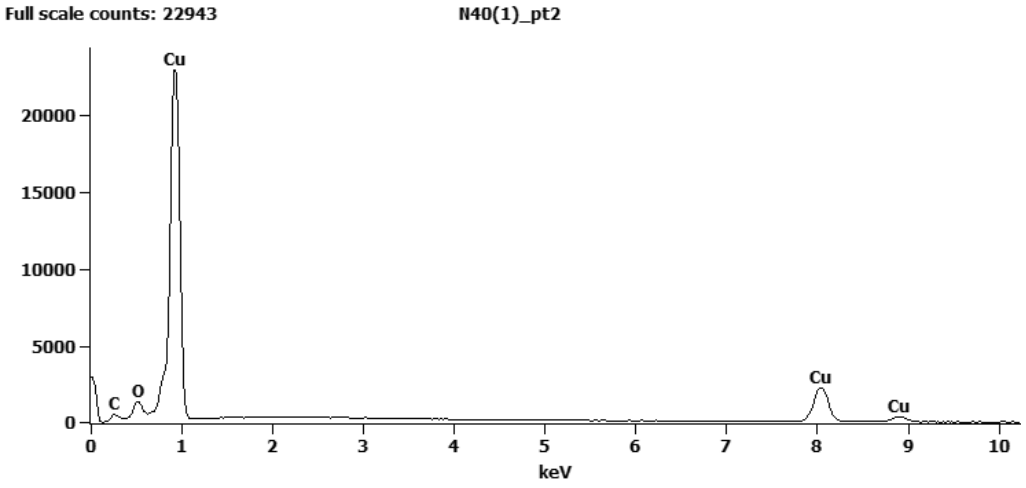
Full scale counts: 22943
N40(1)_pt2
Cu
20000
15000
10000
5000
0
C
O
Cu
Cu
0
1
2
3
4
5
6
7
8
9
10
keV

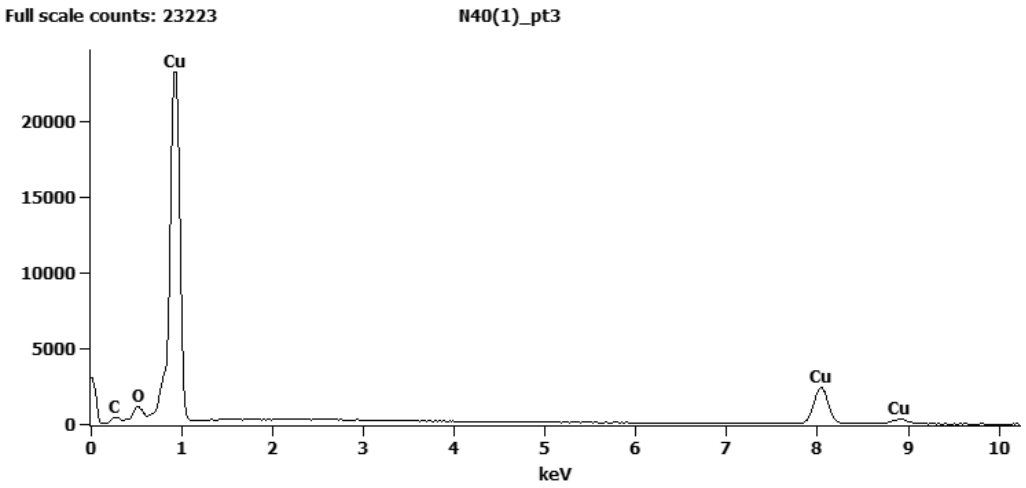
Full scale counts: 23223
N40(1)_pt3
Cu
20000
15000
10000
5000
0
C
O
Cu
Cu
0
1
2
3
4
5
6
7
8
9
10
keV

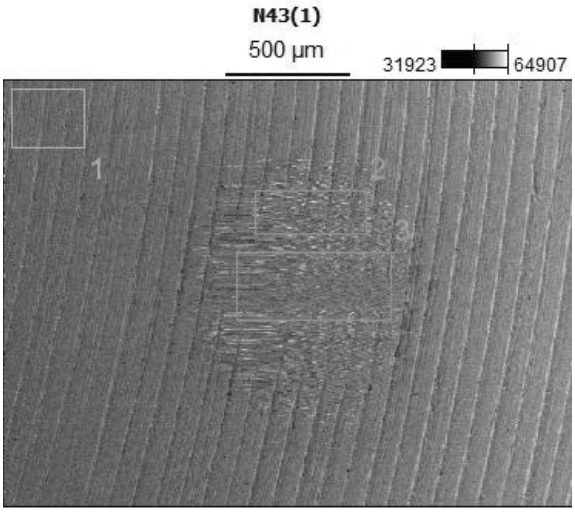

Figure 4S. EDS analysis locations on hydrophobins in a buffer solution-lubricated copper pin. At locations 2 and 3, sulphur is found on the wear track. Outside the wear track no sulphur was observed. Result tables and graphs below.

Weight %

	C-K	O-K	S-K	Cu-K
N43(1)_pt1	7.8	1.4		90.9
N43(1)_pt2	9.3	2.9	0.2	87.7
N43(1)_pt3	9.4	4.1	1.0	85.5

Atom %

	C-K	O-K	S-K	Cu-K
N43(1)_pt1	29.9	4.0		66.2
N43(1)_pt2	33.0	7.7	0.3	59.0
N43(1)_pt3	32.4	10.7	1.3	55.7

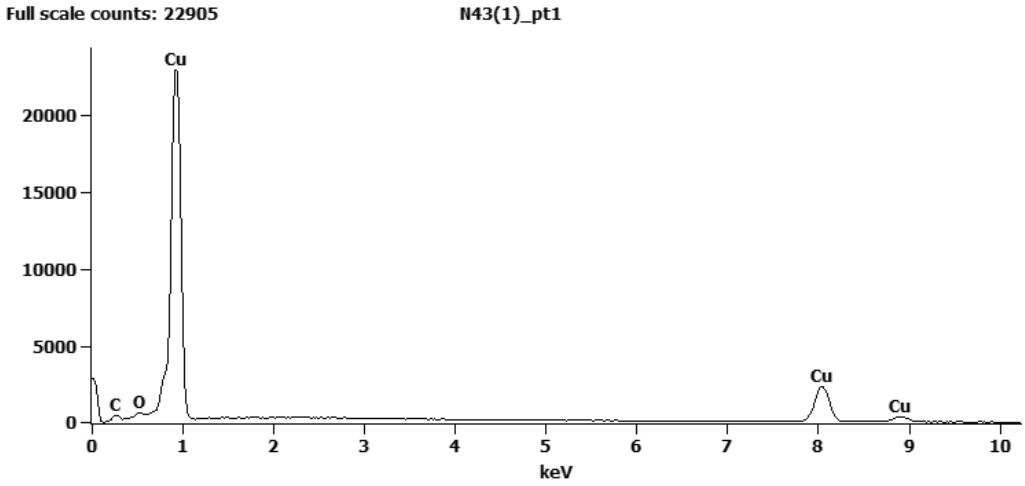

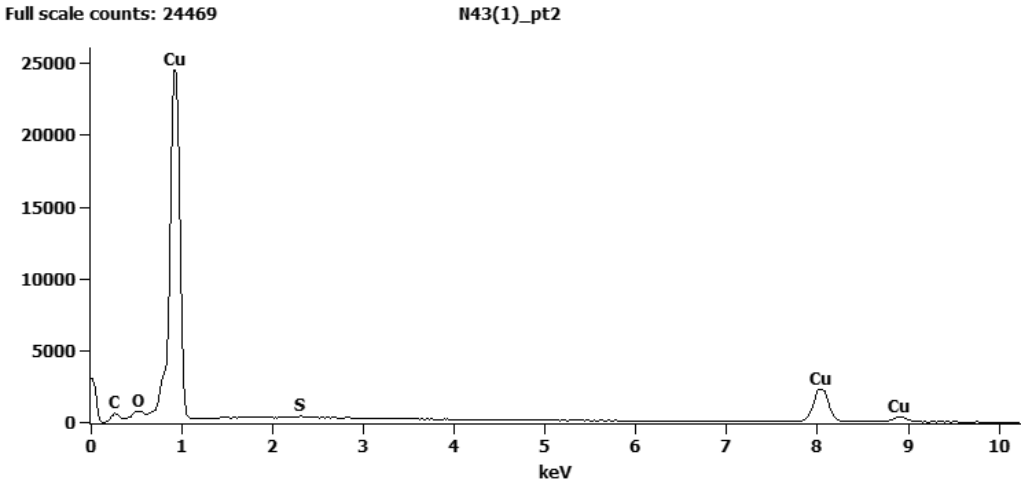
Full scale counts: 24469
N43(1)_pt2
25000
20000
15000
10000
5000
0
Cu
C
O
S
Cu
Cu
0
1
2
3
4
5
6
7
8
9
10
keV

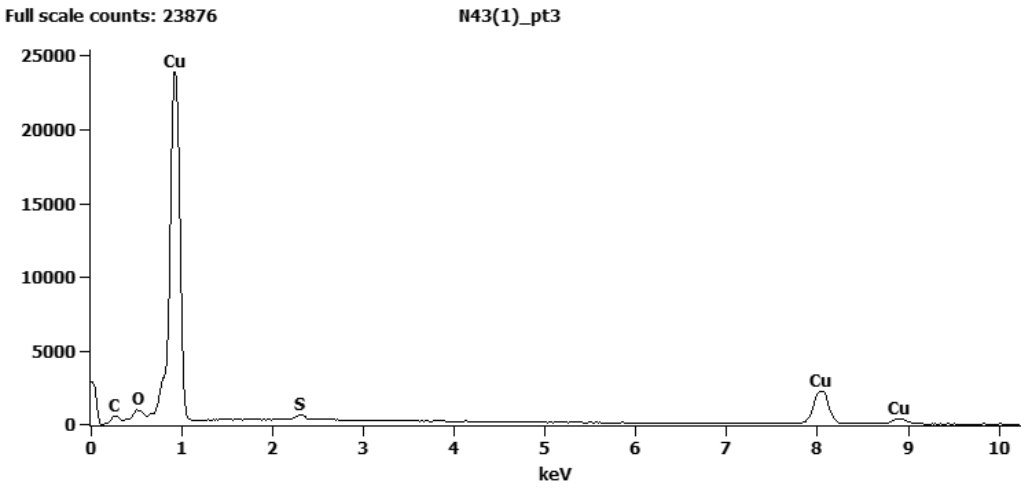
Full scale counts: 23876
N43(1)_pt3
25000
20000
15000
10000
5000
0
Cu
C
O
S
Cu
Cu
0
1
2
3
4
5
6
7
8
9
10
keV

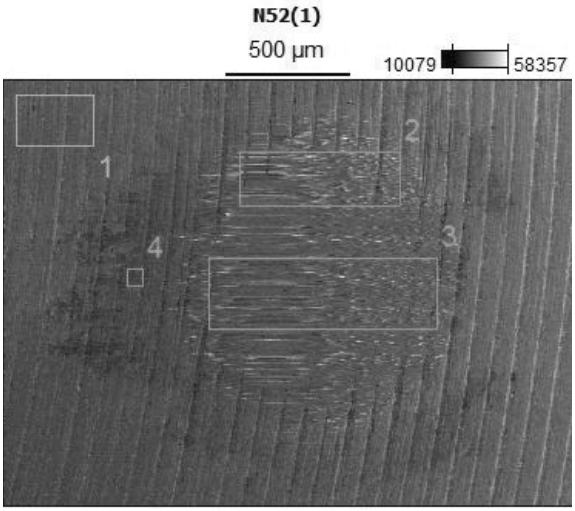

Figure 5S. EDS analysis locations on a hydrophobins in a water-lubricated copper pin. At location 4 nitrogen is observed, which indicates the existence of hydrophobin proteins outside the wear track. Result tables and graphs below.

Weight %

	C-K	N-K	O-K	S-K	Cu-K
N52(1)_pt1	7.7		1.7	0.1	90.5
N52(1)_pt2	7.2		1.9	0.3	90.7
N52(1)_pt3	7.0		2.2	1.1	89.7
N52(1)_pt4	20.3	6.9	4.3	0.7	67.8

Atom %

	C-K	N-K	O-K	S-K	Cu-K
N52(1)_pt1	29.3		4.9	0.2	65.5
N52(1)_pt2	27.9		5.4	0.4	66.3
N52(1)_pt3	27.0		6.5	1.5	65.0
N52(1)_pt4	47.8	13.8	7.6	0.6	30.2

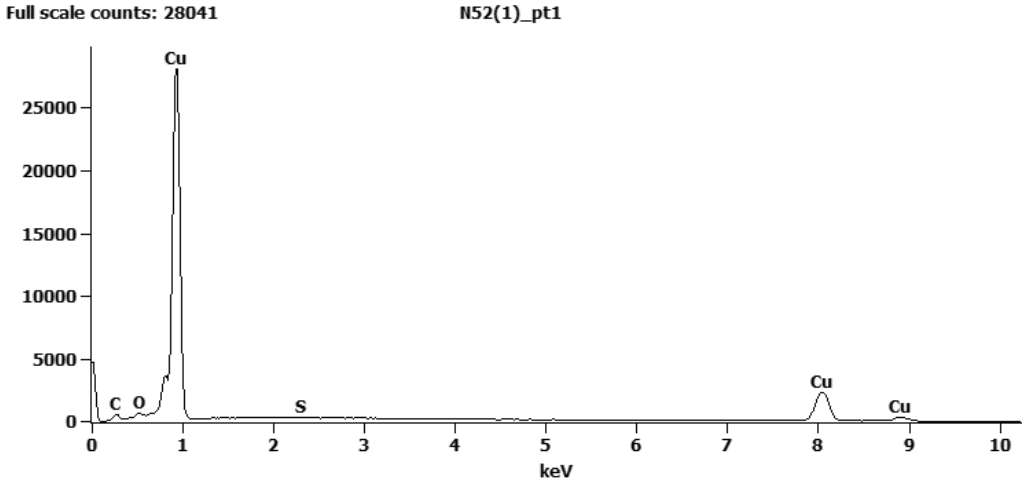

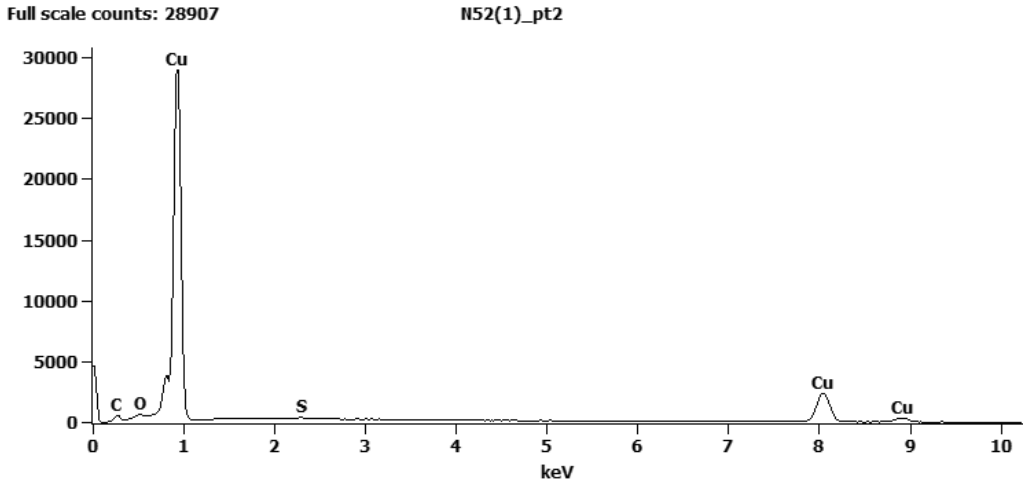
Full scale counts: 28907
N52(1)_pt2
30000
25000
20000
15000
10000
5000
0
Cu
C
O
S
Cu
Cu
0
1
2
3
4
5
6
7
8
9
10
keV

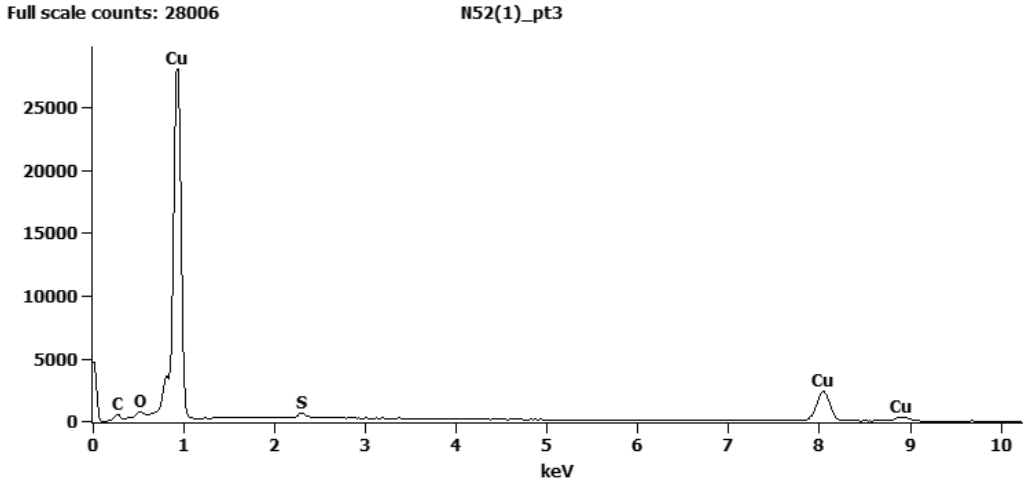
Full scale counts: 28006
N52(1)_pt3
25000
20000
15000
10000
5000
0
Cu
C
O
S
Cu
Cu
0
1
2
3
4
5
6
7
8
9
10
keV

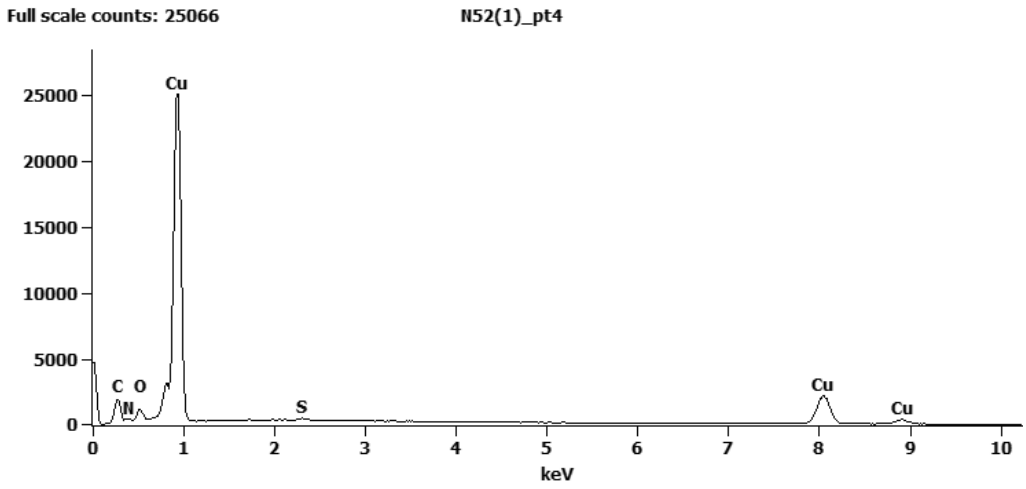
Full scale counts: 25066
N52(1)_pt4
25000
20000
15000
10000
5000
0
Cu
C
O
N
S
Cu
Cu
0
1
2
3
4
5
6
7
8
9
10
keV

VI

Shi Z, Hakala TJ, Metsäjoki J, Szilvay GR, Li F. Lubrication of aluminium versus diamond-like carbon contacts with hydrophobin proteins. *Accepted to Surface Engineering*. DOI: 10.1080/02670844.2015.1114234

Lubrication of aluminium versus diamond-like carbon contacts with hydrophobin proteins

Zhen Shi[a,c], Timo J. Hakala[b], Jarkko Metsäjoki[b], Géza R. Szilvay[b] and Feng Li[a,d,*]

[a]*Key Lab of Nanodevices and Applications, Suzhou Institute of Nano-Tech and Nano-Bionics, Chinese Academy of Sciences (CAS), Suzhou 215123, People's Republic of China*

[b]*VTT Technical Research Centre of Finland, Metallimiehenkuja 8, Espoo, P.O. Box 1000, FI-02044, Finland*

[c]*Advanced Coatings Applied Research Laboratory, Department of Mechanical and Biomedical Engineering, City University of Hong Kong, Kowloon, Hong Kong, China*

[d]*Suzhou JinFu New Material Co., Ltd, Suzhou 215126, China*

*Corresponding author. Tel.: +86 512 62872572; fax: +86 512 62872724

E-mail address: fli2008@sinano.ac.cn

Abstract

Hydrogenated diamond-like carbon (DLC) coatings (a-C:H) and silicon-doped DLC coatings (a-C:H(Si)) of 1 µm thickness were deposited on stainless steel substrates by the inductively coupled plasma chemical vapour deposition technique, including a 300 nm-thick SiN_x interlayer. Tribological experiments for both types of coating under pure and hydrophobin-containing water lubrication were performed using a pin-on-disc tribometer. To better understand wear behaviour, studies of hardness, surface morphology, water contact angle and chemical bonding were carried out using a Nano Indenter, atomic force microscopy, contact angle measurement and X-ray photoelectron spectroscopy, respectively. Silicon doping in the a-C:H coating was found to slightly increase the surface roughness and wettability. The lowest friction coefficient (0.09) was obtained for the a-C:H(Si) coating sliding against an aluminium counterpart in water. The addition of HFBII hydrophobins to water increased both friction and wear of the aluminium counter body, and oxide tribofilm formation was prevented on the aluminium surface.

Keywords: DLC, Water lubrication, Hydrophobins, Friction and wear, ICP-CVD

1. Introduction

Traditional oil-based lubricants have been widely used in many industrial applications such as metal working, for reducing friction, wear and heat between interacting surfaces. However, due to their poor biodegradability and high toxicity,[1] oil-based lubricants involve high energy consumption and risk polluting the environment. Moreover, in certain industries, such as the food industry and the biomedical field, oil cannot be used because of its high toxicity to humans. As a comparison, water-based lubricants have the advantages of low toxicity, biodegradability and fire resistance while maintaining a high level of tribological performance. Thus, due to environmental legislation and safety issues, new lubrication systems containing water-based lubricants should be developed.

In nature, mammal joints, lungs and eyes are water-based lubrication systems, including different kinds of biomolecules, such as proteins, carbohydrates and phospholipids. Usually, biomolecules with lubricating ability consist of hydrophobic and hydrophilic moieties, where friction coefficients (COF) below 0.05 can be measured under low contact pressures.[2] The hydrophilic moiety can bind water onto the surface-adsorbed molecular layer, while the hydrophobic moiety provides good adhesion to the surface. Low friction in biomolecule-lubricated contacts is expected to occur via a hydration lubrication mechanism, where hydrated moieties slide over each other. Thus, perfect alignment of the molecules is essential for good lubrication.[3,4] Depending on the nature of the molecule and its adhesion to the surface, hydration lubrication is very sensitive to normal loads and contact pressures and can occur under contact pressures up to a few megapascals.[5]

Hydrophobins are small fungal amphiphilic proteins that have exceptional film-forming and adhesion properties.[6,7] Their biological roles are related to the control of interfacial forces in fungi. For example, they lower the surface tension of water, mediate adhesion to solids and form protective layers. At the air/water interface, they self-assemble into stable, structured and highly elastic films.[8] It is known that hydrophobins can bind large amounts of water onto their surfaces through their hydrophilic parts.[9] Furthermore, the exceptional thermal stability of hydrophobins has been demonstrated, as no structural changes were observed upon heating to 90°C.[10,11] The high thermal and chemical stabilities have been ascribed to the four intramolecular disulphide bonds that bind the polypeptide chain into a compact globular shape.[12] With strong adhesion to solid surfaces, high water-binding ability and a stable structure, hydrophobins have great potential to act as lubricant additives in water-based systems.

In earlier reports, two hydrophobins, namely HFBI and FpHYD5, have shown their ability to lubricate stainless steel surfaces in aqueous environments.[9,13,14] However, it was observed that an increase in the amount of hydrophobins adsorbed on the surface may increase the friction and wear of sliding contacts.[9,15] Friction coefficients in hydrophobin-lubricated stainless steel contacts were in the range 0.1–0.3, which are similar to that measured on mica surfaces lubricated with nanoscale HFBI.[16]

DLC coatings are known for their high hardness, low friction, high wear resistance, as well as for their biocompatibility, which makes them suitable for biomedical applications.[17] Normally, DLC coatings can be divided into hydrogen-containing (a-C:H) and hydrogen-free (a-C) coatings. The a-C:H coatings display low friction and wear under dry conditions, whereas the friction coefficients increase to more than 0.1 in water or oxygen-containing environments.[18] In contrast, a-C coatings display low friction and wear under humid conditions.[19] In a water environment, low friction

comes from surface graphitisation and thin water-layer formation on the DLC surface.[20] Originally it was supposed that only a-C coatings had good lubrication properties under humid conditions,[21] but lately, silicon-doped a-C:H coatings have also shown super low friction in water environments.[22]

The combination of hard DLC coatings and environmentally friendly hydrophobin-containing water-based lubricants shows great promise as a lubrication system for future use, for example, in the food or biomedical industries. The aim of this paper is to study the tribological behaviours of DLC coatings within a water environment containing hydrophobin proteins. To better understand wear behaviour, studies of hardness, surface morphology, water contact angle and chemical bonding were carried out using a Nano Indenter, atomic force microscopy (AFM), contact angle measurement and X-ray photoelectron spectroscopy (XPS), respectively.

2. Experimental methods

2.1. Coating deposition

Single crystalline silicon (1 0 0) wafers of 50.8 mm diameter and 400±10 μm thickness, along with stainless steel discs (AISI 440B) of 40 mm diameter and 5 mm thickness, were used as substrates. Prior to thin film deposition, the substrates were ultrasonically cleaned with isopropyl alcohol and acetone for 5 minutes each and then washed with distilled water. Experiments were performed using an Oxford Plasmalab System 100 ICP-CVD reactor. The process chamber was first evacuated to a base pressure of 2×10^{-4} Pa. Then, Ar plasma etching was performed for 15 minutes to remove native oxides and contaminants on the substrate surfaces and to promote coating adhesion.[23,24] Ar plasma was obtained at a pressure of 10 mTorr, with the ICP generator and radio frequency (RF) generator power at 1000 W and 100 W, respectively.

The coating deposition rate was evaluated in preliminary experiments in order to control the thickness by altering the deposition time. First, a 300 nm-thick SiN_x interlayer was deposited on

stainless steel (AISI 440B) discs to improve the adhesion between the DLC coatings and the steel substrates with a deposition rate of 33 nm min^{-1}, the working pressure was set at 10 mTorr and the substrate temperature was controlled at 75°C. Following that, DLC coatings were deposited on a SiN_x layer at 30 mTorr, the power outputs of the ICP generator and RF generator being set at 100 W and 250 W, respectively. Table 1 shows the gas flow rates for various deposition regimes. Finally, DLC coatings with 1 µm total thickness were obtained, including a 300 nm-thick SiN_x interlayer. The process times for a-C:H and a-C:H(Si) coatings were 60 min and 35 min, respectively.

Table 1. Gas flow rates for various a-C:H and a-C:H(Si) deposition regimes

Gas flow (sccm)	SiN_x	a-C:H	a-C:H(Si)
CH_4	0	30	30
Ar	0	10	10
SiH_4	40	0	4
N_2	40	0	0

2.2. Preparation of hydrophobins

The hydrophobin protein HFBII was prepared in a recombinant *Trichoderma reesei* strain VTT-D-99745 using a bioreactor. The molecular mass of HFBII is 7200 g mol^{-1} and the protein consists of 71 amino acids. HFBII was extracted from the culture supernatant using an aqueous two-phase system, as described by Hakala *et al.*,[25] and further purified using a Bio-Gel P-6DG size exclusion chromatography column (Bio-Rad) in 20 mM ammonium acetate buffer (pH 8).

HFBII-containing fractions were adjusted with acetic acid to pH 5.5 approximately, and subsequently pooled and freeze dried. For tribological experiments, HFBII powders were dissolved in ultrapure Milli-Q (mQ) water (resistivity 18.2 MΩ·cm) to prepare HFBII solutions with a concentration of 1.0 mg ml^{-1}.

2.3. Coating characterisation

Hardness measurements were carried out using a Nano Indenter (Agilent G200, USA) on silicon wafers, with each hardness value being calculated by averaging the data of six individual indentations. The penetration depths did not exceed one-tenth of the coating thickness to guarantee that the measurements were not significantly influenced by the substrate.

Surface topography of DLC coatings on stainless steel substrates was examined by AFM (XE-120, Parker Systems, Korea) in tapping mode, and images were collected at a fixed scan rate of 0.5 Hz.

Water contact angles were measured by the sessile drop method (CAM 200 optical contact angle measurement system; KSV Instruments Ltd), using the Young–Laplace equation to fit the drop profiles. All measurements were carried out with distilled water at 22.5°C and 50% relative humidity. Three tests were performed on each sample, and the data were reported as mean values and percent uncertainty.

The chemical composition and bonding state of oxygen in the coatings were investigated by XPS on silicon substrates. The spectra were obtained with a Kratos AXIS Ultra DLD (Kratos Analytical Ltd, UK), using Mg Kα radiation as the X-ray source. CasaXPS software was employed to analyse the spectra.

Tribological tests were carried out using a pin-on-disc tribometer designed and manufactured at VTT Technical Research Centre of Finland. The counter body was a spherical aluminium (Al 5083) pin with a radius of 50 mm. The hardness of the aluminium was 82.1 HV_1 and the surface roughness measured with a profilometer was 0.05 µm or lower. The experiments were performed at a normal loading of 2 N, and a sliding velocity of 0.05 m s^{-1} for 40 min was employed to avoid excessive evaporation of the lubricant. A small amount of lubricant (0.6 ml) was added to cover the entire wear track during the experiment. Each test was carried out three times for each

coating/lubricant pair, and following the tests, the disc was cleaned for wear track observation. The volume loss of the spherical aluminium pin was calculated from wear track dimensions measured by optical microscopy.

The wear tracks and the counterpart were examined using scanning electron microscopy (SEM; Zeiss UltraPLUS Thermal Field Emission, Germany). Energy-dispersive X-ray spectroscopy (EDS; Thermo Fisher Scientific UltraDry EDS Detector, USA) was used to analyse the elemental composition.

3. Results

3.1. Surface properties

The hardness values of a-C:H and a-C:H(Si) coatings are about 20.3 GPa and 17.3 GPa, respectively. Surface morphologies of a-C:H and a-C:H(Si) coatings examined by AFM are shown in Figs. 1a and 1b**.** In comparing the morphologies, particles can be observed on the a-C:H(Si) surface, which seem to be nanoclusters formed by silicon species during the film growth. Both a-C:H and a-C:H(Si) coatings have smooth surfaces with values of root mean square roughness (R_q) of 0.71 nm and 2.58 nm, respectively. In comparison, the surface morphology of a bare stainless steel substrate (R_q = 4.59 nm) is shown in Fig. 1c.

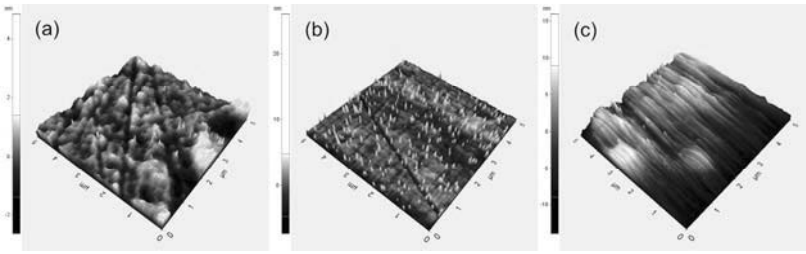

Fig. 1 AFM images of 5 µm × 5 µm scan size of (a) a-C:H coating, (b) a-C:H(Si) coating and (c) bare stainless steel substrate

Figure 2 shows the water contact angle on the coating and bare stainless steel surfaces. It can be observed that these three surfaces have similar wettability. Silicon incorporation in DLC slightly increased the surface wettability, and the contact angle decreased from 77° to 70°.

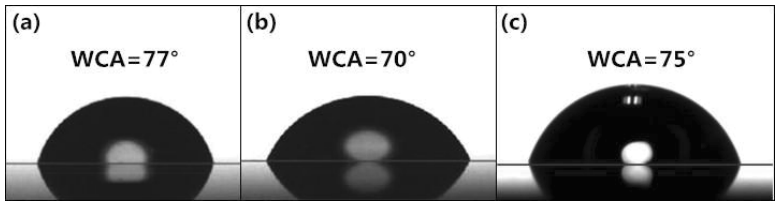

Fig. 2 Water contact angle of (a) a-C:H coating, (b) a-C:H(Si) coating and (c) bare stainless steel substrate

The chemical composition determined from XPS spectra shows the elemental composition of the coatings to be 98.36 at.-% C, 0.47 at.-% Si and 1.17 at.-% O for the a-C:H coating, and 75.25 at.-% C, 21.21 at.-% Si, 2.59 at.-% O and 0.95 at.-% N for the a-C:H(Si) coating. As XPS is a surface analysis technique, the presence of silicon in the a-C:H coating and nitrogen in the a-C:H(Si) coating came from either the process chamber or from atmospheric contamination. The peaks for the O 1s XPS spectrum of the a-C:H(Si) coating can be resolved into two parts: one at 530.9 eV and another at approximately 532.1 eV (Fig. 3). The peak with the lower binding energy is assigned to C–O bonding and that with the higher binding energy to Si–O bonding.[26]

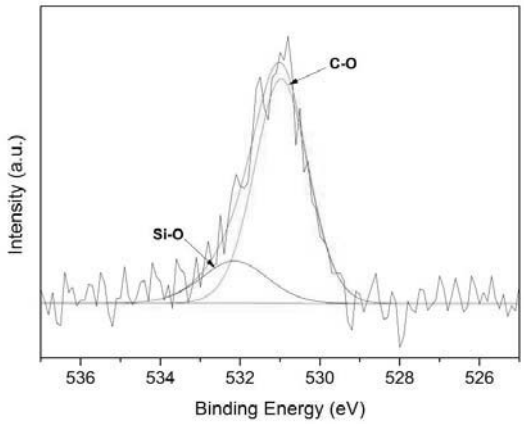

Fig. 3 XPS O 1s spectral deconvolution of the a-C:H(Si) coating

3.2. Friction and wear tests

Figure 4 presents the variation of friction coefficient with time for aluminium versus DLC lubricated contacts, and it can be observed that in water-lubricated experiments, both DLC coatings reduced friction compared with a bare stainless steel surface sliding against aluminium. The lowest friction coefficient of ~0.09 was measured in the aluminium versus a-C:H(Si) contact lubricated with mQ water. The addition of hydrophobins increased the friction coefficient from 0.10–0.15 to 0.20–0.30 (Fig. 5a). The initial Hertzian contact pressure was approximately 80 MPa, calculated using the online program, but it decreased to 9–15 MPa for pure water and to 1–4 MPa for HFBII-containing water lubrication, calculated from the diameters of the wear tracks. The contact pressure reduction is possibly due to the wearing of sliding bodies, which increases the contact area. In our study, friction coefficients remained relatively stable throughout the experiments, and thus the decrease in contact pressure did not affect the lubrication mechanism.

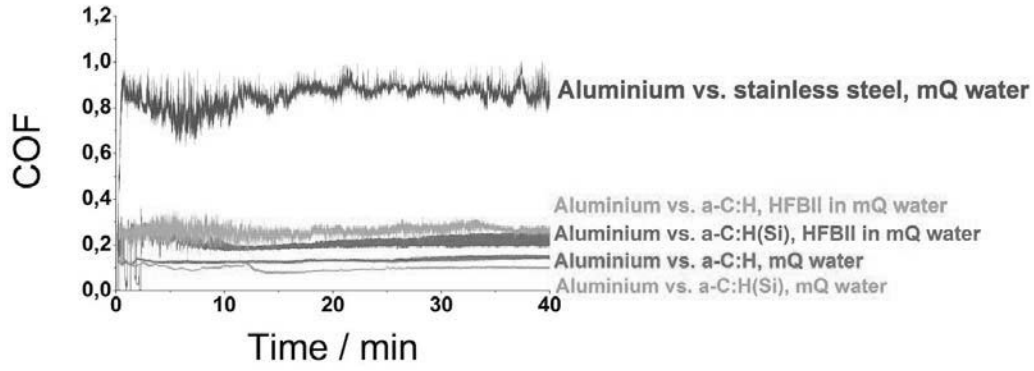

Fig. 4 Friction coefficient variation with time for aluminium versus DLC lubricated contacts. The blue line indicates the aluminium versus stainless steel contact lubricated with mQ water

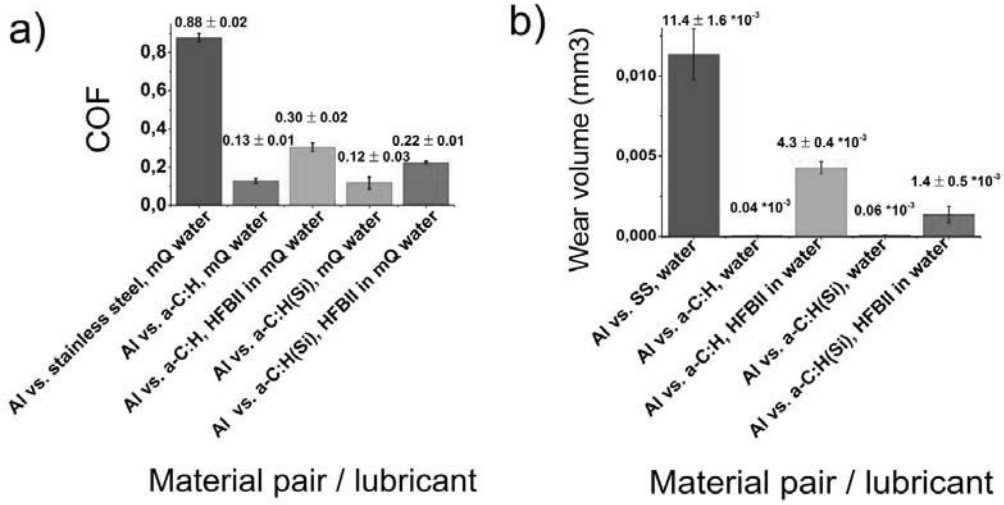

Fig. 5 (a) Friction coefficient and (b) wear volume of aluminium pin in aluminium versus DLC contacts lubricated with mQ water and HFBII in mQ water. The blue column indicates the aluminium versus stainless steel contact lubricated with mQ water

Following the friction tests, wear tracks were studied using SEM. The bare stainless steel disc and the corresponding aluminium pin had the largest wear track dimensions and the worst grooving (Figs. 5b and 6) among all tested material pairs. EDS analyses revealed that there was Al transfer from the pin to the disc. Fe, Cr, O and C were found on a transfer/reaction layer on the pin.

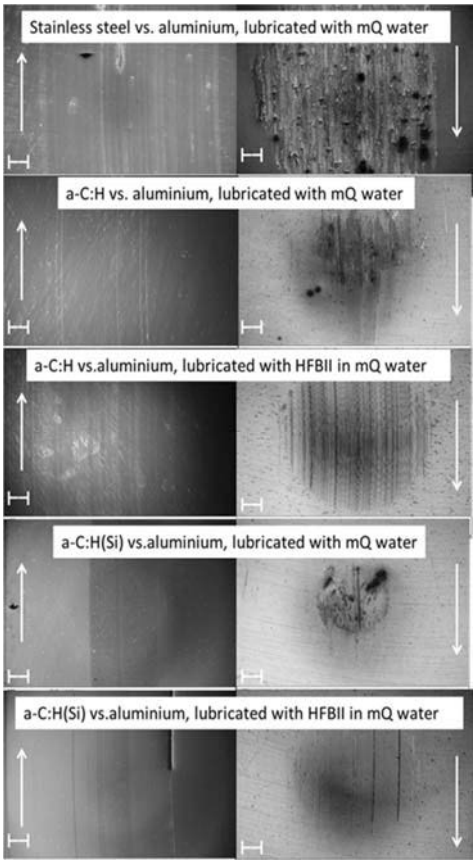

Fig. 6 SEM images of sliding surfaces after pin-on-disc experiments. The left-hand side represents wear tracks on the disc surface, while the right-hand side represents wear on the aluminium pin. The scale bar is 200 µm and the white arrows show the sliding direction

After mQ water-lubricated experiments with DLC coatings, the counter bodies showed very little wear, as presented in Fig. 6. The a-C:H(Si) coating performed especially well: only a few deep grooves were detected on the disc, along with a small worn area on the aluminium pin. There was

no aluminium transfer, but a small number of Si, F and C particles were found in the wear track. A thin tribolayer that contained O, C and possibly traces of pin material was formed on aluminium pins, after sliding against a-C:H and a-C:H(Si) coatings.

The addition of HFBII hydrophobins to water increased the wear volume of the aluminium pins after sliding against DLC surfaces (Fig. 5b)**.** The wear tracks on a-C:H surfaces were almost as wide as those of bare stainless steel discs (topmost pair in Fig. 6). However, the wear loss and Al transfer were small in comparison with aluminium versus stainless steel experiments. In HFBII lubricated experiments, no oxygen-rich tribolayer was found on the aluminium pin as formed in the water-lubricated experiments. HFBII hydrophobins also prevented Al transfer onto the DLC surface, since no trace of Al was found on the discs by EDS.

4. Discussion

Average friction coefficients in all water-lubricated aluminium versus DLC experiments were between 0.11 and 0.13, and the lowest friction coefficient of 0.09 was obtained in a single test. Water was found to lubricate DLC coatings quite well. In fact, lubrication came from the thin water film formed on the DLC surface[20] and the thin tribolayer formed on the aluminium surface during the experiment. In the case of aluminium versus a-C:H(Si), there was a small amount of silicon transferred from the coating surface to the aluminium pin, and friction decreased slightly compared with aluminium versus the a-C:H case. This might be due to the formation of Si–O bonds and graphitisation of the sliding surfaces, which are both beneficial for water lubrication.[22] Figure 2 shows that silicon incorporation into the DLC coating only slightly decreased the water contact angle, because Si–O covalent bond formation leads to a highly polar component of the coating.[27] Thus, the a-C:H(Si) surface showed a slight reduction of the contact angle.

In hydrophobin-lubricated experiments, the average friction coefficients were between 0.20 and 0.34. The increase in friction indicates that the hydrophobins changed the boundary lubrication mechanism of the original DLC coating, since hydrophobins do not significantly affect the lubrication regime through a change in the lubricant viscosity. In this case, hydrophobins prevented the formation of a well-lubricated water layer on the DLC surface and oxygen-containing tribofilm formation on the aluminium surface.

According to the literature, proteins such as albumin can disturb the low friction mechanism of DLC by forming bridges between the sliding surfaces when they are denatured; thus, the adhesion between sliding surfaces increases.[2] Denaturation of the protein may occur due to the increased temperature and shear stress on contact points. In our experiments with hydrophobins, denaturation was not expected to occur because the hydrophobin structure is very stable,[10] and no obvious fluctuation in friction could be observed during the sliding process. Thus, the effect of possible denaturation cannot be seen in friction behaviour.

In a previous study, it was observed that hydrophobins can reduce friction in stainless steel versus stainless steel contacts.[9] Friction and wear are both usually high in such contacts when lubricated with water because water is not capable of forming a lubricating layer or tribofilms on stainless steel surfaces. The situation is completely different for aluminium versus DLC contacts, where the friction coefficient is about 0.1 before mixing any additives. The reason why super low friction coefficients have not been achieved in hydrophobin-lubricated systems may originate from the surface properties of DLC coatings themselves. Low friction coefficients of biomolecule lubricants[2,3] are usually measured on hydrophobic surfaces (water contact angle > 90°) and under relatively low contact pressures. But in this study, the DLC surfaces were not hydrophobic (water contact angle ~70°; Figs. 2a and 2b). Thus, the lack of surface hydrophobicity may affect the

alignment of the molecules, as well as lubrication mechanisms such as hydration lubrication.[4] Hydrophobins would expose their hydrophobic sides to the water interface and sliding could not occur between the hydrated moieties. In these experiments, the upper body also showed wear, which means that a stable molecular layer could not have been formed on both sliding surfaces. Any further reduction in the friction coefficient of aluminium versus DLC contact below 0.1 may need the very high hydration levels provided by hydrophobins, correct alignment and strong adhesion on both sliding surfaces. Hence, sliding can occur between the hydrophilic moieties of hydrophobins, and this is the requirement in hydration lubrication. In hydrophobin-lubricated aluminium versus DLC experiments, the contact pressures decreased from 80 MPa to 1–4 MPa. Thus, it would be possible to achieve super low friction coefficients under these contact pressures with the right selection of molecules and their perfect alignment.

Interestingly, in this study, friction coefficients measured in hydrophobin-lubricated experiments were at the same level (0.1–0.3) as those measured in stainless steel versus stainless steel contacts using hydrophobin additives, as previously reported.[15] We can state that in hydrophobin-containing contacts, hydrophobins played a major role in the lubrication regime. Although the friction coefficients of the original bare stainless steel and DLC coating surfaces in a water environment were quite different, these surfaces showed similar wetting properties (Fig. 2), which affected the lubricating properties of hydrophobins significantly. Thus, following the addition of hydrophobins to water, friction was at the same level in both lubrication systems.

To achieve a better understanding of the effects of hydrophobicity on the tribological performance of hydrophobins, we suggest for future experiments the fabrication of hydrophobic, or even superhydrophobic DLC coatings doped with other elements, such as fluorine, to test their interaction with biomolecule-containing water lubricants.

5. Conclusions

Both a-C:H and a-C:H(Si) coatings were deposited on stainless steel substrates with a 300 nm-thick SiN_x interlayer by the ICP-CVD deposition technique. Surface properties, e.g. surface morphology, wetting behaviour and chemical bonding, were characterised by means of AFM, contact angle measurement and XPS. The tribological behaviour of DLC coatings in both pure and hydrophobin-containing water environments were investigated using a pin-on-disc tribometer. The following conclusions were drawn from this study:

(1) Silicon incorporation into the a-C:H coating slightly increased the surface roughness and wettability.

(2) The prepared hard a-C:H and a-C:H(Si) coatings yielded low friction coefficients (~0.12) when sliding against aluminium in a water environment. Silicon doping in the a-C:H coating enhanced the lubrication ability in water-lubricated contacts, where a friction coefficient as low as 0.09 was measured.

(3) The addition of HFBII hydrophobins to water increased the friction and wear in aluminium versus DLC contacts and prevented oxide tribofilm formation on the aluminium surface.

Acknowledgements

The authors wish to thank the technical personnel at VTT Technical Research Centre of Finland for their technical support on tribology test work, preparation of lubricants and SEM characterisation. The authors also wish to thank the technical personnel from Suzhou Institute of Nano-Tech and Nano-bionics (SINANO) for their technical support on using the thin film coating equipment. This research work was supported financially by the China (Jiangsu) and Finland International R&D Program (BZ2013009), the Finnish Funding Agency for Technology and Innovation (project

Nanolubrication by functional coatings and biomolecules), the Academy of Finland and VTT Technical Research Centre of Finland.

References

1. Y. Shi, I. Minami, M. Grahn, M. Björling and R. Larsson: 'Boundary and elastohydrodynamic lubrication studies of glycerol aqueous solution as green lubricants', *Tribol. Int.*, 2014, **69**, 39.
2. S. Lee, M. Müller, K. Rezwan and N. D. Spencer: 'Porcine gastric mucin (PGM) at the water/poly(dimethylsiloxane) (PDMS) interface: influence of pH and ionic strength on its conformation, adsorption, and aqueous lubrication properties', *Langmuir*, 2005, **21**, 8344–8353.
3. N. M. Harvey, G. E. Yakubov, J. R. Stokes and J. Klein: 'Normal and shear forces between surfaces bearing porcine gastric mucin, a high-molecular-weight glycoprotein', *Biomacromolecules*, 2011, **12**, 1041–1050.
4. J. Klein: 'Polymers in living systems: from biological lubrication to tissue engineering and biomedical devices: a review', *Polym. Advan. Technol.*, 2012, **23**, 729–735.
5. M. Chen, W. H. Briscoe, S. P. Armes and J. Klein: 'Lubrication at physiological pressures by polyzwitterionic brushes', *Science*, 2009, **323**, 1698–1701.
6. G. R. Szilvay, A. Paananen, K. Laurikainen, E. Vuorimaa, H. Lemmetyinen, J. Peltonen and M. B. Linder: 'Self-assembled hydrophobin protein films at the air–water interface: structural analysis and molecular engineering', *Biochemistry*, 2007, **46**, 2345–2354.
7. M. S. Grunér, G. R. Szilvay, M. Berglin, M. Lienemann, P. Laaksonen and M. B. Linder: 'Self-assembly of class II hydrophobins on polar surfaces', *Langmuir*, 2012, **28**, 4293–4300.
8. G. R. Szilvay, A. Paananen, K. Laurikainen, E. Vuorimaa, H. Lemmetyinen, J. Peltonen and M. B. Linder: 'Self-assembled hydrophobin protein films at the air–water interface: structural analysis and molecular engineering', *Biochemistry*, 2007, **46**, 2345–2354.
9. T. J. Hakala, P. Laaksonen, V. Saikko, T. Ahlroos, A. Helle, R. Mahlberg, H. Hähl, K. Jacobs, P. Kuosmanen, M. B. Linder and K. Holmberg: 'Adhesion and tribological properties of hydrophobin proteins in aqueous lubrication on stainless steel surfaces', *RSC Adv.*, 2012, **2**, 9867–9872.
10. S. Askolin, M. Linder, K. Scholtmeijer, M. Tenkanen, M. Penttila, M. L. de Vocht and H. A. B. Wösten:

'Interaction and comparison of a class I hydrophobin from Schizophyllum commune and class II hydrophobins from Trichoderma reesei', *Biomacromolecules*, 2006, **7**, 1295–1301.

11. M. L. de Vocht, I. Reviakine, H. A. Wösten, A. Brisson, J. G. H. Wessels and G. T. Robillard: 'Structural and functional role of the disulfide bridges in the hydrophobin SC3', *J. Biol. Chem.*, 2000, **275**, 28428–28432.
12. J. Hakanpää, A. Paananen, S. Askolin, T. Nakari-Setälä, T. Parkkinen, M. Penttilä, M. B. Linder and J. Rouvinen: 'Atomic resolution structure of the HFBII hydrophobin, a self-assembling amphiphile', *J. Biol. Chem.*, 2004, **279**, 534–539.
13. T. Ahlroos, T. J. Hakala, A. Helle, M. B. Linder, K. Holmberg, R. Mahlberg, P. Laaksonen and S. Varjus: 'Biomimetic approach to water lubrication with biomolecular additives', *J. Eng. Tribol.*, 2011, **225**, 1013–1022.
14. T. J. Hakala: 'A collaborative research on bio-inspired approaches to lubricate engineering materials on nanometer scale', COST Action TD1003, Technical University of Denmark, Kgs. Lyngby, Denmark, 2011.
15. T. J. Hakala, P. Laaksonen, A. Helle, M. B. Linder and K. Holmberg: 'Effect of operational conditions and environment on lubricity of hydrophobins in water-based lubrication systems', *Tribology*, 2014, **8**, 241–247.
16. I. Goldian, S. Jahn, P. Laaksonen, M. Linder, N. Kampf and J. Klein: 'Modification of interfacial forces by hydrophobin HFBI', *Soft Matter*, 2013, **9**, 10627–10639.
17. F. Z. Yang, L. R. Shen, H. L. Zhu, S. Q. Wang, Z. H. Wang and H. F. Liu: 'Study of protective diamond-like carbon films on GCr15 bearing steel', *Surf. Eng.*, 2014, **30**, 836.
18. H. Li, T. Xu, C. Wang, J. Chen, H. Zhou and H. Liu: 'Tribochemical effects on the friction and wear behaviors of a-C:H and a-C films in different environment', *Tribol. Int.*, 2007, **40**, 132.
19. E. Liu, Y. F. Ding, L. Li, B. Blanpain and J.-P. Celis: 'Influence of humidity on the friction of diamond and diamond-like carbon materials', *Tribol. Int.*, 2007, **40**, 216.
20. J. M. Martin, M. I. D. B. Bouchet, C. Matta, Q. Zhang, W. A. Goddard III, S. Okuda and T. Sagawa: 'Gas-phase lubrication of ta-C by glycerol and hydrogen peroxide. Experimental and computer modeling', *J.*

Phys. Chem. C, 2010, **114**, 5003–5011.

21. H. Ronkainen, S. Varjus and K. Holmberg: 'Tribological performance of different DLC coatings in water-lubricated conditions', *Wear*, 2001, **249**, 267.
22. X. Chen, T. Kato, M. Kawaguchi, M. Nosaka and J. Choi: 'Structural and environmental dependence of superlow friction in ion vapour-deposited a-C:H:Si films for solid lubrication application', *J. Phys. D Appl. Phys.*, 2013, **46**, 1.
23. A. Wasy, G. Balakrishnan, S. Lee, J.-K. Kim, T. G. Kim and J. I. Song: 'Thickness dependent properties of diamond-like carbon coatings by filtered cathodic vacuum arc deposition', *Surf. Eng.*, 2015, **31**, 85–89.
24. A. Wasy, G. Balakrishnan, S. H. Lee, J. K. Kim, D. G. Kim, T. G. Kim and J. I. Song: 'Argon plasma treatment on metal substrates and effects on diamond-like carbon (DLC) coating properties', *Cryst. Res. Technol.*, 2014, **49**, 55–62.
25. T. J. Hakala, J. Metsäjoki, N. Granqvist, R. Milani, G. R. Szilvay, O. Elomaa, M. Deng, J. Zhang and F. Li: 'Adsorption and lubricating properties of HFBII hydrophobins and diblock copolymer poly (methyl methacrylate-b-sodium acrylate) additives in water-lubricated copper vs. a-C:H contacts', *Tribol. Int.*, 2015, **90**, 61.
26. J. J. Wang, J. B. Pu, G. G. Zhang and L. P. Wang: 'Interface architecture for superthick carbon-based films toward low internal stress and ultrahigh load-bearing capacity', *ACS Appl. Mater. Inter.*, 2013, **5**, 5019.
27. P. Zhang, B. K. Tay, G. Q. Yu, S. P. Lau and Y. Q. Fu: 'Surface energy of metal containing amorphous carbon films deposited by filtered cathodic vacuum arc', *Diam. Relat. Mater.*, 2004, **13**, 462.

Aalto-DD 144/2015
VTT SCIENCE 118

Friction and wear incur high economic costs globally. It has been estimated that approximately 30% of energy is used to overcome friction. Developing new solutions, such as coatings, surface texturing and lubricants, to reduce friction in the boundary lubrication regime can have great importance to global energy savings in the future.

In this thesis, water-based lubricants with hydrophobin protein (HFBI, HFBII and FpHYD5) and quince mucilage additives were used to lubricate engineering materials such as diamond-like carbon (DLC) coatings, stainless steels and plastics.It was found that hydrophobins can form monolayers on stainless steel, diamond-like carbon (a-C:H) and PDMS surfaces. Increasing the water content in hydrophobin film reduced friction in hydrophobin-lubricated stainless steel vs stainless steel contacts. The same effect was seen in quince mucilage-lubricated UHMWPE vs stainless steel contact.

ISBN 978-952-60-6572-4 (printed)
ISBN 978-952-60-6573-1 (pdf)
ISSN-L 1799-4934
ISSN 1799-4934 (printed)
ISSN 1799-4942 (pdf)

978-951-38-8375-1 (printed)
978-951-38-8374-4 (pdf)
2242-119X
2242-119X (printed)
2242-1203 (pdf)

Aalto University

Department of Materials Science and Engineering
www.aalto.fi

BUSINESS + ECONOMY

ART + DESIGN + ARCHITECTURE

SCIENCE + TECHNOLOGY

CROSSOVER

DOCTORAL DISSERTATIONS